Vascular Smooth Muscle Oxidative Metabolism and Function During Vasospasm After Subarachnoid Haemorrhage

Submitted in partial fulfilment of the requirements for the degree of D.Phil. Biochemistry.

Medical Research Council Biochemical and Clinical Magnetic Resonance Unit,

Department of Biochemistry,

University of Oxford,

South Parks Road,

Oxford.

OX1 3QU

Gail Jean Pyne

Wolfson College,

University of Oxford,

Linton Road,

Oxford.

OX2 6UD

Trinity 1999

Dedication

To Randy.

Not everyone is lucky enough to find their soulmate, but there you were.

May there be many more road trips in our future.

Contents

Acknowledgements

To my Mum and Dad I owe a great deal. They have supported me emotionally, financially and in every other way possible throughout my life, and have put up with me during the most difficult times selflessly, without complaint or expectation of recompense. You're both stars! To the rest of my family, especially Nan and Grandad, who have taught me so much and been so proud of me. I hope I have lived up to and beyond your expectations.

I would like to thank all my friends, a few of whom have stood out that I would like to mention. Bradley Strauchen, Pip for the G & T's, John Bothwell for lunch-time entertainment and Carol, Yvonne and Yvonne who provided excellent research assistance, as well as a shoulder to cry on when needed. A special mention to Mel, OJ. and Nicky whose unflagging enthusiasm is, fortunately, catching! Thanks to Rick Paul for the carrot on the stick.

Thanks to George Radda for taking me into the new and interesting world of the "Radda group", and to Pete Styles for moral support across the Pacific. To my current supervisors, Ruth Dixon I am deeply grateful for all your help and making me do statistics properly, and Tom Cadoux-Hudson for a wealth of ideas and excellent suggestions, I thank you both also for exhaustive checking of this thesis. I also very much appreciate the job I was given at the MRC Collaborative Centre in Mill Hill in between Oxford and Cincinnati.

To Gordie, Jim, and Shawn at Wrighton's of Fritwell for the carotid arteries, steak so fresh it was still mooing and many, many entertaining Monday mornings as well as providing the basis of many excellent dinners. Thanks also to Gordon and all the lads at Mutch meats of Witney for carotid arteries and various other porcine tissues.

Most especially, I wish to thank Joe Clark. He has been the source of my enthusiasm for smooth muscle which I shall never lose, as well as many barbecues and bad jokes! He has been an excellent supervisor and friend and deserves my deepest thanks for all the support, discussions and thesis checking that he has done for me. Cheers!

Publications

Papers

Bearchell, M. C., C. W. G. Redman, G. J. Pyne, T. A. D. Cadoux-Hudson & J. F. Clark. Vascular smooth muscle oxygen consumption is reversibly stimulated by sera from women with preeclampsia. *Am. J. Obs. Gyn.* **179** 1534-1538, 1998.

Abstracts

Pyne, G. J., T. A. D. Cadoux-Hudson, Z. Domingo, G. K. Radda & J. F. Clark. Vascular smooth muscle oxidative metabolism during vasospasm. *Biophys. J.* **72** A59 (1997).

Pyne, G. J., T. A. D. Cadoux-Hudson, Z. Domingo, G. K. Radda & J. F. Clark. Vascular smooth muscle oxidative metabolism during vasospasm. *FASEB J.* **11** A59 (1997)

Pyne, G. J., T. A. D. Cadoux-Hudson, & J. F. Clark. Force-Function relations in vascular smooth muscle during cerebral vasospasm. *Biophys. J.* **74** A256 (1998)

Pyne, G. J., S. Nakayama, T. A. D. Cadoux-Hudson, & J. F. Clark. Altered vascular smooth muscle oxidative metabolism and force generation during magnesium loading and depletion. *FASEB J.* **12** A159 (1998)

Pyne, G. J., S. Nakayama, T. A. D. Cadoux-Hudson & J. F. Clark. Magnesium loading reduces excessive oxidative metabolism and tension in response to subarachnoid haemorrhage *in vitro. British Neurosurgical Research Group Annual Meeting* ***5th annual meeting abstract book.*** (1998)

Abstract

Vascular smooth muscle oxidative metabolism and function during vasospasm after subarachnoid haemorrhage.

Gail Jean Pyne, Wolfson College, University of Oxford. D.Phil. Trinity 1999.

Aims: The purpose of the research presented in this thesis is to elucidate the mechanism of the stimulation of oxidative metabolism and contractile function that occurs in vascular smooth muscle during cerebral vasospasm (CV) after subarachnoid haemorrhage (SAH). The biochemical mechanisms leading to CV were investigated using an *in vitro* model of CV developed for this research. CSF (cerebrospinal fluid) from SAH patients at risk of vasospasm which stimulated oxygen consumption (CSF_S) was used to model vasospasm. The hypothesis is CSF_S contains a substance which stimulates tension generation over that of CSF_N,(non-stimulatory cerebrospinal fluid) and also inhibits the myosin light chain phosphatase.

Methods: The porcine carotid artery was used as a model for the human basilar artery. The rate of oxygen consumption (JO_2) was measured in response to CSF_S and tension generation was also examined. Various agents were used to treat or pretreat the tissue such as magnesium and α_1-adrenergic receptor agonists. Their effects on the CSF_S-induced stimulation were measured to study the mechanism of vasospasm. A myosin light chain phosphatase (MLCP) assay was developed to study the mechanisms leading to CV.

Results and conclusion Addition of CSF_S to the porcine carotid artery is a reliable and reproducible *in vitro* model of CV. Using this model, it was found that Mg^{++} loading and α_1-adrenergic receptor agonists attenuated the vasospasm, but a non-specific endothelin antagonist had no effect. Acute addition of 12mM Mg^{++} relaxed the tissue from a CSF_S induced contraction significantly and rendered the contraction rinsible. Okadaic acid (1nM), a phosphatase inhibitor, had very similar effects to CSF_S because it stimulated JO_2 and slowed relaxation after a stretch. There was also significant inhibition of phosphatase caused by the CSF_S. Vasospasm appears to be caused by a combination of a contractile stimulus, and inhibition of MLCP activity.

Abbreviations

(A)MDP	(Actin and) myosin bound to ADP and phosphate
(A)MT	(Actin and) myosin bound to ATP
$[Mg^{2+}]$	Magnesium concentration in moles per litre (M)
$[Mg^{2+}]_i$	Intracellular magnesium concentration
$[Mg^{2+}]_o$	Extracellular magnesium concentration
^{14}C	Carbon isotope with a M_r of 14
A	Actin
ADP	Adenosine 5' diphosphate
AM	Actomyosin
ATP	Adenosine 5' triphosphate
ATPase	ATP hydrolysing activity
Ca^{2+}	Calcium ion
CaCaMKII	Calcium-calmodulin dependent protein kinase 2
CaD	Caldesmon
CaM	Calmodulin
cAMP	Adenosine 3'5' cyclic monophosphate
CaP	Calponin

CaT	Caltropin
CC	Contractile component
cGMP	Guanosine 3' 5' cyclic monophosphate
CO_2	Carbon dioxide
CSF	Cerebrospinal fluid
CSF_N	Non- stimulatory (with respect to JO_2) CSF
CSF_S	Stimulatory (with respect to JO_2) CSF
CV	Coefficient of variation
DAG	Diacyl glycerol
DAGK	Diacyl glycerol kinase
ET	Endothelin
IP_3	Inositol 1,4,5 trisphosphate
JO_2	Rate of oxygen consumption (μmol O_2 min^{-1}g dwt^{-1}
KCl	Potassium chloride
kDa	KiloDaltons
M	Myosin
MgADP	Magnesium adenosine diphosphate
MgATP	Magnesium adenosine 5' triphosphate
MHC	Myosin heavy chains

MLC_{17}	Essential myosin light chains
MLC_{20}	Regulatory myosin light chains
MLCK	Myosin light chain kinase (a calcium-calmodulin activated kinase)
MLCP	Myosin light chain phosphatase (probably a PP1 or PP2A)
NMR	Nuclear magnetic resonance
OA	Okadaic acid
PCA	Perchloric acid
PIP_2/ PIP_3	Phosphatidylinositol bis/trisphosphate
PKA	cAMP dependent protein kinase
PKC	Protein kinase C (usually Ca^{2+} dependent)
PKCε	DAG dependent, Ca^{2+} independent PKC
PKG	cGMP-dependent protein kinase
PLC/D	Phospholipase C/D
PP1	Type 1 protein phosphatase
PP2A/ C	Type 2 protein phosphatase (subtype A or C)
PSS	Physiological saline solution
SAH	Subarachnoid Haemorrhage
SEC	Series Elastic Component
TpM	Tropomyosin

Contents

1.Introduction

1.1 Overview

Smooth muscle is a unique and versatile tissue. It is found throughout the body, lining all hollow organs. Many of the most important functions of the body rely on the appropriate actions of smooth muscle. These include digestion of food and expulsion of the resultant waste products, intake of oxygen and importantly, the delivery of oxygen rich blood to vital organs and removal of oxygen depleted blood to be re-oxygenated. For a tissue that plays such an important role in homeostasis of numerous bodily systems, it is underrepresented in medical research compared to skeletal and cardiac muscle.

1.1.1 Types of smooth muscle

The ordinary function of smooth muscle comprises interaction between a number of components resulting in tension generation, tension maintenance or relaxation. There are many kinds of smooth muscle with a wide range of functional and physiological differences. Somlyo and Somlyo[260] described two kinds of smooth muscle based on their response to stimuli such as calcium and noradrenaline: a "spike-generating" type based on portal vein responses and a "gradedly responsive" type with the examples being the aorta and the pulmonary artery. These were termed tonic (gradedly responsive) and phasic (spike-generating) smooth muscle by the way that they contracted in response to certain stimuli[260]. They showed that depolarized phasic muscle contracts and relaxes rhythmically upon initial stimulation and further stimulation will increase the magnitude of the oscillation, maintaining the same trough tension but with increasing peak tensions[79, 260]. Depolarized tonic smooth muscle does not oscillate, but rather increases tension in response to a stimulus[97, 260]. There are some smooth muscles, such as the hepatic portal vein, which have a tonic and phasic element[246]. Unlike in skeletal muscle, where there are

cells with tonic activity and others with phasic activity[147], each individual smooth muscle cell appears to have both phasic and tonic capability[161]. In these muscles, both the basal tone and the peak height are increased in response to a stimulus[260]. Tonic vascular smooth muscle is the tissue under investigation in this thesis.

1.1.2 Smooth muscle contraction

Vascular smooth muscle has unique metabolic and functional properties. It is well matched to its function in that, although generation of tension consumes energy, it is able to maintain tension for extended periods of time with relatively little energy consumption[185], therefore being capable of maintaining blood pressure in an economical fashion. The energy metabolism of vascular smooth muscle is introduced in more detail in Section 1.3. Smooth muscle contraction, like striated muscle, is regulated by calcium. Unlike skeletal muscle, however, the calcium activates contraction indirectly, whereas in skeletal muscle, calcium binds directly to the thin filaments to relieve inhibition. The components of the smooth muscle contractile apparatus, as well as the mechanism of contraction and its control by calcium and other factors are detailed in section 1.4.

1.1.3 Passive elastic recoil

Apart from the closely regulated active contraction element of smooth muscle contraction, there is an elastic component to the function of smooth muscle. Vessel walls also contain a number of other components, including connective tissues collagen and elastin which do not have contractile function, but contribute to the passive elastic capacity of the vessels. The smaller the vessels, the greater the proportion of the elastic to smooth muscle component of the tissue[181]. This means that large blood vessels, such as the aorta, have proportionally less elastic component to contractile component than a small blood vessel such as an arteriole. The purpose of this passive elastic recoil in the arterial system is, in the large vessels, to modulate turbulence from blood flow and in the smaller vessels, to aid in maintenance of tension and vascular tone. As the blood is pumped from the heart

into the major arteries, they stretch and then recoil to minimise turbulence and to aid the movement of the blood through the vessels[181].

1.1.4 Metabolism in vascular smooth muscle

ATP production and utilisation in smooth muscle is thought to be compartmented [122, 219].The ATP that fuels contraction appears to come almost exclusively from the oxidative metabolism of glycogen derived glucose in the muscle. This was shown by way of a number of experiments, mainly in the laboratory of R. J. Paul. It was shown that oxygen consumption was increased concomitant to a stimulation of contraction without increased production of lactate[124]. This was further clarified by the use of radiolabelled glucose as a substrate. External glucose metabolism, assessed by measuring radiolabelled lactate and CO_2 production, did not increase during contraction. This suggests that glycogen-derived glucose is oxidatively metabolised preferentially over extracellular glucose to fuel contraction [25]. The ability of the tissue to perform oxidative metabolism can be impaired through sustained stimulation of contraction beyond the oxidative capacity of the tissue or exposure to hypoxic conditions. In these situations, lactate production was found to increase upon stimulation of contraction[122, 217] This suggests possible supplementation of aerobic glycogen-derived glucose metabolism by anaerobic glucose metabolism. This increase in lactate production can also be seen when cyanide is used to inhibit oxidative metabolism in working muscle[123]. What, then, is responsible for the relatively large basal lactate production seen in smooth muscle? This has been shown to be derived from anaerobic metabolism of extracellular glucose to fuel cell homeostasis, membrane pump and channel activity[125]. This was determined by the incubating the tissue in ^{14}C-labelled glucose and subjecting it to osmotic stress or inhibition of membrane pumps with agents such as ouabain. The production of ^{14}C labelled lactate was found to be increased under these conditions. Oxygen consumption has been shown to be linearly correlated to isometric force[221]. This was elucidated using simultaneous force and oxygen consumption measurements. The relationship between rate of O_2 consumption (JO_2) and

force changes according to the level of myosin regulatory light chain (MLC_{20}) phosphorylation[308]. These concepts are further described in section 1.3.

1.1.5 Pathologies due to inappropriate smooth muscle responses

What happens when vascular smooth muscle reacts inappropriately to physiological signals? There are a number of leading causes of mortality related to disruption of smooth muscle function. These include hypertension leading to stroke, myocardial infarction, kidney disease and atherosclerosis, which may lead to plaque detachment and ischaemic heart disease or stroke. The particular pathology dealt with in this thesis is one that occurs after a haemorrhagic stroke. Blood enters the cerebrospinal fluid, after rupture of a vessel due to trauma or aneurysm, in the subarachnoid space, resulting in a condition known as subarachnoid haemorrhage. Four to seven days later[294], 40% of the surviving patients develop a vascular condition known as cerebral vasospasm[113]. This severe and chronic spasm or pathological vasoconstriction of the cerebral arteries can lead to cerebral ischaemia, impaired recovery, further stroke and death[113]. Vasospasm also occurs in the coronary arteries[132] and mesenteric arteries[154] so it is a common problem to multiple vascular beds.

1.2 Hypothesis

There are currently many theories as to the cause of cerebral vasospasm. These include structural alterations[62, 113] or contractile dysfunction[38, 187] due to metabolic[49, 179] and signalling[38, 186, 201] perturbances. The aim of the work presented in this thesis is to determine the state of the oxidative metabolism in the porcine carotid artery during incubation in cerebrospinal fluid from patients with cerebral vasospasm after subarachnoid haemorrhage. I aim to demonstrate, using a model developed in this laboratory that, although there may be some stimulation of contraction involved, the ætiology of cerebral vasospasm may be one of a pathological failure to relax. This is possibly caused by

inhibition of myosin light chain phosphatase, which, in conjunction with a contractile stimulus, likely to be protein kinase C activation[201], culminates in an unresponsive spasm.

1.3 Vascular smooth muscle energy metabolism

It is postulated that glycolytic metabolism fuels membrane pumps and cell homeostasis and that oxidative metabolism fuels contractile function. Glycolytic and oxidative metabolism will be introduced separately at first, followed by a description of the relationship between oxidative metabolism and contractile function that forms the basis of the experiments in this thesis.

1.3.1 Glycolytic metabolism

Vascular smooth muscle is a very glycolytic tissue and has a relatively high basal rate of lactate production. As much as 80 or 90% of the glucose taken up by vascular smooth muscle is metabolised to lactate, the remainder recovered as CO_2[41]. This was determined using ^{14}C labelled glucose as a substrate in the solution bathing the muscle and monitoring the fate of the label. The wall of some arteries is rich in glycogen, but this is not generally reduced by more than 50% during physiological stimulation and is thought to act as a reserve for periods of high tension development under anaerobic conditions[156]. It has been reported that glycolytic metabolism mainly fuels membrane pumps, but is able to compensate for oxidative metabolism during sustained contraction or hypoxia[122, 219]. This was introduced in section 1.1.4.

1.3.2 Oxidative metabolism

Most of the ATP demand, up to 70%, in smooth muscle has been reported to be met by oxidative metabolism. Conversely, it has been calculated that 80% of oxygen consumption in smooth muscle is to meet contractile energy demands[44]. Oxygen consumption in smooth muscle, as in most tissues, occurs in the mitochondria through

oxidative phosphorylation producing ATP. The way in which this energy is utilised was introduced in 1.1.4 and is presented in the next section.

1.3.3 Coupling of energy metabolism to contractile function

The experiments that were performed to elucidate the compartmentation of smooth muscle metabolism are presented in section 1.1.4. The theory that oxygen consumption is coupled to contractile activity is further confirmed by studies examining the link between oxygen consumption and phosphorylation of MLC_{20}. Phosphorylation of MLC_{20}[38] and therefore tension correlates linearly with oxygen consumption[307] in the initial stimulation of tension. During tension maintenance, the rate of oxygen consumption drops off due to the economical latch mechanism employed in smooth muscle, as do levels of MLC_{20} phosphorylation. During active tension generation, the coupling of oxygen consumption to contractile function is thought to be so tight that oxygen consumption can be used to estimate levels of contractile activity[307]. This means that substances that induce tension in smooth muscle should also stimulate oxygen consumption and this is often the case.

The tight coupling of oxygen consumption to tension generation forms the basis of the investigations presented in this thesis. To further support this putative coupling of energy production to utilisation, it has been reported that PCr (phosphocreatine) and ATP are not at equilibrium in smooth muscle[122, 124]. This phenomenon was first reported by Born[31]. Ishida and Paul[122] measured the ATP and PCr content of guinea pig taenia coli under various conditions. They found that the tissue contained 1.5 μ mol/g ATP and 2.5 μ mol/g PCr under aerobic conditions exposed to 45.4mM potassium chloride. During hypoxia (substitution of N_2 for O_2), the PCr concentration fell to 10% of control, correlating with the drop in tension. After the tissue had reached a steady tension around 10% of control, ATP began to decrease until it was 50% of the pre-hypoxic concentration. Upon addition of supraphysiological concentrations of glucose (55mM) to the hypoxic tissue, the ATP content recovered to 80% of control and the tension increased to 40% of

control. PCr content did not significantly rise. If, instead of glucose addition, re-oxygenation was carried out, different results were observed. PCr was seen to increase rapidly, recovering to control levels within 5 minutes of re-oxygenation, and actually overshooting the control concentration. ATP concentration was restored to control levels after 5 minutes of re-oxygenation. They also found that total phosphagen levels did not correlate with tension in the taenia.

The disruption of the creatine kinase equilibrium could have occurred in several ways: lowered pH due to lactate accumulation during hypoxia; loss of adenylate or creatine; impaired creatine kinase activity and compartmentation of phosphagens. The authors determined that the change in pH that would occur in their system would not account for such a difference in recovery of phosphagens after hypoxia by the two methods described[122]. Although adenylate loss (estimated at 30%) may account for the left shift in the relationship between PCr and ATP after re-oxygenation, however, it does not account for the recovery of ATP concentrations without significant change in PCr when glucose was added to the hypoxic tissue. The creatine concentration appears to be sufficient as PCr concentration recovers after re-oxygenation. Creatine kinase (mitochondrial CK) activity was found to be at or above control levels at 1000 μ mol/min/mg mitochondrial protein, thus making the possibility of insufficient CK activity unlikely.

The authors came to the conclusion that phosphagens in smooth muscle are compartmentalised. They postulate that there may be a pool of ATP not accessible to contractile proteins and also an ATP pool not accessible to CK based on the results described above. A system of PCr shuttles is proposed, whereby mitochondrial CK converts ATP to PCr, with the products being ADP and a proton that may stimulate further ATP production at the mitochondria. This PCr is then converted to ATP by cytoplasmic CK (MB isozyme in smooth muscle[42]) thus absorbing the proton produced by cytoplasmic ATP hydrolysis and maintaining cytosolic pH even during substantial ATP hydrolysis under aerobic conditions.

1.4 Vascular smooth muscle contraction

The events occurring during contraction of smooth muscle appear simple in themselves, although they are not yet fully elucidated. Vascular smooth muscle contains a number of different contractile proteins. Calcium binding, or calcium-activated covalent modification, usually phosphorylation-dephosphorylation events control many of these. Unlike skeletal muscle, which is thin filament regulated, smooth muscle is controlled at the thick filaments via the phosphorylation by a calcium-dependent protein kinase at a particular site on the MLC_{20} regulatory subunit[56]. The next few pages discuss this control mechanism and the other components that affect smooth muscle contractile function.

1.4.1 Components of the contractile cycle

The sliding of myosin over actin generates tension. In smooth muscle this is accompanied by calcium regulated ATP hydrolysis by myosin and myosin phosphorylation by myosin light chain kinase (MLCK). The main contractile work of smooth muscle involves thick filaments and thin filaments[93, 182, 290]. The thin filaments contain actin and several regulatory proteins, as described in table 1.1, include calcium-binding proteins. The thick filaments comprise one pair of myosin heavy chains (MHC) which have an intrinsic ATPase activity and two pairs of so called light chains, a pair of essential light chains (17kDa known as MLC_{17}) and a pair of regulatory light chains (20kDa known as MLC_{20}). It is the latter light chains that are phosphorylated at a specific site and modulate the activity of the ATPase in the MHC. Table 1.1 lists the components of the contractile cycle. The dependence upon calcium and phosphorylation are given, along with the mediator of that response. That is, a plus sign (+) next to MLC_{20} under calcium indicates that calcium leads to contraction when acting on the MLC_{20}. A minus sign (-) would indicate no contraction, or relaxation.

Table 1.1: Calcium and phosphorylation control of contractile cycle components.

Component	Ca^{2+}	mediated by	phosphorylation	mediated by
MLCK	+	Calmodulin	–	CaCaMKII
MLCP	–	MLCK:MLCP ratio	+	PKC?
MLC_{20}	+	MLCK (CaCaM)	+	MLCK
MLC_{20}	–	DAG/IP_3	–	PKC
Caldesmon	+	CaM + Caltropin inhibit	+	CaCaMKII + MAPK
Calponin	+	DAG/IP_3 + CaM	+	PKC + CaCaMKII
Calmodulin	+	Ca^{2+} + CaD inhibition	NA	NA
Caltropin	+	inhibits Caldesmon	NA	NA
Tropomyosin	+	CaD	+	inhibits CaD

Table 1.1. The effect of calcium and phosphorylation on some components of the contractile cycle. A + sign next to a component indicates an effect of calcium/ phosphorylation leading to contraction. A – sign, conversely, indicates an effect leading to relaxation or inhibition of contraction. Where an effect is mediated by another molecule, this intermediate is listed in the column headed "mediated by". Where a component is not phosphorylated, and therefore there is no intermediate molecule, NA (not applicable) is placed in the relevant column.

The components listed in Table 1.1 all have specific effects on the contractile cycle of smooth muscle and the components pertinent to this thesis are introduced in more detail below.

The contractile cycle of smooth muscle contains a number of steps that form the cross bridge cycle. This actomyosin ATPase cycle is summarised in Figure 1.1.

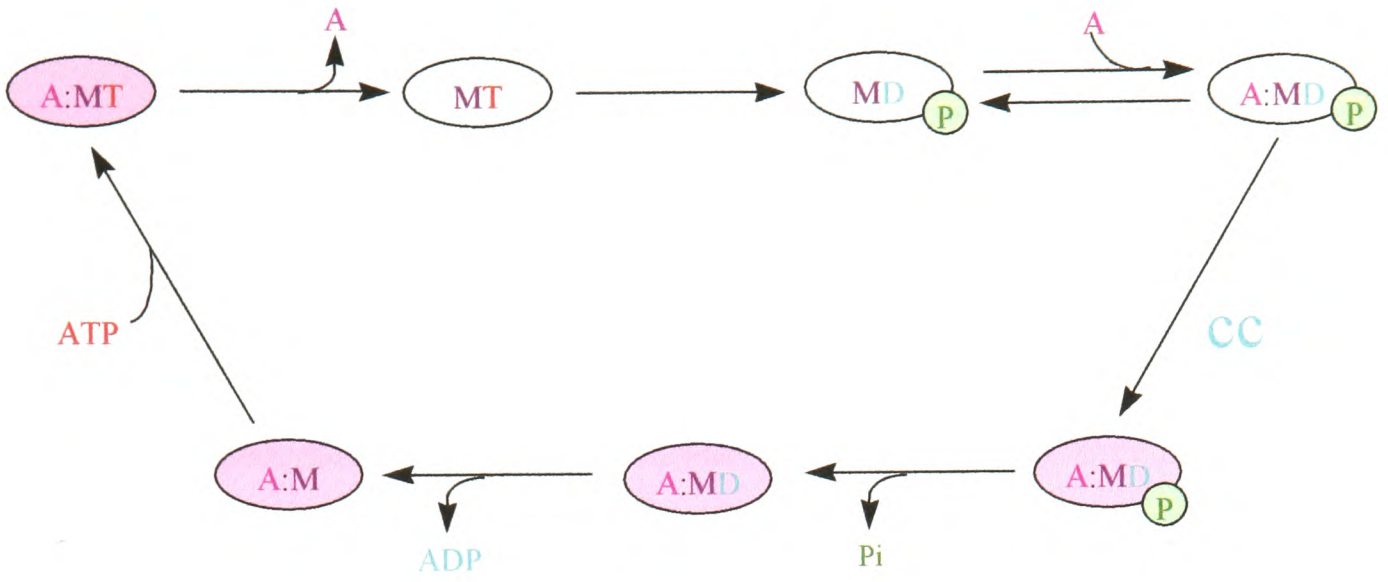

Figure 1.1 The Actomyosin ATPase cycle adapted from Biochemistry of Smooth Muscle Contraction[261]. MT, MD and MDP are myosin bound to ATP, ADP and ADP + P_i bound respectively; A is actin: A:M (x) is actin bound to myosin species; cc indicates a conformational change that may take place without change of substrates. The pink shaded states are those that are thought to be tightly bound, load bearing states[261].

Beginning with myosin bound to MgATP (MT), the cycle progresses as follows. The ATPase activity of the myosin head cleaves the ATP to ADP and P_i, which both remain bound to the myosin. In a reversible step, actin binds to myosin forming what is thought to be a non-load-bearing cross bridge. Cycling between these two states, with the concomitant hydrolysis of ATP by the myosin ATPase, is the tension-generating step in the cycle. It is then thought that a conformational change without loss of substrates to a more tightly bound cross bridge occurs[86, 182] and that this is the load-generating state. The inorganic phosphate is then removed by a phosphatase, leaving actin bound to myosin and MgADP. This is known as a latch bridge. It is now generally accepted that the latch bridge requires MgADP to be bound[259]. MgADP dissociates to form the nucleotide-free state. The area of Figure 1.1 that is shaded indicates the strongly bound states.

1.4.2 Tension generation

As described above, the cycling of cross bridges with the concomitant hydrolysis of MgATP enables the generation of tension in vascular smooth muscle. Unlike skeletal muscle, where the actomyosin ATPase is constitutively active, smooth muscle actomyosin ATPase must be activated before tension can be generated[183]. As mentioned briefly in

1.4.1, smooth muscle myosin consists of 2 pairs of light chains as well as the pair of heavy chains containing the MgATPase activity. It is the 20kDa regulatory light chains (MLC_{20}) that are phosphorylated in order to activate the MgATPase activity of myosin. The initiating step in generating tension in smooth muscle is the phosphorylation of MLC_{20} by myosin light chain kinase (MLCK). Under physiological conditions, MLCK phosphorylates serine 19 of the MLC_{20} in the following amino acid sequence *in vitro* [223] as well as in intact muscle[17, 48];

acetyl-ser[1]-ser-lys-arg-ala[5]-lys-ala-lys-thr-thr[10]-lys-lys-arg-pro-gln[15]-
arg-ala-thr[18]-ser[19]-asn[20]-val-phe-ala-....

If the MLCK concentration is raised to supraphysiological levels, threonine 18 may also be phosphorylated[119]. The significance of this threonine phosphorylation has yet to be determined. Protein kinase C also phosphorylates MLC_{20}, at serines 1 and 2 and threonine 9 which decreases the myosin MgATPase activity by half[197], although this has not been demonstrated *in vivo*. Activation of myosin then allows actin and myosin to associate and dissociate, with the concomitant hydrolysis of ATP and active tension results. The level of phosphorylation of MLC_{20} in a population of myosin light chains is proportional to the tension generated[6, 133, 137, 287] although there is controversy as to whether the phosphorylation of MLC_{20} is correlated to cross bridge cycling rates (as estimated from shortening velocity measurements) or not[250]. The increase in phosphorylation of the MLC_{20} appears to actually occur before tension development in response to an agonist[18, 61]. Hasegawa *et al*[94] reported that phosphorylation of the MLC_{20} elicited a conformational change in the myosin such that it is able to interact with actin and become active[37, 93, 209]. The nature of this conformational change is not yet resolved. If two successive stimulations are applied to smooth muscle, there is no increase in phosphorylation with the second stimulation, although tension is generated. This indicates that the first increase in MLC_{20} phosphorylation has performed the task of activating the actomyosin ATPase[22]

What of the enzyme that catalyses this reaction, myosin light chain kinase (MLCK)? MLCK depends upon on magnesium, calcium and calmodulin for its activity. MLCK exists in smooth muscle cells at a concentration of between 3-4 μM and that of its physiological substrate, MLC_{20}, ranges between 70 and 80 μM[92, 263]. MLCK is a calcium-calmodulin dependent protein kinase and there are two distinct gene products found in both skeletal and smooth muscle, the muscle and non-muscle forms of the enzyme. The muscle form of MLCK has a molecular weight of 165kDa and contains at has a calmodulin binding domain, allowing calcium regulation. The N terminus of the calmodulin-binding domain is a pseudosubstrate autoinhibitory region, forms of which are found on most protein kinases[145]. Paul and Ruegg[222] reported that there is an absolute requirement of MLCK for magnesium. They showed that magnesium-free solutions inhibit the enzyme. This is probably due to the requirement of MLCK (as of all protein kinases) for MgATP. MLCK is phosphorylated and inhibited by calcium-calmodulin dependent kinase 2 (CaCaMKII) and cAMP dependent protein kinase (PKA).

The thin filaments comprise actin, caldesmon, calponin and tropomyosin. Actin is the major protein found in the thin filaments of smooth muscle. *In vitro*, it exists in two forms; G-actin, which is monomeric and globular, and polymeric filamentous F-actin. The length of F-actin is varied and therefore a precise mass cannot be calculated, but G-actin has a molecular mass of 42kDa[93]. *In vivo,* the predominant form is the F actin, which polymerises in an ATP dependent manner and forms the structural basis of the thin filaments.

There is thin filament regulation of smooth muscle contraction mediated by a number of proteins that are controlled by phosphorylation events and calcium binding. As several agents have been found to elicit contraction without phosphorylation of the myosin light chains[305], it has been postulated that there is a significant involvement of the thin filaments of smooth muscle[305].

Caldesmon is able to bind to filamentous actin, tropomyosin, myosin and calcium-calmodulin (Ca^{2+}CaM)[111]. If tropomyosin is absent, the binding of caldesmon to actin is very weak and so it is likely that caldesmon mainly binds to tropomyosin containing thin filaments *in vivo*. Caldesmon acts as an inhibitor of actin-myosin interaction by reducing the affinity of actin for myosin and this inhibition is relieved by the Ca^{2+}CaMKII phosphorylation of caldesmon and the direct binding of Ca^{2+}CaM at the carboxyl terminal of caldesmon[101, 109]. In summary, caldesmon is able to reduce the affinity of myosin for actin without slowing cross bridge cycling rate. It is phosphorylated and inactivated by Ca^{2+}CaMKII and also inhibited by the direct binding of Ca^{2+}CaM[101, 109, 111].

Calponin, another thin filament protein, also binds to F-actin[268] and inhibits the myosin ATPase[304]. It appears to inhibit the ATPase activity of myosin heads bound to actin by competitive inhibition with myosin[173]. Unlike caldesmon, inhibition by calponin decreases the V_{max} of cross bridge cycling[196], not the affinity of actin for myosin and tropomyosin does not affect the affinity of calponin for actin[304]. Calponin does not appear to be regulated *in vivo* by direct binding with calcium, although *in vitro* calponin binds to caltropin, calmodulin and calcium only at high ratios[73, 302]. It is phosphorylated and inactivated (thus allowing contraction) by CaCaMKII[304] and PKC[186]. Dephosphorylation (and restoration of its inhibitory activity) of calponin is thought to be mediated by a type 2 protein phosphatase[303]. The effects and control of calponin are not as well substantiated as those of caldesmon. Several of the control mechanisms described here have been refuted by some groups, or may not occur *in vivo*[4, 20]. The actual *in vivo* activity of calponin, therefore, is not fully understood.

1.4.2.1 Summary of tension generation

Tension generation in smooth muscle is initiated by the CaCaM-dependent phosphorylation of the MLC_{20} by MLCK. This activates the myosin MgATPase activity of the myosin head and allows active contraction by interaction with actin with concomitant

ATP utilisation. The thin filament proteins caldesmon and calponin modulate this interaction, which decreases myosin affinity for actin and rate of actin and myosin interaction respectively. MLCK, caldesmon and calponin are all phosphorylated and inhibited by Ca^{2+}CaMKII.

1.4.3 Tension maintenance

Vascular smooth muscle is unique in that it is able to maintain tension for long periods of time with little ATP consumption[233]. This is achieved by the ability of smooth muscle cross bridges to enter what is known as the "latch state"[56, 86]. This is essential to the function of vascular smooth muscle, which is to maintain blood pressure and vascular tone over long periods. It is thought that the state of the cross bridges during this sustained tension maintenance is attached, dephosphorylated cross bridges with Mg^{2+}ADP bound, termed "latch bridges". These latch bridges are very slowly cycling, allowing tension maintenance at high economy, as the ATP consumption has been shown to be 300 times lower than that of skeletal muscle when maintaining tension[182]. The latch state is characterised by moderate to basal phosphorylation of the MLC_{20} with high force, reduced ATP consumption and reduced contraction rates[185]. There may also be increased responsiveness to calcium[63]. In order for tissue to be able to enter the latch state, there must be normal activity of MLCP and decreased intracellular calcium, as seen after stimulation with histamine[22]. After the initial influx of calcium, if the histamine is still present, the calcium concentration falls below the level at which it can stimulate MLCK, the latch state results and Mg^{2+}ADP may play a role as a determinant of the latch state[198]. If, as proposed by Nishiye *et al*[198], Mg^{2+}ADP were required to be bound to the AM complex for latch bridges to maintain tension, increased Mg^{2+}ADP concentrations in the smooth muscle cells would stabilise the latch state. It has also been suggested that increased MLCP activity may be responsible for the latch state, but the evidence for this is based on a mathematical model[60].

1.4.4 Smooth muscle relaxation

Dephosphorylation of the MLC_{20} by myosin light chain phosphatase is associated with smooth muscle relaxation. Haeberle *et al*[85] showed that relaxation was associated with a significant, but not complete dephosphorylation in skinned fibres and studies in intact muscle also show this relationship[93]. When the rates of dephosphorylation were examined along with the rates of relaxation, the rates were found to vary up to 5 fold at room temperature, even within the same laboratory[93]. This variation is more than can be explained by the high temperature dependence of myosin light chain kinase[175], showing that more controlled studies are required to examine this relationship. Magnesium is not thought to influence the activity of myosin light chain phosphatase[222], although there exists in smooth muscle a magnesium-activated protein phosphatase, PP2C. It is perhaps possible that if such a phosphatase were able to dephosphorylate myosin, raised magnesium concentrations may induce formation of latch bridges and promote relaxation.

The enzyme responsible for the dephosphorylation of MLC_{20} is myosin light chain phosphatase. It is the balance between this and myosin light chain kinase that determines whether the tissue is relaxed or contracting[70]. The nature and even the type of phosphatase involved in the contractile cycle have not been fully characterised.

Serine/ threonine Phosphatases can be classified according to the composition of the holoenzyme and the specificity of the targeting subunits. Type 1 protein phosphatases (PP1) consist of a 37 kDa catalytic subunit (PP1C) which assembles with one of a number of various targeting subunits including a glycogen targeting subunit, inhibitor 1 and inhibitor 2. In smooth muscle, the PP1 holoenzyme has been found to comprise the 37 kDa catalytic core associated with two targeting M subunits[23]. These M subunits have been found to be 110 and 20 kDa in size and have been found to enhance the dephosphorylation of myosin by approximately 13-fold[58]. Glycogen phosphorylase kinase β subunit is dephosphorylated by a PP1. Type 2 phosphatases are further divided into PP2A, PP2B and PP2C. PP1, PP2A and PP2B are all from the same gene family, with PP2C coming from a

different gene. PP2A comprises the core assembly of PP2Ac (catalytic subunit) and a 65kDa A subunit and one of a number of regulatory B subunits including several T antigens. Glycogen phosphorylase kinase α subunit is dephosphorylated by a PP2A. PP2B (also known as calcineurin) is calcium dependent. The A subunit has an amino terminal catalytic site, a binding site for calcium-calmodulin and the regulatory B subunit and a carboxyl terminal autoregulatory site. PP2C dephosphorylates autophosphorylated Ca^{2+}CaM kinase II in brain and may be involved in osmoregulation[296]. It is Mg^{2+}-activated, but the mechanism by which this is effected is not yet known. Further discussion of phosphatases in smooth muscle can be found in Chapters 6 and 7.

A trimeric enzyme with 130, 38 and 20 kDa subunits (suggesting a PP2A[151]) has been identified in pig bladder[249] chicken gizzard[7, 247] and turkey gizzard[215, 258]. It is now the consensus of opinion that myosin light chain phosphatase is a type 1 protein phosphatase[7, 77, 174, 199] although confusion still exists, as some groups have found it to be a type 2A phosphatase[59, 297]. When gizzard actomyosin was isolated, it was found that the major phosphatase associated with it is type 1[127]. Phosphatases purified from the cytosolic fraction, however, are predominately type 2A phosphatases[59]. The variety of subunits found by various researchers may be due to the existence of targeting subunits. Phosphoprotein phosphatases often vary only in the targeting subunit that is associated with the core enzyme. Just as there are many kinases which are very specific for particular substrates, there are also a number of phosphatases characterised to date from the same gene[47] and there is evidence to support the existence of interchangeable subunits that allow greater specificity[7, 247, 249].

Another type 2 phosphatase, protein phosphatase 2C, has been found to be able to dephosphorylate phosphorylated myosin light chains at least *in vitro*. It is independent of calcium but dependent upon magnesium for its activity. Protein phosphatase 2C is a monomeric 43-48kDa enzyme[214] existing as two isoforms, PP2Cα and β. These isoforms are products of separate genes[277].

Protein phosphatase 2C was at first classified as smooth muscle phosphatase 2. These were shown to be one and the same[214] by examining substrate specificity, its insensitivity to inhibitor-1 and inhibitor-2 and the fact that the enzyme has an absolute requirement for Mg^{2+} for its phosphatase activity[204]. It is a cytosolic enzyme[45].

The substrates known to be dephosphorylated by PP2C include glycogen synthase (sites 1a and 2), pyruvate kinase, ATP citrate lyase, acetyl CoA carboxylase, HMG CoA reductase and its kinase, histone H2B and most importantly phosphorylated myosin light chains in smooth muscle[45, 75, 120]. Its role in smooth muscle contraction has not yet been elucidated.

It was, at first, found that supraphysiological [Mg^{2+}] (3mM) was required to achieve half maximal activation of PP2C towards hormone sensitive lipase *in vitro*[204]. A role for arachidonic acid was then discovered. The presence of arachidonic acid reduced the activation concentration of Mg^{2+} to 1mM, around physiological concentration[142]. It has been found to be essentially insensitive to okadaic acid[75].

Recently, a mechanism to control myosin light chain phosphatase has been postulated[115]. They report a phosphorylation and inhibition of the myosin-bound phosphatase in smooth muscle. The trimeric holoenzyme appears to dissociate when the 130kDa subunit is phosphorylated, thus abolishing phosphatase activity. The kinase responsible has not been determined, although the authors suggest a possible role for PKC, as the reaction was chelerythrine sensitive and a PKC specific amino acid sequence being the site of phosphorylation, even though the reaction was phorbol ester and phospholipid insensitive. These experiments were, however, performed on isolated, purified systems and the authors postulate the role of artifactual involvement.

1.5 Vasospasm

Vasospasm can occur in a number of vascular beds. It occurs in the coronary arteries, as well as the mesenteric arteries and a number of other vessels but by far the most frequently researched form of vasospasm is that which occurs in the cerebral vessels after subarachnoid haemorrhage[38, 49, 71, 158, 160, 245, 283, 320].

1.5.1 Subarachnoid haemorrhage

A ruptured vessel due to trauma or aneurysm results in leakage of blood into the space between the brain and the layer of cells that line the pia mater, the arachnoid cells. This space, known as the subarachnoid space, has cerebral spinal fluid within it, the sterile, salt and protein containing liquid that is continuously produced in the ventricles of the brain and buffers the brain. Blood mixes with this CSF and undergoes the normal process of clotting and degradation, unless removed. This type of cerebrovascular accident, known as aneurysmal subarachnoid haemorrhage afflicts 6-16 people in every 100,000 worldwide[53] with the highest rates reported in Finland and Japan[141, 237]. Men aged between 75 and 84 years are most at risk and the initial bleeding results in the death of 50-70% of those affected. Cerebral vasospasm, severe, chronic, contraction of the cerebral vessels in the area of the blood clot, occurs in around 50% of the subarachnoid haemorrhage patients that survive the initial insult[167]. The diagnosis and risk factors, *in vivo* models and putative ætiology are the subject of this section.

1.5.2 Risk factors and diagnosis of cerebral vasospasm

Cerebral vasospasm does not manifest as a clear-cut set of clinical signs. A number of factors must be taken into account in order to assess a patient and make a diagnosis. The Fisher grading system[71] is based on the volume of blood that has entered the CSF as assessed by CT scan on admission. The higher the grade (out of 5) the more blood is present. Patients with a Fisher grade of 4 or 5 are considered to be at risk. Another grading system derived from the Glasgow Coma Scale called the WFNS (World Federation of

Neurological Surgeons) grade is used to assess neurological deficit in the patients. It is graded 1 to 5, each grade representing a range of the Glasgow Coma Scale, with 5 being comatose and 1 being practically normal. Patients with a grade 3 or above are considered to be at risk of developing spasm. Magnetic resonance imaging allows us to non-invasively assess the cerebral blood flow, areas of low perfusion indicating significant risk and cerebral arterial narrowing on angiography being a very good indicator of impending vasospasm. Hypertension, family history of stroke, polycystic kidney disease and connective tissue disorders are also risk factors[113].

The results of vasospasm can be severe debilitation and death. Patients who may have appeared to begin to recover from the stroke may suddenly decline in neurological function. The vasospasm may significantly impair recovery, or even lead to further strokes. When this occurs, the chances of recovery are significantly reduced. Current therapy for the treatment of vasospasm involves administration of Nimodipine (Bayer®) to the patients directly after admission by way of a prophylactic. This and other therapies will be introduced in section 1.5.3.

1.5.3 Current theories on the ætiology of vasospasm

There are some unique characteristics of the spasm seen in this pathology which may be indicative of the pathological mechanisms involved. It does not begin to develop until several days after the subarachnoid haemorrhage[294]. It is a chronic spasm and is essentially irreversible, in that it does not respond to a variety of therapeutic strategies[283]. There have been a number of compounds that have reached clinical trials and a brief description of these and the results is presented here.

Table 1.2: intervention studies.

Agent	Action	Trial	Outcome	Reference
Nimodipine	Ca^{2+} channel blocker	open, human	ineffective for spasm	15, 34, 82, 91, 153, 224,

				242, 309
Nimodipine	Ca^{2+} channel blocker	open, human	reduced spasm	30, 81, 241
Nimodipine	Ca^{2+} channel blocker	double blind, human	ineffective for spasm	8, 78, 193, 200
HA 1077	Ca^{2+} antagonist	Rat: spontaneous tone	dilated cerebral vessels	273
HA 1004	Ca^{2+} antagonist	Rat, A23187 induced spasm	reversed spasm	274
Nicardipine, Diltiazem, Verapamil	Ca^{2+} channel blockers	Rat, A23187 induced spasm	reversed spasm	274
Tirilazad Mesylate and U74389G	Lipid peroxidation inhibitor	Double haemorrhage, dog	Prevention, not reversal	157, 162
Nicaraven	hydroxyl radical scavenger	placebo controlled, double blind, human	improved neurological outcome	11
Disulfiram, n-butyl picolinamide	Dopamine β-hydroxylase inhibitors	Breach of basilar artery, cat	prevents spasm	27
E5880	Platelet activating factor inhibitor	Double haemorrhage, rabbit	Ineffective on spasm	105
ML-9	Myosin light chain kinase inhibitor	Double haemorrhage, dog	Ineffective on spasm	143
Nicorandil	Raises cGMP	Double haemorrhage	Ameliorated spasm	164

Magnesium sulphate	Ca^{2+} antagonist	Randomised, double blind, human	Inconclusive, no side effects	179
AT877	Ca^{2+} antagonist	Randomised placebo controlled, double blind, human	Reduced spasm on angiography	244
Bosentan, PD155080	ETA and ETB antagonist	Double haemorrhage, dog	Reduced spasm	245, 320
Aminophylline, nifedipine, papaverine.	Phosphodiesterase inhibitor, Ca^{2+} antagonist	Double haemorrhage	Ineffective	283
Histidine	Oxygen radical scavenger	Single haemorrhage, rabbit	Prevented spasm when added before SAH (!)	69

Table 1.2. A summary of the numerous clinical trials with their outcomes. Trial column indicates the nature of the patient-researcher interaction. Open indicates that all the patients are taking the drugs. Double blind indicates that neither side knew (until after the study) who was on the drug and who on the placebo and placebo controlled is open but with placebo controls. The patients are never aware of what they are taking to eliminate psychosomatic effects. Where animal studies are quoted, the type of model used is indicated.

The significance of the outcome of some of these studies is discussed in further detail in 3.1.1 and 7.1.1. These intervention studies provide insight into the putative mechanism of vasospasm and particularly the involvement of calcium movements in this pathology.

1.5.4 Possible ætiology of vasospasm

1.5.4.1 Energy metabolism changes

The metabolic changes seen in the vessels during cerebral vasospasm after subarachnoid haemorrhage are not well documented compared to the contractile changes[138, 313]. Kim *et al*[138] reported that levels of high energy phosphates (ATP, GTP and phosphocreatine) were significantly reduced and that ratios of ATP:ADP, GTP:GDP and PCr:tCr (phosphocreatine: total creatine) were also very much reduced. This kind of metabolic perturbance was also reported in another paper by the same group a year later[313]. They describe a loss of total adenylate fuel and postulate that this is a metabolic failure. The metabolic changes were observed before the angiographically visible onset of vasospasm.

Takai and co-workers assign the decrease in guanosine phosphates to the production of cGMP, which is an essential part of the nitric oxide signalling pathway for the relaxation of smooth muscle[116]. Nitric oxide, at levels of less than 1μM, selectively activates soluble guanylate cyclase, which in turn raises intracellular cGMP concentrations. cGMP activates PKG and ion channels. The exact mechanism by which cGMP elicits relaxation is not known, but one theory is that PKG inhibits phospholipase C, thus decreasing the IP_3 induced elevation of calcium and PKG also phosphorylates and inhibits calcium channels[271].

1.5.4.2 Postulated mechanisms

There are many papers that postulate the involvement of breakdown products of blood in the ætiology of cerebral vasospasm[33, 35, 106, 139, 152, 293]. Many researchers have studied these breakdown products, some looking at individual components, others approaching it by investigating which signalling pathways are activated[38, 49, 165, 248, 291, 293, 310, 316].

What characterises the contraction of cerebral vessels in vasospasm? Many authors agree that there is an increase in intracellular calcium concentration during vasospasm and presume this is the reason for the vessel contraction[38, 139, 164, 165, 187, 201, 248, 312]. This rise in intracellular calcium has been attributed to a number of causes, some of which are introduced below.

The protein kinase C family (currently) consists of 13 classified isoenzymes. These can be characterised according to their sensitivity to calcium, diacyl glycerol, phospholipids and their specificity[171]. The classical isoenzymes (cPKC's) comprise the α, βI, βII and γ protein kinases (βI and βII products of alternative splicing). These isoenzymes are activated by phosphatidylserine in a calcium dependent manner and also bind diacyl glycerol, which increases their affinity for Ca^{2+} so that physiological concentrations of calcium can activate them[272]. The novel (nPKC's) PKC isotypes consist of the η, ε, δ and θ isoenzymes. These are insensitive to calcium, but are activated by phorbol esters or diacyl glycerol in the presence of phosphatidylserine[206]. The atypical PKCs (aPKC) are the ι and ζ isoenzymes. These are neither calcium nor diacyl glycerol/ phorbol ester sensitive[207]. The fourth and final recently described group is the PRK isoenzymes comprising PRK 1, 2 and 3. Their specificity remains to be elucidated[180].

Smooth muscle has been found to contain several of these isoenzymes. PKC isoenzymes α and δ have been found in all smooth muscles examined, and ε and ζ are found in most. βII was extracted from porcine carotid artery, and one group found η in the rat aorta, but this is likely to be endothelial contamination, as η is thought to be endothelial cell-specific[252].

Activation of protein kinase C has been frequently implicated in vasospasm[165, 187, 201, 248, 293, 312]. The ε isoenzyme has often been postulated as being involved in the ætiology of vasospasm[112, 298]. The mechanism most frequently proposed for the vasospasm is that of a slow, accumulation of DAG in the smooth muscle cells resulting in a prolonged

activation of PKCε[165, 201, 312]. This mechanism is described in more detail in chapters 4 (4.1.1.3 and figure 4.1) and 7 (7.1.5).

It is known that there are at least two separate kinds of PKC-induced tension in vascular smooth muscle[289]. The mechanism mediated by phospholipase C occurs thus. An agonist, such as an α_1-adrenergic receptor agonist like noradrenaline binds to the α_1-adrenergic receptor extracellularly. A conformational change through the membrane enables activation of phospholipase C by a stimulatory G protein. This enzyme cleaves phosphatidyl inositol in the membrane to diacyl glycerol and IP_3. IP_3 opens ligand (IP_3) gated calcium channels in the sarcoplasmic reticulum, eliciting a rise in intracellular calcium concentration. This, along with DAG, activates PKCα, which phosphorylates and inactivates caldesmon (and calponin), allowing tension development as previously introduced. Upon sustained activation of PKC, however, a different PKC isoenzyme is stimulated[289]. It is likely that this is PKCε, which is stimulated by DAG but does not require calcium and has been shown to translocate to the plasma membrane in response to sustained stimulation of contraction[289]. PKCε activation is mediated by PLD, which cleaves phosphatidylcholine to give phosphatidic acid (PA) and choline. PA is then able to be cleaved by phosphatidic acid phosphohydrolase to diacyl glycerol. Interestingly, this DAG is different in fatty acid composition than the DAG from PIP_2 or PIP_3 breakdown. It is postulated that this may change the affinity of DAG kinase, responsible for the breakdown of this molecule and therefore increase the half-life of DAG[289]. Possible mechanisms for the induction of this isoenzyme are discussed in Chapter 7 (7.1.5).

A number of researchers believe that endothelin 1 is the molecule responsible for delayed vasospasm and some have shown that endothelin concentrations in the patients are elevated after subarachnoid haemorrhage[144, 240]. Endothelin 1 is produced as a result of the cleavage of big endothelin by endothelin converting enzyme[311]. Big endothelin is in turn produced by the cleavage of preproendothelin in vascular endothelial cells[311] amongst

others. The production of preproendothelin is stimulated by agonists which increase intracellular calcium[311]. Endothelin 1 has also been linked to coronary vasospasm[148].

The mechanism of action of endothelin has been characterised using a variety of investigations[5, 40, 117, 264, 288, 299]. The stimulation of contraction of the vessels in response to endothelin 1 has been shown to be both calcium dependent and calcium independent. This latter response is unaffected by H1-histamine, serotonin, cyclooxygenase, lipooxygenase and α_1 adrenergic receptor[311]. This suggests that an increase in intracellular calcium concentration is not mediated through phospholipase C, but rather through ligand gated calcium channels. In human cerebral vessels, endothelin A (ETA), but not ETB receptors are found[225]. The two distinctly localised receptor subtypes may account for the calcium independent and calcium dependent actions of endothelin 1. It has been further clarified that endothelin 1 binding to ETA receptors activates the G-protein mediated activation of phospholipase C, which forms diacyl glycerol (DAG) and inositol trisphosphate (IP_3). IP_3 releases intracellular Ca^{2+} stores and diacyl glycerol activates protein kinase C, which may phosphorylate and activate chloride channels[117]. As chloride leaves the cell, the membrane depolarises and voltage dependent calcium channels open further elevating intracellular calcium concentrations. This is one interpretation of how endothelin may cause contraction. It is also postulated that endothelin-1 receptors are coupled to chloride channels. Receptor binding of ET-1 activates and opens the channels, allowing the efflux of Cl^- (down the voltage gradient). This results in depolarization of the cell membrane, opening of voltage dependant Ca^{2+} channels and increased intracellular Ca^{2+} concentrations. This is a rapid Ca^{2+} influx, which leads to smooth muscle contraction and PKC activation. This has been observed in several arterial myocytes[16, 236]

The involvement of endothelin in cerebral vasospasm is by no means undisputed[228]. The issue of receptor tissue and animal specificity and the use of endothelin antagonists are discussed in Chapter 7.

1.5.4.3 Phosphorylation events in vasospasm

Two groups have estimated myosin light chain phosphorylation in models of cerebral vasospasm. Harada *et al*[90] used a rat femoral artery model of vasospasm to investigate the time course of MLC_{20} phosphorylation after application of blood. They found a significant increase in MLC_{20} phosphorylation, which then declined suddenly at day 7 after the blood exposure. This puzzling finding was shown to be due to a similar decline in the concentration of MLC_{20} in the vessels. The authors are uncertain as to the cause of both the elevated phosphorylation and the loss of protein in their model. Butler *et al*[38] used the double haemorrhage model in the dog and reported similar results. They report a very significant increase in MLC_{20} phosphorylation in vasospastic tissue but do not attempt to explain the reasons for this. The phosphorylation of MLC_{20} is discussed in more detail in Chapters 6 and 7 (7.1.3, 7.1.4 and 6.1).

1.6 Aims

The purpose of the research presented in this thesis is to determine the changes in oxidative metabolism and contractile function that occur in vascular smooth muscle during cerebral vasospasm after subarachnoid haemorrhage as induced in this model, using the porcine carotid artery and cerebrospinal fluid from vasospastic patients. In order to achieve this, I will describe and validate an *in vitro* model of cerebral vasospasm and then use this model to investigate the biochemical changes occurring in the vascular smooth muscle. The oxygen utilisation and contractile function of the porcine carotid artery will allow illustration of the functional impact of this pathology and enable characterisation of the phenomenon using a number of pharmacological and biological agents to elucidate a putative mechanism for this type of vasospasm.

The thesis is divided into several sections. Chapter two gives the methods used to obtain the data presented in this thesis. Chapter three introduces and validates the *in vitro* model of vasospasm developed for the investigation of the pathology in question and also

describes the efforts made to extract or purify the vasoactive component of the vasospastic cerebrospinal fluid. Chapters four, five and six contain experimental data obtained using the model introduced in Chapter three and other methods which characterises the stimulation of O_2 consumption and tension generation in the porcine carotid artery. Chapter five deals specifically with the effect of magnesium on these observations and Chapter six presents experiments determining the involvement of phosphatases in the pathology. These results are discussed as an overall picture in the discussion, Chapter seven.

1.7 Hypotheses

A number of hypotheses guided this research. These being:

- the spasm seen in cerebral vasospasm after subarachnoid haemorrhage is *a pathological failure of the smooth muscle to relax*, coupled to a physiological vasoconstriction

- this failure to relax involves inhibition of myosin light chain phosphatase resulting in increased MLC_{20} phosphorylation

- A factor in the CSF of these patients causes the observed cerebral vasospasm.

2.Materials and Methods

2.1 Introduction

A number of experimental techniques were used to obtain the data presented in this thesis. The majority of these were established and well-documented techniques. A few techniques were developed to investigate phenomena.

Tension generation in isolated vascular preparations has long been used to gauge whether a patient's CSF is vasospastic or not[33, 35, 114]. This method was compared in this thesis with stimulation of O_2 consumption in the porcine carotid artery. A fuller discussion of the comparison of these methods can be found in Chapter 3.

Porcine carotid arteries were chosen as the experimental tissue due to several characteristics. (i) The Large White pig has a similar body mass to a human; (ii) the porcine carotid artery is subject to approximately the same blood pressure as a human basilar artery and (iii) the tissue is readily available, easy to obtain and robust, remaining viable with sufficient substrate for up to 72 hours[29, 102].

2.2 Materials

2.2.1 Equipment

Instrument	*Supplier*
Centrifuge MSE Centaur 2E *Rotor MS43124-1263*	MSE (Fisons), Crawley, Sussex, UK. Tel. +44 1293 531 100
Chart recorders *Model 80300-10*	Kipp and Zonen supplied by ISC Laboratories: http:\\www.iscpubs.com

Constant temperature circulator. *Model TD*	Grant Instruments, Cambridge, CB2 5QZ Tel. +44 1763 60811
Electrophoresis Cell *X-Cell II*	Novex, Brüningstraße 50, Gebäude 0584, Frankfurt 65429, Germany. Tel +49 69 3058 2100
Force transducers *Model A49588*	Harvard Apparatus Inc. 84, October Hill Rd., Holliston, Mass. 01746 USA. Tel +1 800 272 2775
Freeze Dryer *Modulyo EF4*	Edwards Instruments, High Canons, Well End, Borehamwood, Herts. WD6 5PL Tel. +44 181 207 5044
Homogeniser *Polytron Kinematica*	Polytron Devices Inc. PO Box 398, Paterson, New Jersey, USA. 07544 Tel +1 973 345 5885
ModelMaker software *Version 3.0.*	Cherwell Scientific Publishing Ltd., The Magdalen Centre, Oxford Science Park, Oxford. Oxon. UK. OX4 4JA Tel. +44 1865 784 800
Oxygen monitoring software *Version 1.11*	Hansatech Instruments Ltd. Narborough Rd, Pentney, Kings Lynn, Norfolk, UK. PE32 1JL UK. Tel. +44 1760 338877
Oxygen monitoring system	Yellow Springs Instruments Inc.

Probe 05520-13	Lynchford House, Lynchford
Monitor 05520-34	Lane, Farnborough, Hampshire.
	UK. Tel. +44 1252 514 711
Picolog software	Pico Technology Ltd.
version 4.04	149-151 St. Neot's Rd,
	Hardwick, Camb. UK. CB3 7QJ
	Tel. +44 1954 211 716
Scintillation counter	Beckman Instruments Inc.
Model LS 1701	Viewfield Rd., Viewfield
	Industrial Estate, Glenrothes,
	Fife. KYE 2RD Scotland.
	Tel. +44 1592 771 234
Spectrophotometer	Beckman Instruments Inc.
Model DU7500	as above.
Water deioniser	Millipore (UK) Ltd.
Model Milli-RX	The Boulevard, Blackmoor Lane,
	Watford, Herts. WD1 8YW
	Tel. +44 1923 816 375

2.2.2 Chemicals

Substance	*Supplier*
MOPS/ MES/ Sample buffer (SDS PAGE)	Novex, *Ibid.*
γ-^{32}P labelled ATP	Nycomed-Amersham, Amersham
99.9% γ-^{32}P	Place, Little Chalfont,
	Amersham, Bucks. HP7 9NA
	UK. Tel. +44 1494 544 000
Bio-Rad Dye reagent concentrate	Bio-Rad Laboratories Ltd.
	Bio-Rad House, Marylands Ave.,

	Hemel Hempstead, Herts. UK. HP2 7TD Tel +44 181 328 2000
Calmodulin *Bovine Brain*	Calbiochem-Novabiochem (UK) Ltd. Boulevard Industrial Park, Padge Rd, Beeston, Nottingham. UK. NG9 2JR Tel. +44 1159 430 840
Cholesterol Esterase *Pseudomonas fluorescens*	Boehringer Mannheim & Roche, F. Hoffmann La Roche Ltd. Diagnostics Division, CH-4070, Basel, Switzerland. Fax. +41 61 699 3030
Endothelin-1 *Porcine*	Alexis Corporation (UK) Ltd. 3, Moorbridge Ct, Moorbridge Rd., East Bingham, Nottingham, UK. NG13 8QG Tel. +44 1949 836 111
Express Ion Q mini columns *Strong anion exchange gel*	Whatman International Ltd. Whatman House, St. Leonards Rd., Maidstone, Kent. UK ME16 OLS Tel. +44 1622 676 670
L-Lactate Dehydrogenase *Bovine heart*	Boehringer Mannheim
ML-9 Hydrochloride	Alexis Corporation (UK) Ltd.
Myosin Light Chain Kinase *Chicken gizzard*	Mike Walsh, Department of Physiology, Univ. Calgary, Canada.

	e-mail walsh@ucalgary.ca
Okadaic acid (free acid)	Sigma Aldrich Co. Ltd. Fancy Rd., Poole, Dorset, UK. BH12 4QH Tel. +44 1202 733 114
PD142893	Sigma Aldrich Co. Ltd.
Smooth Muscle Myosin Light Chains *Chicken gizzard*	Alexis Corporation (UK) Ltd.

All other chemicals were AnalaR reagents obtained from BDH-Merck Ltd., Merck House, Poole, Dorset. BH15 1TD

Normal PSS was made according to the protocol of Krebs and Henseleit[146]. Before addition of the calcium solution, the PSS was bubbled for at least 15 minutes with 95% O_2/ 5% CO_2. The calcium was then added, and the buffer sealed until use. The PSS was not seen to drop below pH 7.1 or rise above pH 7.4 during the course of experiments, or during storage of tissue. Potassium chloride was substituted isoosmotically for sodium chloride in order to make 70mM KCl buffer for inducing isometric contractions. Essentially calcium free buffer contains no calcium and 1mM EGTA to keep extracellular calcium to a minimum. This buffer is required for the dissection of rat aortas and human basilar arteries, to avoid stressing the tissue. All of the buffers were made with distilled-deionised water and stored at 4°C for up to one week.

2.2.3 Buffers

Chemical	Normal PSS (mM)	Ca^{2+} Free PSS (mM)	KCl PSS (mM)
NaCl	118	118	54
$NaHCO_3$	25	25	25
KCl	5.7	5.7	70
$MgSO_4$	1.2	1.2	1.2
$CaCl_2$	2.5	1mM EGTA	2.5
Glucose	11	11	11
NaH_2PO_4	0.75	0.75	0.75

Table 2.1: Physiological saline solutions used in the research presented in this thesis. In all cases, the solutions are bubbled for at least 15 minutes with 95% O_2/ 5% CO_2 and stored in a sealed container at 4°C.

2.2.4 Tissue collection and storage

2.2.4.1 Porcine Tissue

Porcine carotid arteries from Large White Land pigs were harvested from a nearby abattoir (G. B. Wrighton's and Sons, Fritwell, Bicester, Oxon. or Mutch Meats, Witney, Oxon.). The carotids were taken from the pig carcass within 20 minutes of slaughter and immediately placed in cooled (4°C) physiological saline solution (PSS, see Table 2.1) which had been bubbled with 95% O_2/5% CO_2 and sealed. The carotids were conveyed to the laboratory and dissected free of connective and adipose tissue, taking particular care to remove all traces of blood. The cleaned tissue was stored in PSS at 4°C and the PSS was changed at twelve-hour intervals. In this way, the carotids remained viable for up to 72 hours[43].

2.2.4.2 Rat tissue

Animals were treated according to Home Office guidelines under Schedule 1. Rats were stunned with a blow to the head and killed by cervical dislocation and aortas were collected immediately before use. The thoracic and abdominal aortas were removed quickly and placed in cooled (4°C) essentially calcium free PSS. The adipose tissue and connective tissue were carefully removed in essentially calcium free PSS and the cleaned tissue was stored in PSS for up to 1 hour prior to use.

2.2.4.3 Human vessels

Central Oxford Research Ethical Committee (COREC) approval was granted for experiments involving human tissue. Human basilar arteries were obtained with next of kin post mortem consent from the Neuropathology Department of the Radcliffe Infirmary, Woodstock Road, Oxford. The arteries were taken from brains submitted for post-mortem with causes of death other than vascular disease. Tissue showing clear signs of arteriosclerosis was discarded. The arteries were collected within 72 hours after post-mortem and placed in cooled (4°C) PSS. They were found to have stable rates of oxygen consumption when tested up to 24 hours later.

2.2.4.4 Cerebrospinal fluid

COREC approval was granted in order to collect Cerebral Spinal Fluid (CSF) from patients at time of surgery or from the lumbar drain. Either or both these procedures are routinely carried out on all subarachnoid haemorrhage patients. The fluid was collected and immediately centrifuged for 15 minutes at 3000rpm (1500 × *g* calculated from a nomogram supplied by the company, see 2.2.1) to remove brain tissue and contaminating blood. Lumbar drain CSF was collected into sterile Cordis® bags and frozen at -20°C until further processing. The volume of CSF required for force measurements was freeze-dried and stored at –20°C until needed for experiments. CSF for force measurements was reconstituted so that the concentration was approximately equal to whole CSF. Although

the CSF was obtained from low risk patients with respect to HIV and Hepatitis B, all samples were handled as biohazardous material and disposed of according to local regulations.

2.2.5 Patient population

Cerebrospinal fluid was collected from the Radcliffe Infirmary, Oxford, Addenbrooke's Hospital, Cambridge and the Frenchay Hospital, Bristol. The criteria for determining which patients were at risk of vasospasm are discussed in Chapter 7. Cerebrospinal fluid was collected from all patients within 36 hours of the initial haemorrhage either at the time of surgery or subsequently through a lumbar drain. Where CSF was collected over a period of time from a single patient, the first collection is used in the experiments to eliminate any dilution effects. Both stimulatory (CSF_S) and non-stimulatory (CSF_N) cerebrospinal fluid was collected from patients who have suffered a subarachnoid haemorrhage. The way in which this CSF was treated subsequently is reported in 2.3.5.

Samples from patients with complications such as systemic infection, or those on non-typical therapy were not included in this cohort. Typical therapy for cerebral vasospasm after subarachnoid haemorrhage usually includes treatment with a calcium channel blocker, Nimodipine® (Bayer).

2.3 Methods

2.3.1 Oxygen consumption measurements

Clark-type polarographic oxygen probes (Yellow Springs Instruments) immersed in magnetically stirred sample chambers were used to measure the oxygen consumption of various tissues (Figure 2.1).

The chambers were jacketed with water and kept at a constant temperature using a Grant constant temperature circulator. The porcine carotid arteries were cut into 1 cm rings, debrided of endothelium and split lengthways to form a strip. Physiological saline solution (50ml) was bubbled with 95% O_2/ 5% CO_2 and then filtered through a 0.2μm Millipore filter to removed bacteria. This PSS was then sealed in a plastic tube and placed in a water bath at 30°C. Six millilitres of this PSS (Table 2.1) was added to each chamber and allowed to equilibrate with air at the experimental temperature (30°C or 37°C) for at least 10 minutes. The Lucite® plungers encasing the probes (see 2.2.1) were then inserted into the chambers and the background respiration of the PSS was monitored for at least 30 minutes. Any significant rate of background respiration (>10% of rate from carotid alone) resulted in the chambers and plungers being removed and washed, as respiration in the absence of tissue was presumed to be due to bacterial contamination. The pH of the PSS was not found to change significantly during the course of the experiment.

The carotids were then placed in the PSS and allowed to respire for at least 30 minutes to obtain a baseline respiration rate. When tissue viability had been established, that is a stable rate of oxygen consumption had been observed for at least 30 minutes, agents were added through a capillary in the plunger using a Hamilton syringe and their effects on the respiration of the tissue monitored. The output was recorded on a Kipp and Zonen (2.2.1) chart recorder. If the oxygen levels fell below 15%, the PSS was replaced.

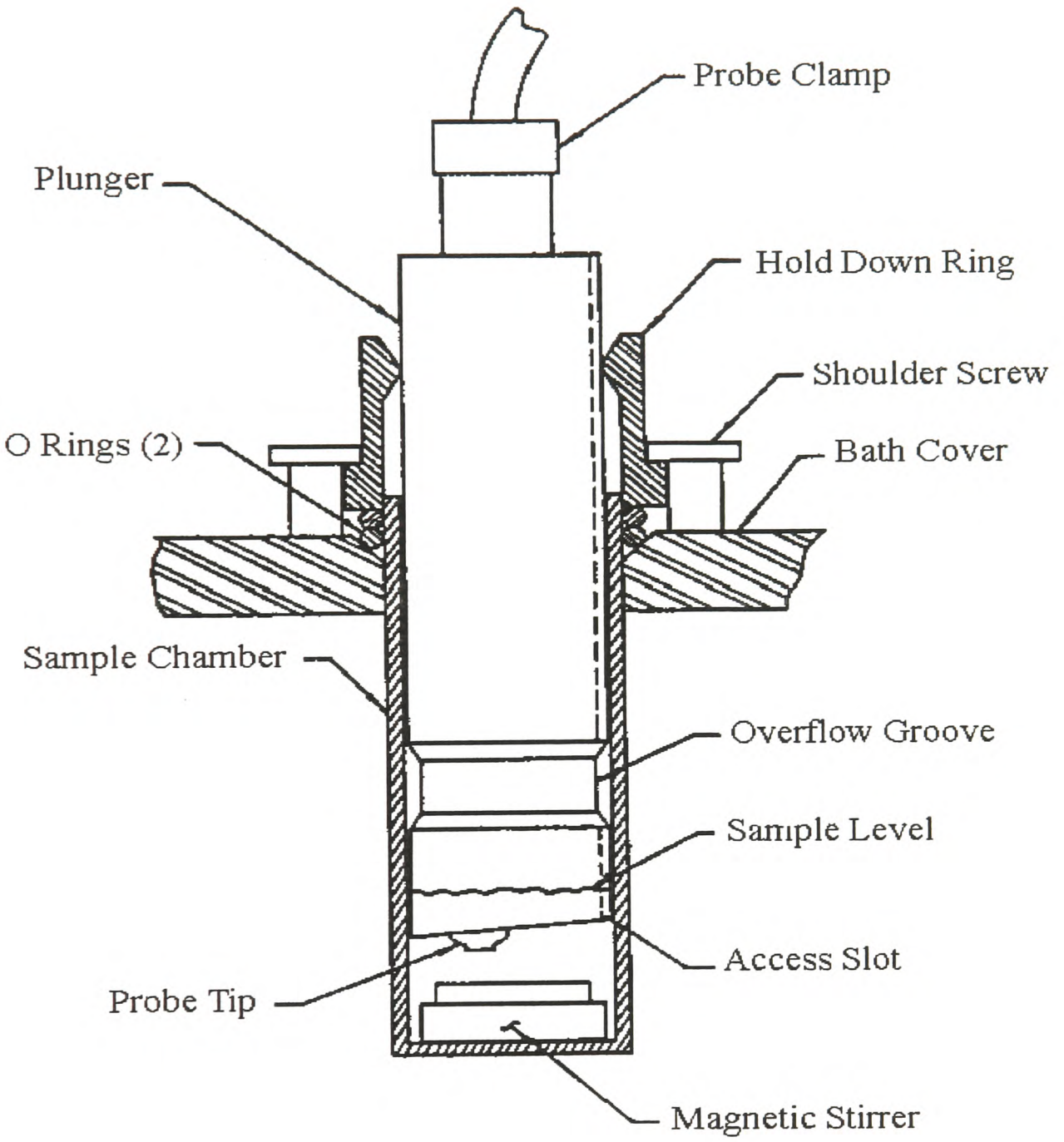

Figure 2.1: The Yellow Springs Instruments Clark type oxygen electrode apparatus used for the oxygen consumption measurements.

In order to convert the data into amount of oxygen consumed per unit time per gram dry weight of tissue, the following formula was used.

$$\frac{x[O_2]V}{tx_{max}M} \qquad \text{(i)}$$

Where;

x is the deflection in cm across the chart paper in 30 minutes

$[O_2]$ is the oxygen tension of buffer and is dependent on temperature; (At 30°C, it is 0.26 μmol O_2 ml^{-1} and at 37°C, it is 0.202 μmol O_2 ml^{-1}. This is the amount of O_2 dissolved in PSS per ml.)

V is the volume of buffer in the chamber in ml;

t is the length of time over which each measurement is taken in minutes;

x_{max} is the full scale deflection of the chart recorder in cm;

M is the mass of the tissue after at least 24 hours of drying in air at 25°C in g.

This calculation yields a value of O_2 consumption with units μmol O_2 min^{-1} .g dwt^{-1}.

To ensure consistency in the oxygen consumption measurements, the electrodes were calibrated periodically. This was achieved by placing the electrode in PSS equilibrated with 95% O_2/ 5% CO_2 to obtain a maximum, followed by addition of an excess of sodium thiosulphate to obtain a zero reading. The chart recorders were adjusted manually to zero in the presence of sodium thiosulphate. If the reading obtained in 95% O_2 equilibrated PSS was anomalous, the membranes were replaced and the electrodes cleaned before further recalibration.

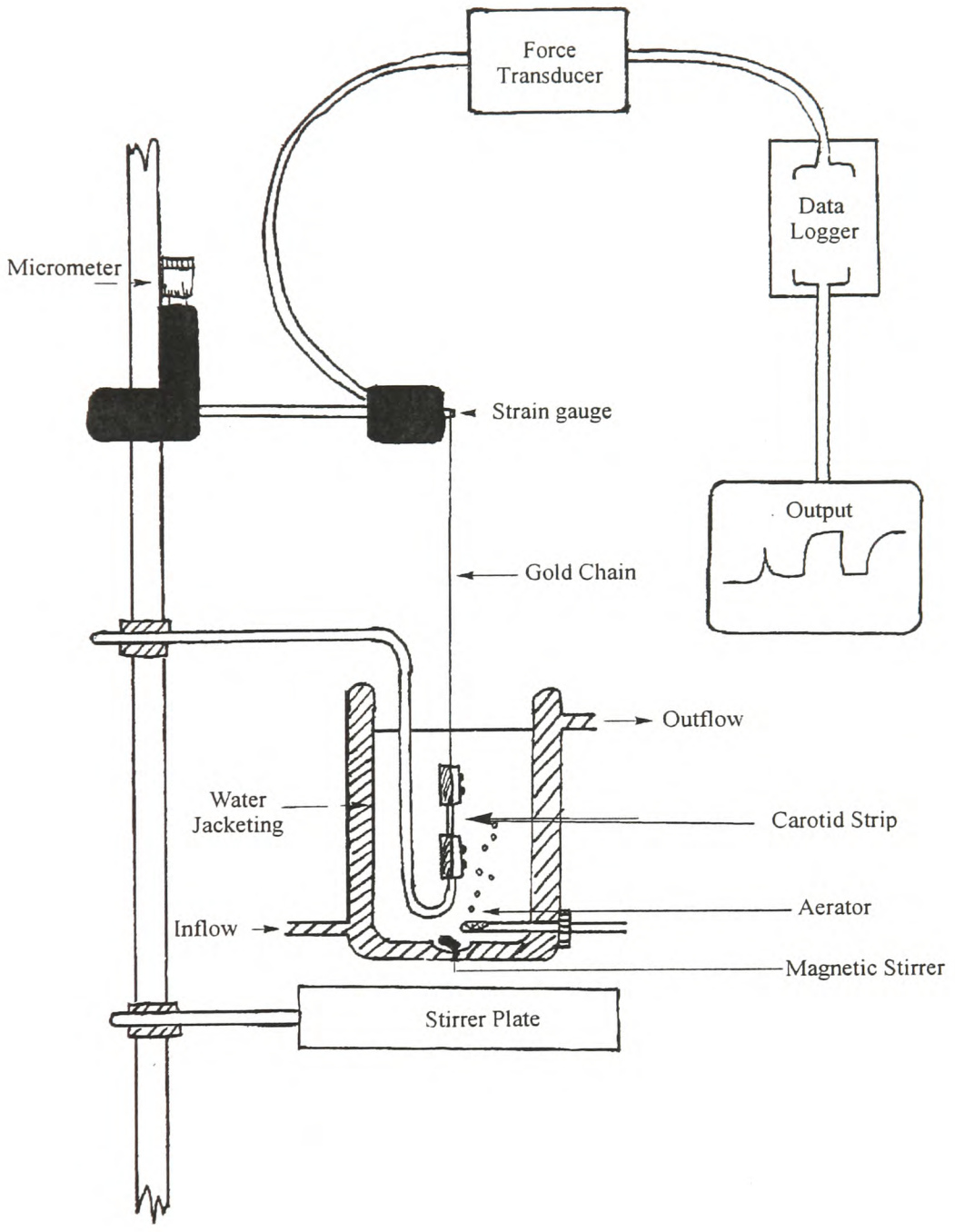

Figure 2.2: The water jacketing maintains the buffer at a steady 37°C via a circulating pump. The buffer in the organ chamber is also bubbled with 95 % O_2/ 5% CO_2 and stirred using a glass coated magnetic flea. The tissue can be stretched in a controlled and reproducible manner using the micrometer.

2.3.2 Force measurements

The force measurement apparatus (Figure 2.2) consists of a force transducer (Harvard Apparatus) interfaced with a PC using Pico Technology Picolog (version 4.04) software. The tissue was mounted in a clamp with perspex and stainless steel blocks. The lower clamp was fixed on a stainless steel arm and the upper clamp was attached via a non-corroding gold chain to the strain gauge.

The tissue was split longitudinally and strips of smooth muscle (intima and media) are teased from the adventitia (Figure 2.3). The strips of smooth muscle taken in this way are not perpendicular to the length of the artery, but at an angle as demonstrated by Herlihy and Murphy[102].

Strips 1mm wide were mounted in the clamp and immersed in a water jacketed chamber containing PSS aerated with 95% O_2/ 5% CO_2 at 37°C. Buffers were stored in jacketed reservoirs at 37°C and aerated with 95% O_2/ 5% CO_2. The tissue was judged to be healthy if the "Herlihy Hop" was observed[102]. This contraction and relaxation, known as the Herlihy Hop, occurs in porcine carotid artery in response to being moved from buffer at 4°C to buffer equilibrated at 37°C and bubbled with 95% O_2/ 5% CO_2. If this did not occur, the tissue was judged to be unfit for experimentation and discarded. The tissue was allowed to equilibrate in the buffer at resting tension, that is the tissue was lengthened until resistance is just registered on the transducer, for at least one hour after mounting and then stretched to 120% of the resting length, measured to 0.5mm using a ruler. This has been shown to be the optimum length (L_O) for the porcine carotid artery[57].

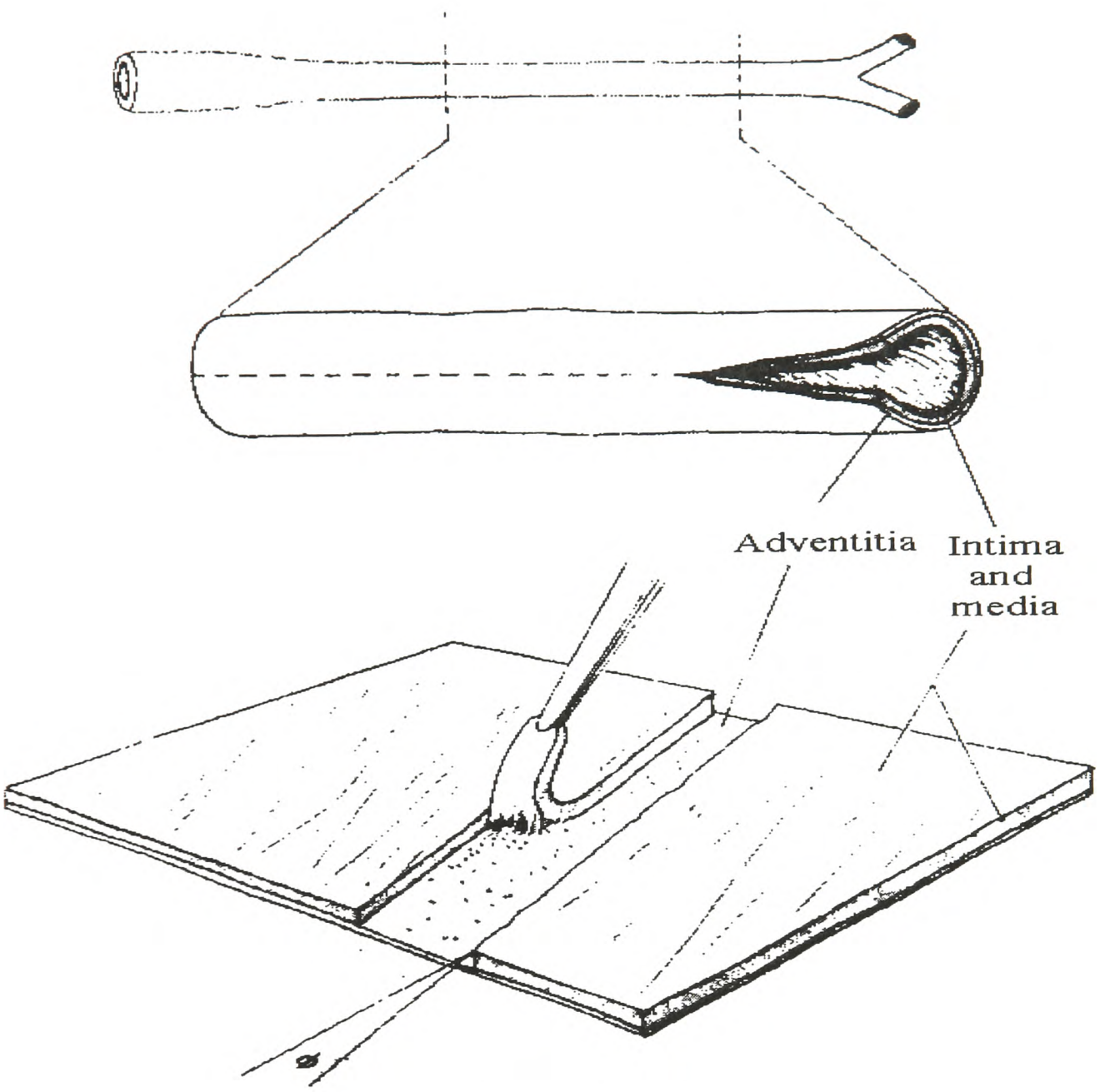

Figure 2.3: Strips of smooth muscle are peeled from the connective tissue with forceps. Care is taken to exert as little shear stress as possible on the tissue. This figure reproduced from Herlihy and Murphy[102]

The tissue was allowed to equilibrate for at least an hour, until a baseline tension was reached. The tissue was then exposed to pre-warmed and aerated 70mM KCl buffer until a steady maximum was observed. KCl was then rinsed off and the KCl contraction repeated once a steady baseline was achieved. The KCl induced isometric tension was taken to be 100% of the tissue's maximum force (F_{Max}). When a stable baseline was achieved after the second KCl contraction and rinse, the experimental protocol was begun.

In order to convert this into force per cross sectional area (Nm^{-2}), the following calculations were performed.

1. The force transducers were calibrated using standard weights and this enabled conversion of the data stored in millivolts to g.

2. The length and width of the tissue were measured to the nearest 0.5mm and the wet mass was recorded.

3. The cross sectional area was calculated using the following formula;

$$CSA = \frac{M}{L_i \rho} \qquad \text{(ii)}$$

where:

CSA is the cross sectional area of the tissue in m^2;

M is the wet mass of the tissue in kg;

L_i is the initial length of the tissue in m after the stretch by 120% and

ρ is the density of the tissue, taken to be 1050 kg m^{-3}. [102]

The force per cross sectional area was thus calculated using the following formula;

$$F = \frac{d \times g}{CSA} \qquad \text{(iii)}$$

where

F is the force per cross sectional area Nm^{-2},

d is the mass exerted by the tissue calculated using the data collected by the Picolog software and the manual calibration, in kg,

g is acceleration due to gravitational force, taken to be 9.81 ms^{-2},

CSA is the cross sectional area, in m^2, calculated from equation (ii).

2.3.2.1 Stretch-release measurements and analysis of relaxation

When vascular smooth muscle is stretched to 1.5 times the L_i (initial length) and then quickly released back to L_i, there is a regeneration of tension. During a stretch, myosin light chains (MLC_{20}) are phosphorylated in proportion to the amount of stretching the cross bridges are subjected to. The rate and magnitude of tension regeneration after a stretch are dependent upon the magnitude of the phosphorylation that occurred during the stretch phase[19].

The tissue was prepared and treated with KCl as described above. Before and after the addition of any agent, the tissue was stretched to 1.5 times its resting length and then quickly released back to the L_i within 4 seconds. The velocity of the regeneration of tension was analysed using ModelMaker (Cherwell Scientific Publishing) software version 3.0. A typical stretch-release response is represented in Figure 2.4. The data was fitted using the formula for a rectangular hyperbola: $y = a[(bx) \div (1 + bx)]$

where a is the maximum value and b is the gradient of the initial velocity. This equation was chosen as it best represents smooth muscle tension generation[86].

The relaxation of tissue after a stretch was measured in the fast phase (termed a) and the slow phase (termed b) and is represented in Figure 2.4. The rate of relaxation at these two positions was calculated by fitting a line to the tangent at the initial fast relaxation phase, and another to the second slow phase of relaxation as shown in Figure 2.4. The lines were fitted using the equation $y = mx + c$ where c is the y intercept and m is the gradient of the line giving the velocity.

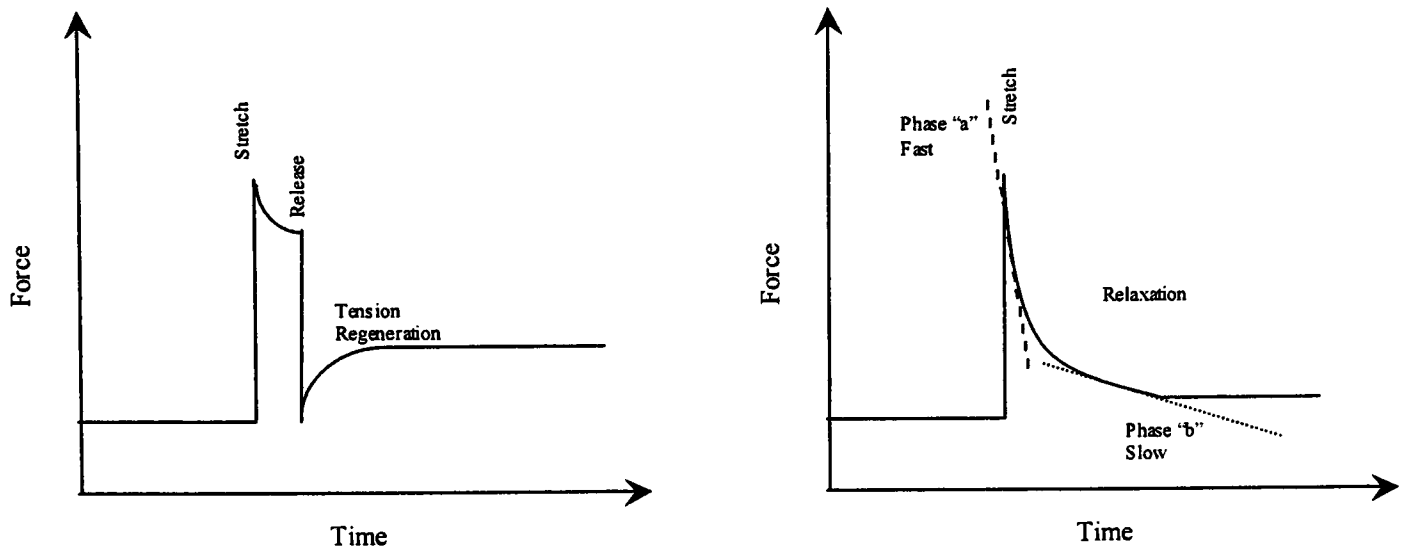

Figure 2.4: Schematic representations of regeneration of tension after a stretch, and relaxation after a stretch in the porcine carotid artery.

2.3.3 Concomitant measurements

A Lucite plunger used in the oxygen consumption measurements was adapted in order to monitor oxygen consumption of tissue at the same time as tension development. Figure 2.5 illustrates the adaptations made by Shinsuke Nakayama, Department of Physiology, University of Nagoya Medical School, Nagoya, Japan.

The calculations used to process the data were the same as for the individual measurements, using equations (i), (ii) and (iii).

Carotid rings were prepared by cutting with a scalpel a 0.3-0.4cm length of carotid. The tissue was allowed to equilibrate and respire in the O_2 electrode chamber for at least 40 minutes. It was then stretched to the L_O for the porcine carotid artery (1.5 times the resting length) and allowed to equilibrate for a further 30 minutes. CSF and other agents were added by means of a Hamilton syringe through a capillary in the plunger. In order to obtain a dose response curve to calcium, the tissue was equilibrated in essentially calcium free buffer with 70mM KCl. The calcium was added in increments of 0.2 mM from 1mM to 2.6 mM.

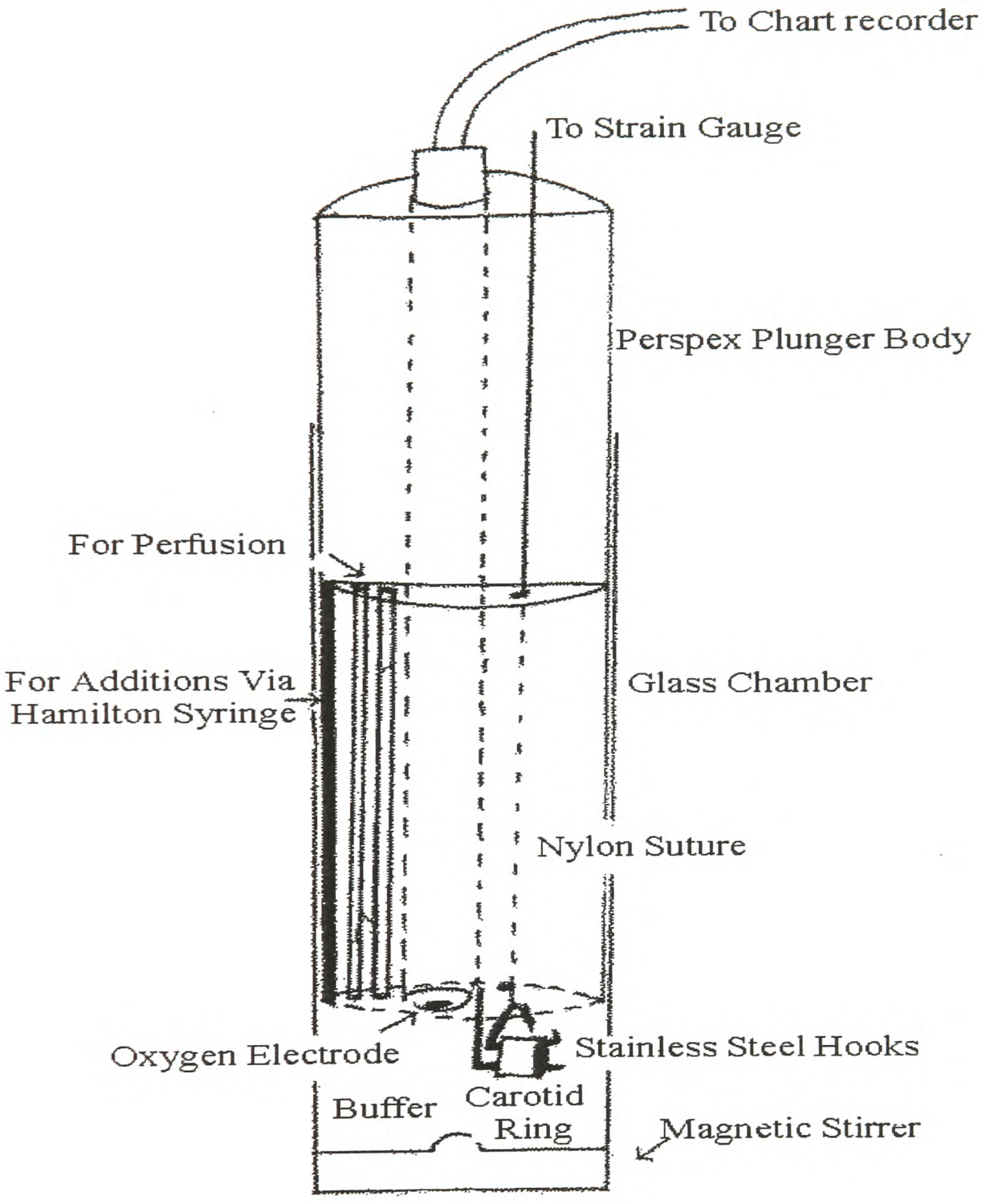

Figure 2.5. Holes were drilled in the plunger to allow continuous flow of buffer and attachment to a force transducer. A metal L-shaped bar was affixed to the bottom of the plunger so that tissue could be hooked over this and a triangle of metal attached to the force transducer.

2.3.4 Testing the model parameters

In order to determine the suitability of using the stimulation of O_2 consumption by

CSF_S as a model for cerebral vasospasm after subarachnoid haemorrhage, a number of experiments were performed. The rate of oxygen consumption of porcine carotid arteries at 30°C was recorded and the rate at 180 minutes was used for statistical analysis. Variation between carotids from different animals was calculated by allowing untreated carotids to consume oxygen. Variation between carotids from different animals when stimulated with equal concentrations of one CSF_S or 1 nM okadaic acid was also calculated. Variation within animals was determined by recording the oxygen consumption at 180 minutes of different sections of the same carotid and of different sections of the same carotid stimulated by CSF_S at 180 minutes. Recording the response of different sections of the same carotid to different CSF_S samples allows us to estimate the variation between patients.

In order to compare this model with the more established method of measuring the stimulation of tension development by CSF_S, some CSF_S samples were used to examine tension development. Concomitant measurements were used to show the relationship between tension and O_2 consumption under normal and vasospastic conditions. The normal relationship can be demonstrated by preparing the tissue as described in Endo[65]. Essentially calcium free conditions were achieved by incubating the tissue in 0.1mM EGTA and 10 mM caffeine[64]. The tissue was then exposed to 70 mM KCl PSS (2.2.3) and the tension and rate of O_2 consumption recorded. The calcium concentration was then increased in a stepwise fashion and the tension and O_2 consumption measurements recorded at each plateau. To examine the effect of CSF on this relationship, a number of CSF samples were chosen that gave a range of high O_2 consumptions. As the CSF_S effect is not reversible by rinsing (see Figures 3.2 and 5.5), each CSF was applied to a different piece of carotid. When a stable tension and O_2 consumption were reached (180 minutes), it was recorded. The CSF was added as for tension measurement experiments and the experiment was carried out at 37°C instead of the usual 30°C (see 3.3.3 and Table 3.2).

2.3.4.1 Choosing the appropriate tissue

In order to determine the most suitable tissue to use in this model, the responses of vascular smooth muscle tissues from various vascular beds and different animals were examined. The tissues were exposed to a 1 in 30 dilution in PSS of CSF_S (as defined using the porcine carotid artery) in the oxygen electrode chamber at 30°C. The magnitude of the stimulation, and the intrinsic variation of the tissue were calculated, the results of which are seen in Chapter 3. The porcine carotid artery, porcine basilar artery, human basilar artery, rat thoracic and abdominal aorta and the guinea pig thoracic and abdominal aorta were all tested. The results from the porcine carotid, human basilar artery and rat thoracic aorta are shown in 3.3.3.

2.3.5 Defining CSF_S from CSF_N.

Whether a CSF was defined as stimulatory (CSF_S) or non-stimulatory (CSF_N) for the purpose of these investigations was determined using oxygen consumption measurements. A CSF sample that stimulated the rate of O_2 consumption to above 0.4

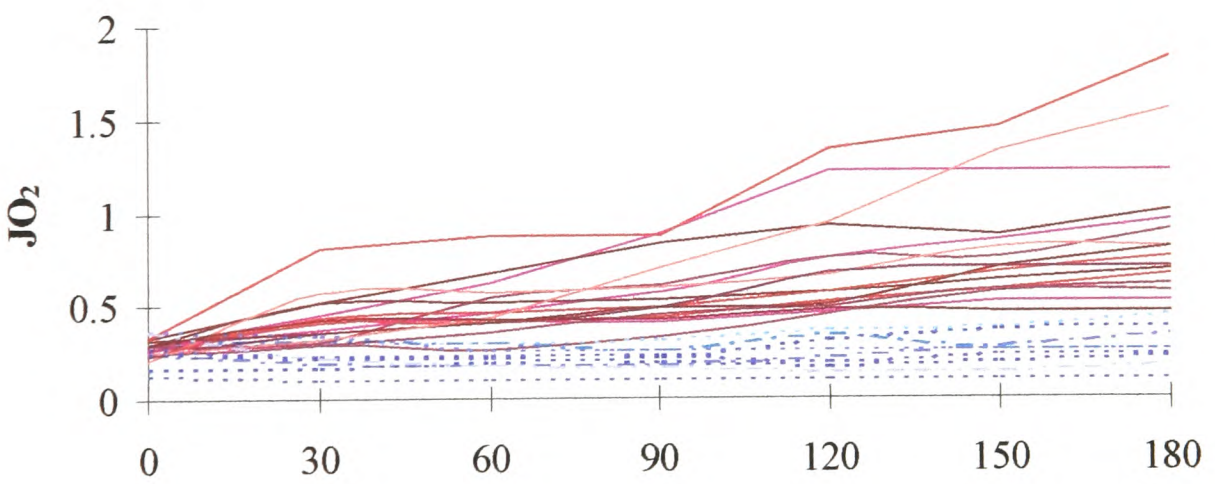

Figure 2.6: The spectrum of responses obtained upon addition of CSF to porcine carotid artery. The response is measured as JO_2 at 180 minutes in µmoles O_2 min^{-1} g dwt^{-1}. The dashed lines represent those CSF samples falling below 0.4 µmoles O_2 min^{-1} g dwt^{-1} of stimulation and thus classified as CSF_N. Solid lines represent CSF_S samples, that is CSF samples that stimulated O_2 consumption to above 0.4 µmoles O_2 min^{-1} g dwt^{-1} at 180 minutes. CSF_S, n=16; CSF_N, n=7.

μmol min^{-1}g dwt^{-1} (in the porcine carotid artery at 30°C) at 180 minutes was determined to be CSF_S and anything below that, CSF_N. Such a distinction needed to be made as the CSF samples that were run gave a spectrum of rates of O_2 consumptions with no clear delineation between CSF_S and CSF_N. This range of responses can be seen in Figure 2.6.

2.3.6 Agonist and inhibitor studies

Table 2.2 shows the agents used to characterise the nature of the CSF_S stimulation of O_2 consumption. In order to solubilise some of the inhibitors, methanol was used as the solvent in some cases. The maximum volume of inhibitor added to a 6ml chamber was 100 μl. Addition of 100μl of methanol to 6ml of buffer did not affect the respiration of the arteries.

2.3.7 Perchloric acid extraction of tissue

The tissue was quick frozen in N_2(l) and ground with a mortar and pestle that had been pre-cooled to N_2(l) temperature. The tissue was added to pre-weighed tubes containing 12% perchloric acid, approximately 100mg (wet mass) tissue per 1ml PCA. The tubes were weighed again to allow accurate estimation of the mass of tissue extracted and then the contents were thoroughly homogenised using a Polytron Kinematica homogeniser. The tubes were balanced and centrifuged for 15 minutes at 3000rpm (1500 × g). The supernatant was carefully decanted for soluble metabolite assay and the pellet kept for the protein assay.

CSF and blood plasma samples did not require homogenisation and the rest of the protocol was as previously described. A small volume of concentrated PCA was added to liquid samples so that the solution contained 12% PCA v/v. The acidified samples were then centrifuged and the protocol followed as for tissue samples. The PCA extract supernatant was quickly neutralised using solid TRIS-base to minimise the volume. The entire

procedure was carried out at <4°C. It was found that extracting the CSF using 12% perchloric acid was effective in removing protein.

Agent	**Inhibits**	**Receptor**	**Final conc.**	**Solvent**
Dobutamine	-	α_1/ β_2 AR	296 nM	Buffer
Endothelin	-	ETA & ETB	10^{-5} M	Buffer
Histamine	-	Histamine	10^{-5} M	Buffer
Noradrenaline	-	α_1 AR	10^{-5} M	Buffer
Okadaic Acid	PP2A >PP1	-	1nM[1]	Methanol
PD142893	ETA & ETB	-	1μM	Methanol
PKA Inhibitor	Protein kinase A	-	1μM	Methanol
Staurosporine	Protein kinase C	-	1nM	Methanol

Table 2.2: Agonists and inhibitors employed to investigate the stimulation of smooth muscle O_2 consumption by CSFs. All chemicals were dissolved, where possible, in buffer (physiological saline solution) or in methanol where necessary.

2.3.7.1 Concentration of CSFs

The observation that a known protein phosphatase 2A inhibitor, okadaic acid, elicited a response that closely mimicked CSFs led to the adaptation of the extraction

[1] unless otherwise specified

procedure for okadaic acid derived by Tachibana *et al*[266]. Flowchart 2.1 illustrates the extraction procedure used to remove as many vasoactive impurities as possible from the CSF_S. It was found that 500ml of CSF, when lyophilised, yielded approximately 1.5g of dry powder and this powder was PCA extracted and the supernatant retained. The precipitate was resuspended and washed in methanol three times and once in acetone. The washes were combined with the supernatant for rotary evaporation. This aqueous concentrate was washed three times with n-hexane and the hexane fractions discarded. No activity, assayed using oxygen consumption, was found in the hexane washes. The aqueous fraction was loaded onto a 1cm × 2cm silicic acid column (Whatman International) with a 0.5ml void volume, which had been pre-equilibrated in methanol. The product was washed whilst bound to the silicic acid column using a decreasing concentration of methanol in water as shown on flowchart 2.1 in order to remove salts and sugars. The column was then eluted with a hexane/ acetone mixture (5:1). This eluent was dried under $N_2(g)$ and the product tested for activity.

The product was a white powder that exhibited activity when added to porcine carotid artery in the O_2 electrode. In order to achieve a stimulation equivalent to a 1 in 30 dilution of CSF_S, freeze dried CSF had to be diluted 1 in 10,000. Extracted CSF, however, had to be diluted 1 in 15,000 representing a purification assessed by the bioassay of approximately 1.5 times from the freeze dried, un-extracted CSF to the final product. The aim of this extraction was to remove any contaminating vasoactive compounds without diminishing the activity of the CSF in the O_2 electrode assay. This was assessed to have been done, as the product was still active in our bioassay, yet many impurities will have been removed by this protocol. This extracted product was used at a 1 in 15,000 dilution to pre-treat the tissue in which phosphatase activity was assayed in Chapter 6.

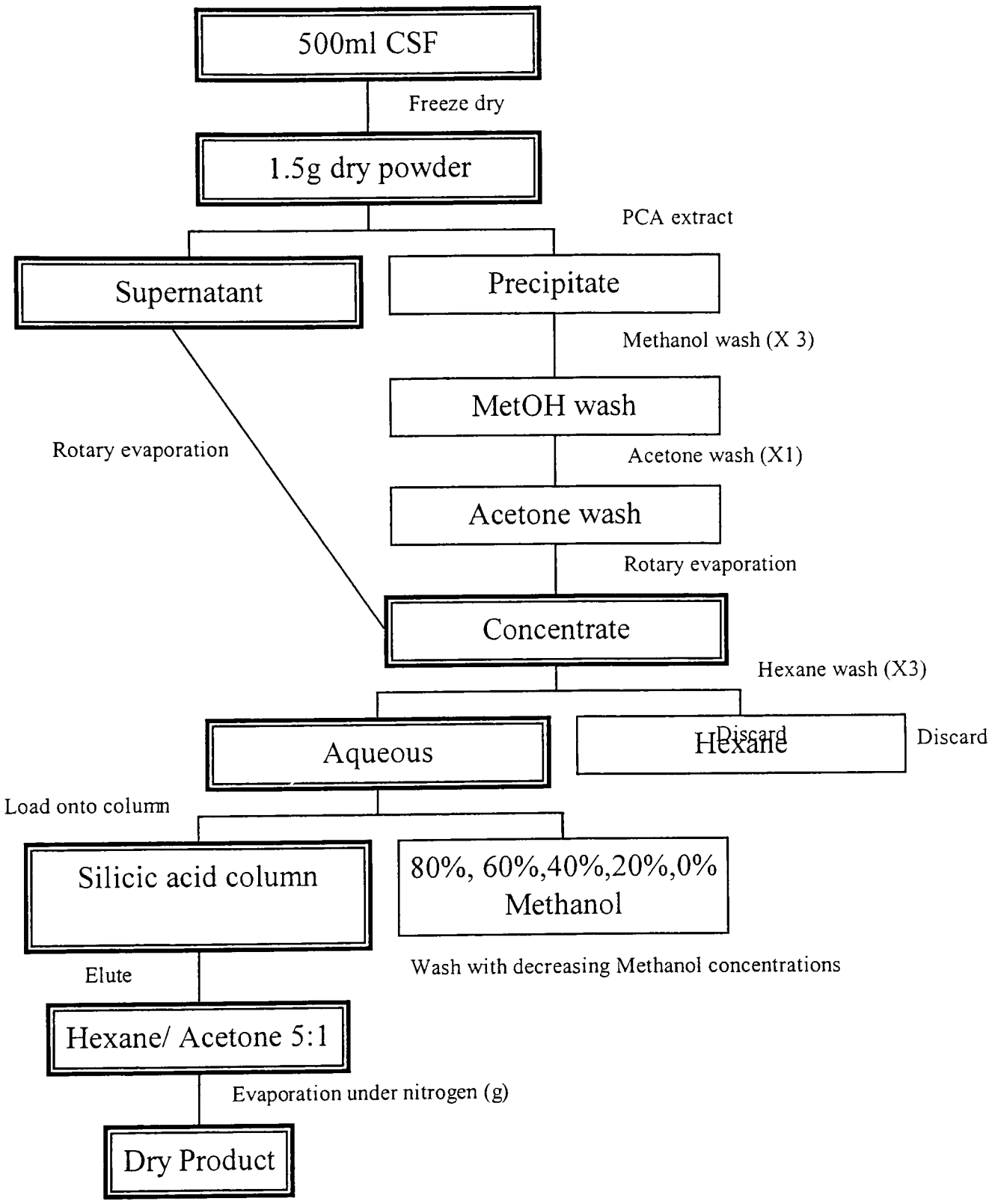

Flowchart 2.1. This flowchart illustrates the steps involved in the removal of vasoactive contaminants from Freeze-dried CSFs. The extract was assayed for stimulation of O_2 consumption in the porcine carotid artery after each step.

2.3.8 Lactate determination

Supernatant from the PCA extraction procedure was used to estimate tissue or CSF L - Lactate content. The reaction buffer consisted of the following components:

5% Hydrazine Hydrate; 1mM EDTA; 0.2M TRIS; 0.1M NAD (made up just before use). The buffer was adjusted to pH 9.5 using 5M HCl.

A standard range was set up in triplicate, each cuvette containing 10U L- lactate dehydrogenase, 1 ml reaction buffer, 0.9 ml H_2O, varying volumes of 1mM lactate solution (between 0 and 0.1ml of 1mM lactate solution). This gives a range of 0 - 0.1μM. Varying volumes of H_2O were added so that the total volume in each cuvette was 2ml. Sample tubes contain 1ml reaction buffer, 10U L- Lactate Dehydrogenase, 0.8ml H_2O and 0.2 ml sample at an appropriate dilution. The cuvettes were mixed by inversion, making sure not to contaminate the samples by using parafilm over each cuvette and then left to react for 40 minutes at room temperature. The absorbance readings of each cuvette were read at 340nm after 40 minutes and blanked against a tube containing 1ml reaction buffer, 10U L- Lactate Dehydrogenase and 1 ml of H_2O. Each sample was assayed in triplicate. This assay was adapted from that of Passonneau and Lowry[213].

2.3.9 Protein determination (Lowry)

The pellets from the PCA extraction procedure (which contain precipitated protein) were resuspended in 1M NaOH (25mg tissue per ml NaOH) and heated to 60°C for 1 hour. The sample was then homogenised, vortexed and a fraction of each sample diluted 1 in 10 in H_2O. A standard range was set up in triplicate, ranging from 0 to 1 mg Bovine Serum Albumin (BSA). 40μl of diluted sample was added to 60μl H_2O. One ml of buffer containing 0.46mg/ml $CuSO_4$, 0.82mg/ml $NaO_2CCH(OH)CH(OH)CO_2Na.2H_2O$ and 90mg/ml Na_2CO_3 in 0.091M NaOH was added to each tube (including standard curve and non-proteinous controls). All tubes were vortexed and allowed to stand at room temperature for 10 minutes. 3ml of a buffer containing 9% Folin and Ciocalteau's

Phenol[155] reagent in H_2O were added to each tube. The tubes were then incubated at 50°C for 10 minutes and the absorption at 650nm recorded. This assay was taken from that reported by Lowry[155].

In order to assess the effect of CSF_S and CSF_N on resting porcine carotid, five incubation conditions were set up. Tissue was incubated in PSS alone, a 1 in 30 dilution of CSF_N, a 1 in 30 dilution of CSF_S and 1 μM Okadaic acid. The carotid arteries were placed in the flasks and maintained, stirred and bubbled with 95% O_2/ 5% CO_2 at room temperature. Aliquots (200μl) were taken at timed intervals and assayed for lactate content.

2.3.10 Magnesium loading and depletion

To study the effect of depleting or loading tissue with magnesium, the following protocol was undertaken. Lengths (approximately 4cm) of porcine carotid artery were placed in one of the three buffers detailed in Table 2.3. It has been shown previously that in order to deplete vascular smooth muscle significantly of magnesium it is necessary to remove extracellular calcium[191, 211, 222].

The tissue was incubated, stirred and bubbled with 95% O_2/5% CO_2, for at least 2 hours at room temperature (22°C). These are the conditions that have been shown to be necessary to load or deplete smooth muscle of magnesium [189, 190].

Although the actual intracellular concentration of magnesium was not measured in these experiments, it is predicted that the level of loading/ depletion will be similar in the porcine carotid to the guinea pig taenia, where these values have been measured. The porcine carotid artery has an intracellular free magnesium concentration of 0.48 ± 0.02 mM at pH 7.1 and in the presence of 15 mM glucose[55]. If the prediction were true, under the conditions described above, depleted porcine carotid artery would contain around 0.048 mM intracellular free magnesium and loaded tissue, 1.2 mM intracellular free magnesium.

Chemical	Control [Mg^{2+}] (mM)	Loading [Mg^{2+}] (mM)	Depletion [Mg^{2+}] (mM)
NaCl	138	138	116
$KHCO_3$	5.9	5.9	5.9
$CaCl_2.9H_2O$	2.4	2.4	0[2]
$MgCl_2.2H_2O$	1.2	12	0
Glucose	11.8	11.8	11.8
HEPES	5	5	5
EDTA	0	0	0.1
pH	7.4	7.4	7.4

Table 2.3: In all experiments, the loading/ depleting buffer was replaced by control buffer containing 1.2mM magnesium before carrying out any protocol. It has been reported that the loaded/ depleted condition of the tissue is maintained in control buffer for up to 2 hours[191].

2.3.11 Sodium dodecyl sulphate polyacrylamide gel electrophoresis

An X Cell II™ Mini Cell system (Novex, San Diego, CA.) was used to determine the protein profile of whole and PCA extracted CSF. NuPage (10% Acrylamide/ Bisacrylamide gel) gels were used which were Bis/ Tris HCl buffered at pH 7. The buffers used are detailed in Table 2.4

[2] successful magnesium depletion requires essentially calcium free conditions.

Chemical	Sample Buff. (40ml)	MOPS (1000ml)	MES (1000ml)
MOPS [3]	0	5.23g	0
MES [4]	0	0	4.88g
TRIS-Base	0.1705g	3.03g	3.03g
TRIS-HCl	0.1665g	0	0
Sucrose	1g	0	0
10% SDS	0.2g	5g	5g
EDTA	0.0015g	0.15g	0.15g
Serva Blue G250	0.001875g	0	0
Phenol Red	0.000625g	0	0
Ultrapure Water	40ml	1000ml	1000ml
pH	8.5	7.7	7.3

Table 2.4: Composition of the buffers used to load and run the samples for SDS-PAGE.

Samples were incubated with sample buffer for 10 minutes at 70°C and then 25µl was loaded into each well. The gels were 1mm thick, with 10 wells and 2 were run at once. MOPS buffer was used where good separation of larger molecules (200kDa-55kDa) was

[3] 3-(N-Morpholino) Propane Sulphonic Acid

[4] 2-(N-Morpholino) Ethane Sulphonic Acid

required and MES where good separation of the smaller molecular weight proteins (2.5kDa-36kDa) was required. The gel was allowed to run for 35 minutes in MES buffer or 50 minutes in MOPS buffer. In both cases, the voltage was set at a constant 200 V, the expected current at the beginning of the run was 110mA per gel and at the end, 70 mA per gel. On each gel, a pre-stained molecular weight protein ladder and an unstained ladder were run to assess efficacy of staining and molecular weight of unknown proteins.

At the end of the electrophoresis, the gels were removed from the cassette and placed in a staining solution consisting of 0.13% Coommassie blue (w/v), 50% methanol (v/v) and 10% acetic acid (v/v) for 2.5 hours on a gently shaking tray. After this period of staining, the gels were rinsed and placed in destaining solution overnight. The destainer consisted of 25% methanol (v/v) and 17% acetic acid (v/v). After destaining, the gels were rinsed in ultrapure water and photographed.

2.3.12 Myosin light chain phosphatase assay

Myosin light chain kinase substrate derived from smooth muscle was purchased from Alexis Corporation (product no.162-013-M001). The substrate consisted of a fragment of the smooth muscle myosin light chain 13 amino acids long and having the following amino acid sequence:

H-^{11}Lys-Lys-Arg-Ala-Ala-Arg-Ala-Thr-Ser-Asn-Val-Phe-Ala^{23}-NH_2

This peptide derives from the smooth muscle regulatory light chain of chicken gizzard and contains the phosphorylatable residue **Ser^{19}**. The necessary^{136} basic residues, **Lys^{11}**, **Lys^{12}** and **Arg^{13}** are present, ensuring maximal activity of smooth muscle myosin light chain kinase.

2.3.12.1 *phosphorylation of the substrate with ^{32}P.*

The smooth muscle myosin light chain kinase was purchased from Dr. Michael P. Walsh of the University of Calgary, Canada. The kinase was isolated[194] and purified[195] from chicken gizzard in the laboratory of Michael P. Walsh. The activity of the enzyme in the presence of 0.1 mM Ca^{2+} and 1μM Calmodulin was 10 μmoles P_i incorporated min^{-1} mg^{-1} kinase.

The buffers used in this protocol are detailed in Table 2.5. They are adapted from an existing protocol[215]. The substrate molecules were phosphorylated with ^{32}P by incubating in buffer R with myosin light chain kinase (0.2 μg/ml) and 10μM γ-^{32}P ATP (50 μCi) for 20 minutes at room temperature (around 20°C), shaking gently. The ^{32}P phosphorylated substrate was separated from the excess γ-^{32}P-ATP, Ca^{2+}, calmodulin and any free P_i using an ion exchange column. Express ion-Q strong anion exchange columns (Whatman International) were used. The columns were 1cm in diameter and 1cm in length, with a column volume of 1 ml. The ^{32}P phosphorylated substrate was loaded onto the column in buffer R and rinsed with 5 column volumes of buffer R without calmodulin to remove all extraneous radioactive ATP and free phosphate (see 2.3.13.3). The substrate was eluted using 2 column volumes of buffer E. The eluted substrate was diluted to 300 mOsm with water.

Chemical	**Homogenization (H)**	**Reaction(R)**	**Elution (E)**
	mM	**mM**	**mM**
NaCl	-	-	500
TRIS-HCl	20	50	-
$(CH_3CO_2)Mg.4H_2O$	-	10	-
$CaCl_2.6H_2O$	-	0.2	-
Calmodulin	-	0.001	-
Sucrose	250	-	-
EGTA	10	-	-
EDTA	1	-	-
β-Mercaptoethanol	10	-	-
PMSF[5]	1	-	-
Leupeptin	0.02%	-	-
TRITON-X100	0.1%	-	-
pH	7.5	7	7

Table 2.5. The buffers used for the phosphatase assay are adapted from Pato *et al*[215].

[5] Phenyl Methyl Sulphonyl Fluoride

2.3.12.2 Partial purification of myosin light chain phosphatase from treated tissue

The porcine carotid arteries from which the myosin light chain phosphatase activity was to be assayed were prepared in the following way. Lengths of porcine carotid artery, approximately 4 cm long with internal diameter of 4mm were turned inside out and slipped over a glass rod with a diameter of 1.5 times the lumenal diameter (6 mm) of the carotid. Pre-stretching must be done in order to induce the myosin light chain phosphatase because at rest, the enzyme has been reported to be minimally active[79, 215]. Tissue was incubated in 95% O_2/ 5% CO_2 gassed buffer for 1 hour at room temperature under the following conditions:

1. Control: PSS
2. CSF_N: PSS and CSF_N at a dilution of 1 in 30
3. CSF_S: PSS and CSF_S at a dilution of 1 in 30
4. Okadaic acid: PSS and 1nM okadaic acid (Positive control).

For each experimental condition, 5 pieces of carotid were used and for CSF_N and CSF_S incubations, 5 different patient CSF samples were used. After 1 hour of incubation, the carotids were removed from the glass rods and allowed to relax for 30 seconds in order to maximise the activity of the myosin light chain phosphatase. The tissue was weighed and then fast frozen in $N_2(l)$ and powdered using a pre-cooled stainless steel mortar and pestle. The powder was carefully decanted into pre-weighed tubes of buffer H so that the tissue suspension was around 100mg per ml of buffer. A homogeniser (Polytron Kinematica) was used to further grind the tissue. The suspensions were centrifuged (MSE Centaur 2E) at 3000 rpm (1500 × *g*) for 10 minutes. The supernatant was decanted and the pellet discarded.

2.3.12.3 Control experiments

A number of control experiments were carried out to determine the specificity and sensitivity of the assay.

The amount of radiolabelled ATP getting through the removal procedure was assessed by carrying out the entire procedure and assay in the absence of substrate. In this case, MLCK had no substrate to phosphorylate and so only residual radiolabelled ATP was present in the assay mixture. This also gave an indication of non-specificity of MLCK and effectiveness of ML-9 in this assay. If the ML-9 is ineffective at inhibiting the kinase, MLCK (albeit without calcium and calmodulin) may phosphorylate the natural substrate in the phosphatase preparation and give false positive results.

Carrying out the assay without the addition of the phosphatase preparation gave an indication of the levels of non-specific phosphate cleavage. This control experiment was carried out at 22°C and 37°C in order to determine any advantage of running the assay at a physiological temperature over running it at a lower temperature in order to minimise non-specific cleavage of radiolabelled phosphate.

The optimum time of incubation for this enzyme was also determined by plotting the phosphate released against time. The incubation time was taken from the part of the relationship that was linear, significantly below the plateau reached at longer time periods. The results of these control and optimisation experiments are given in Chapter 6, section 6.3.3.

2.3.12.4 The assay

One millilitre of each supernatant containing the myosin light chain phosphatase (obtained as described in section 2.2.13.2) was added to the prepared radiolabelled substrate and incubated in the presence of ML-9 Hydrochloride (Alexis corporation UK Ltd), a potent myosin light chain kinase inhibitor. This was added to prevent the ^{32}P

phosphate groups being rebound to the substrate during the course of the reaction. ML-9 was used at a concentration of 30 μM, which has been shown to be a concentration that inhibits kinases fully without interfering with phosphatase function[128]. A 30-minute incubation was then carried out at room temperature. 20°C was chosen in order to prevent non-specific phosphate dissociation whilst still keeping within a reasonable time course. Perchloric acid at -20°C was added to each tube to a final concentration of 12% in order to precipitate the myosin light chain phosphatase substrate. The assay tubes were centrifuged so that the substrate precipitated in the pellet and the supernatant contained liberated ^{32}P phosphate. The amount of phosphate liberated from the phosphorylated substrate depended on the activity of the phosphatase: the more phosphate liberated, the greater the activity of the phosphatase. The supernatants were decanted into microvials and Cherenkov counted in a scintillation counter (Beckman LS 1701). A calibration curve of the radiolabelled ATP solution used in the experiment was also run in triplicate, so that the level of phosphorylation could be accurately determined.

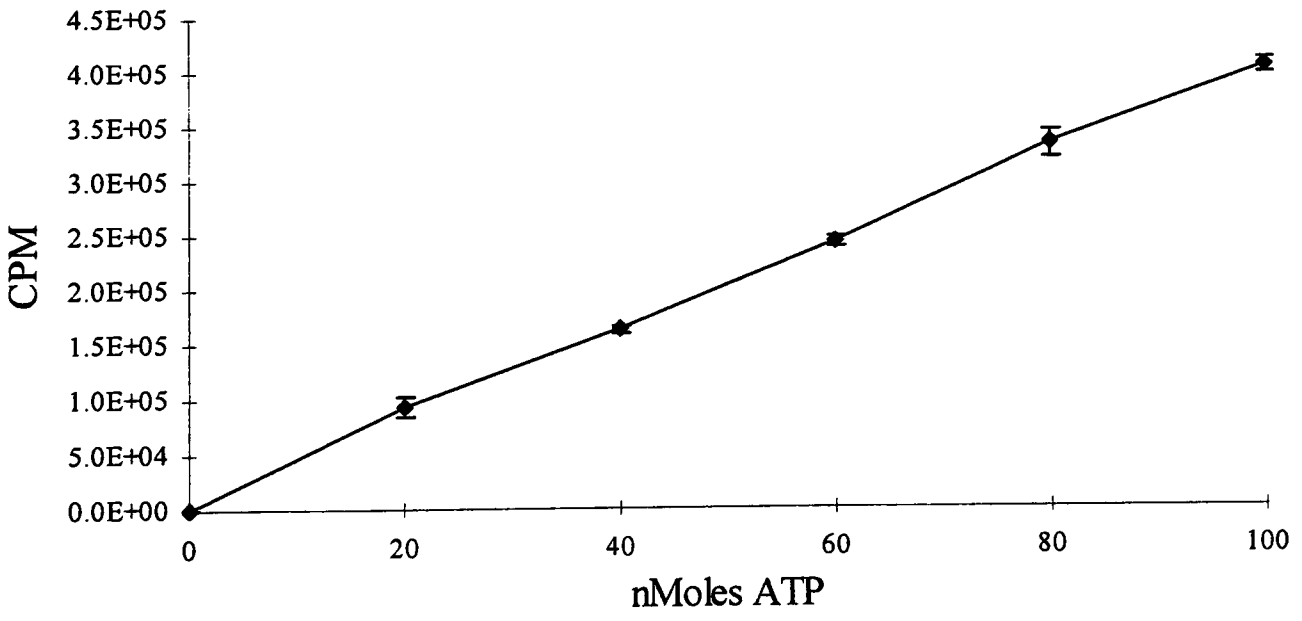

Figure 2.7: The relationship between counts per minute obtained using Cherenkov counting and the amount of ^{32}P labelled ATP present. The errors are standard deviations and n=3.

The results, obtained in counts per minute, were converted into moles of phosphate using the calibration curve (shown in Figure 2.7) and the assay was also carried out in the absence of substrate in order to determine non-specific binding.

2.3.13 Statistical analysis and curve fitting

Statistical significance was determined using two-tailed analysis of variance (ANOVA). The ANOVA function of Microsoft Excel version 5 was used to calculate significance. A 95% confidence limit was considered to be statistically significant. A curve fitting program, ModelMaker version 3.0, was used to fit curves to experimental data in order to obtain rate constants. The program utilises the least squares method to fit curves to the data. Curve fitting was used to analyse the tension generation and regeneration of tension after a stretch and release data.

3.The Experimental Model and extraction of CSF_S

3.1 Introduction

The relevance of the investigation into the pathology of cerebral vasospasm after subarachnoid haemorrhage presented in this thesis depends on the accuracy, reproducibility and reliability of the methods used to model vasospasm *in vitro*. In order to enhance the reproducibility of the model, various ways of treating the CSF samples were investigated to remove known vasoactive compounds.

The aim of this chapter is to introduce the models that have been used in the past and thoroughly characterise the model that was developed and used in this thesis. I aim to show that the model that has been used for these investigations is robust, reproducible and reliable enough to be able to postulate theories on the phenomenon of vasospasm based on the results obtained.

3.1.1 Existing models for cerebral vasospasm after subarachnoid haemorrhage

There are many different models for the phenomenon of cerebral vasospasm after subarachnoid haemorrhage reported in the literature[38, 49, 140, 159, 160, 165, 229, 293, 294]. The *in vivo* models involve the injection of autologous blood into the arachnoid space or ventricle of the brain. The single haemorrhage model has been used with dogs[134] amongst other species[65, 104]. This model requires the injection of autologous blood into the cisterna magna and waiting for vasospasm to occur, usually 5-7 days later. This model has been criticised because it was found to lack reproducibility[134]. The autologous blood, when injected into the animal's brain, did not go to the same region of the brain every time and therefore vasospasm was distributed differently in each animal, making direct comparison difficult.

The single haemorrhage model has subsequently been replaced with what is known as the two haemorrhage or double-haemorrhage model[134, 283].

The double-haemorrhage model is frequently carried out on dogs[163, 164, 283]. While anaesthetised and intubated, the animal is kept at a constant temperature and its blood pressure monitored continuously while the right vertebral artery is cannulated approximately 3cm proximal to where it enters the foramen transversarium. Angiography is performed before 4ml of CSF is replaced with 4ml of autologous non-heparinized blood in the cisterna magna. The blood is allowed to clot around the basilar artery and another angiogram taken to assess acute vasospasm. The dog is left to recover for the next day (day 2) and then the replacement of 4ml of CSF with 4ml of blood was repeated as just described with an angiogram before and after the procedure. The dog was then allowed to rest for a day, followed by a fifth angiogram to assess the extent of vasospasm induced. On day 7, vasospasm reaches a peak[294] and images are taken or basilar arteries are harvested for experimentation. Depending on the aim of experiment, different imaging techniques are used. For the determination of vasospasm, angiography is the most appropriate, whereas studies of changes in cerebral blood flow and perfusion are better carried out using magnetic resonance imaging. To correlate the volume and distribution of the subarachnoid clot *in vivo*, computerised tomography in conjunction with angiography is used.

Other models of cerebral vasospasm have been reported[74, 106]. One vasospasm model used a non-cellular blood material glue that has been named Fibrin Glue[74]. Fibrin glue is composed of fibrinogen and thrombin which, when mixed, mimic the final stages of the clotting cascade to form a fibrin clot[279]. It is used as a topical haemostat and to hold together tissues such as nerves while they heal. In the model described above by Honda and Terao, the glue is used to coat the cerebral vessels of dogs so that the CSF is not able to circulate freely around the vessels. They found vasospasm in the animals with most vessels coated with the glue. As a model, it is very invasive, as the animal has to be anaesthetised and have the brain vessels exposed in order to paint on the glue. This model also does not

involve any contact between blood and the artery, as the glue forms a barrier[279] and is therefore not as physiological as the double haemorrhage model. There is also evidence that fibrin glue coating of the vessels may actually prevent vasospasm after subarachnoid haemorrhage by keeping the clot separated from the arteries[74].

There are few established *in vitro* models of cerebral vasospasm after subarachnoid haemorrhage. Various simulations have been used and most use tension development as an indication that vasospasm has been induced[62, 152, 284]. Vasospasm can be induced in vascular smooth muscle in several ways. Balloon angioplasty, platelets, whole blood and longitudinal stretching[62, 152, 284] have all been used to simulate vasospasm *in vitro,* but these types of studies have been criticised[295]. The main point of contention is that the time course of vasospasm in man and animal models is between 4 and 12 days[294] and the *in vitro* models previously used have been on an acute time scale (hours). This disparity in time scale results in difficulty in applying the results to the pathology in humans.

3.1.2 Developing a new model

In order to investigate the phenomenon of cerebral vasospasm after subarachnoid haemorrhage *in vitro*, a reliable, sensitive and reproducible model needed to be developed. Preliminary investigations from this thesis showed that cerebral spinal fluid from patients at risk of cerebral vasospasm stimulated the rate of oxygen consumption of the porcine carotid artery *in vitro*[228]. Further investigation showed that stimulation was not seen in response to CSF from patients without vasospasm (a more complete presentation and discussion of these results can be found in Chapter 4). It was proposed that this observation could be developed into an *in vitro* model of cerebral vasospasm after SAH.

An *in vitro* demonstration of the effect of CSF_S has existed since 1964[35]. Strips of human basilar artery were exposed to cerebrospinal fluid from patients with angiographically visible vasospasm (no other parameters were used). CSF was lyophilised and reconstituted so that the final concentration that the tissue was exposed to was

approximately that of undiluted CSF. Boullin *et al*[33] observed that a relaxation occurred followed by a slow insidious development of tension that was irreversible. Since then, other authors have also reported that CSF from patients who have had a subarachnoid haemorrhage and were at risk of vasospasm (see 2.2.5) elicited tension development in smooth muscle[33].

This tension generation was sometimes found to be irreversible and unresponsive to known vasorelaxants[283]. There have, however, in recent years been suggestions that a disorder of the oxidative metabolism of the muscle may precede any observable changes in contractile function[38, 89, 227, 313]. If this is indeed the case, then an assay that detects disruption in the metabolism of the tissue may prove simpler and more accurate than tension generation. In the porcine carotid artery, tension generation and oxygen consumption are coupled such that changes in oxygen consumption can be directly correlated with changes in activation of smooth muscle[216] as discussed in Chapter 1.

Investigations were carried out in order to ascertain the sensitivity, reproducibility and reliability of the use of the oxygen electrode to detect stimulation of vascular smooth muscle O_2 consumption by CSF_S. The response to CSF_S was also assessed using force measurements in order to determine whether CSF_S was stimulatory with respect to tension generation as well as O_2 consumption.

3.1.3 Extraction of the active constituent from CSF_S

The CSF that is collected from patients who have had a subarachnoid haemorrhage is a cocktail of biological molecules and ions resulting from the leakage of blood into the cranial cavity and CSF. Various methods were employed to ensure that the sample that was used in the model was as free from known vasospastic compounds as possible without destroying its spasminogenic activity. The extraction procedure described in 2.3.8 has an acid extraction as it's first step, which would remove endothelin, and acid-labile prostaglandin-type vasoconstrictive agents.

Although the main thrust of this thesis is towards understanding the changes in the biochemistry of the smooth muscle used in the model, some attempts were made to isolate the constituent of CSF_S that caused the stimulation of O_2 consumption in these experiments. In this section, the various methods employed to try and elucidate the nature of the molecule or molecules that may be causing an increased rate of oxygen consumption will be presented.

3.2 Methods

3.2.1 Collection of CSF

CSF was obtained in a number of ways. In some cases, the subarachnoid haemorrhage patient undergoes an operation to clip the burst vessel, and CSF is collected at this time. This usually takes place within 24 hours of the initial haemorrhage, and contains a large proportion of blood compared to CSF collected by lumbar drain. Brain tissue may also contaminate these samples and because of this, results obtained using these samples are not included in the data presented in this thesis.

The CSF used in this study was collected using lumbar drain collection. This procedure is carried out on most subarachnoid haemorrhage patients (whether they have had the aneurysm clipped during surgery or had a coil inserted to seal the breach) in order to relieve pressure on the brain. These drains may remain in place for a number of days, and a large volume of CSF can be collected from a single patient. Great pains are taken by the clinical staff to keep these CSF collections sterile. This CSF is collected from as early as 24 hours to around 5 days after the initial haemorrhage.

3.2.2 Preparation of CSF

The method developed for the partial extraction and concentration of CSF_S is detailed in 2.3.8. At each stage of the extraction procedure during its development, all fractions were retained and tested for stimulatory activity using the porcine carotid activity

in the oxygen electrode. In this way, any loss of activity could be accounted for, and the method refined.

To determine the effect of freeze-thaw cycles on unextracted CSF, samples were stored at -20°C for 12 months. The samples were defrosted and tested in the oxygen electrode each month. As the impurities were removed from the CSF_S, the activity became more heat and freeze-thaw cycle labile. In the cleanest form of the extracted CSF_S, the activity appeared to diminish rapidly when exposed to light.

Because of this, CSF used in the phosphatase assay (Chapter 6) was extracted immediately (within 24 hours) before use and kept cold and in the dark.

Lyophilised, perchloric acid extracted CSF was used only in the force measurement experiments, whereas the phosphatase assay used CSF that had been extracted according to the methods in 2.3.8. In all other cases, unless otherwise specified, untreated CSF was used.

3.3 Results

3.3.1 Statistical characteristics of the model

Table 3.1 gives the coefficient of variation for several sets of conditions. The means and standard deviations have units of $\mu mol\ min^{-1}\ g\ dwt^{-1}$ and the coefficient of variation is a percentage. The coefficient of variation is an expression of the standard deviation of a population as a percentage of the mean. This allows comparison between different sized means. These data show that the variation between pigs and the variation within pigs when unstimulated are not dissimilar. The greatest variation is seen when different pig carotids are stimulated by the same CSF_S.

Parameter	n	μ (mean)	σ ($s.d._{n-1}$)	C.V. ([σ/μ] × 100) %
Between pigs: control	9	0.162	0.017	10.8
Between pigs: Okadaic acid (1nM)	14	0.887	0.105	11.8
Between pigs: CSF_S	8	1.040	0.128	12.3
Within pig: control	8	0.159	0.016	10.2
Within pig: Okadaic acid (1nM)	8	0.891	0.098	11
Within pig: CSF_S	5	0.739	0.082	11.1

Table 3.1: These statistical analyses show that the model yields data which is both reliable and reproducible. The coefficient of variation is at or below 12.3%, which is an acceptable level of error for a bioassay.

The variation between patients was calculated from all the CSF_S samples that were run, giving a coefficient of variation of 47%, as might be expected from a human patient population.

3.3.2 Sources of error

Other aspects of the suitability of the model were also investigated. Possible interference by oxygen producing or consuming organisms in the chambers were investigated by running null control experiments. The oxygen consumption of chambers containing PSS alone or PSS and CSF without tissue was monitored over several hours to this end. It was found that no significant oxygen consumption in either the buffer only, or the CSF and buffer chambers was observed until after 360 minutes at 30° or after 300 minutes at 37°C.

The temperature that the assay was to be run at required careful consideration. The force measurement assays in the literature are run at 37°C, as are our force measurement assays. The O_2 consumption measurements were taken at 30°C, in order to minimise temperature-induced mitochondrial breakdown and several experiments were also run at 37°C in order to be able to compare the O_2 consumption and force measurement data. Table 3.2 shows the ratio of the rate of oxygen consumption over a 7°C rise in temperature (Q_7)

Condition	**JO_2 @ 30°C**	**JO_2 @ 37°C**	**Q_7**
Control	0.16 ± 0.017	0.39 ± 0.031	2.44
CSF_N	0.17 ± 0.021	0.41 ± 0.033	2.41
CSF_S	0.70 ± 0.160	0.70 ± 0.240	1.00
1nM Okadaic acid	0.84 ± 0.098	0.94 ± 0.108	1.12

Table 3.2: Control is carotid in PSS alone. For each condition, n=8 and errors are standard deviations. JO_2 is in units of μmol $O_2.min^{-1}.g\ dwt^{-1}$ calculated taking the amount of oxygen dissolved in the buffer to be 0.21 μmol $O_2.ml^{-1}$ at 30°C and 0.202 μmol $O_2.ml^{-1}$ at 37°C.

The unstimulated tissue (with CSF_N or no CSF) showed Q_7 values of 2.44 and 2.41, meaning that when the temperature is raised by 7°C, the rate of O_2 consumption (JO_2) in increased 2.44 or 2.41 times. However, the stimulated tissue showed Q_7 values of 1.00 and 1.12 representing little difference between the stimulated rates at 30° C and 37°C. n=8 for each experiment.

The effect of time on the activity of the CSF was also investigated and no significant reduction of activity was observed in CSF samples that were freeze/ thawed once a month for 1 year (data not shown). The variation between stimulation at 180 minutes over 12 months lies within one standard deviation due to the variation between pigs.

The time at which the CSF was collected subsequent to haemorrhage did not seem to affect the stimulatory or non-stimulatory nature of the CSF, or the magnitude of the stimulation. A bag of CSF collected from a patient after 24 hours had the same magnitude of stimulation of O_2 consumption as a bag from the same patient collected after 5 days. This is illustrated in Figure 3.1.

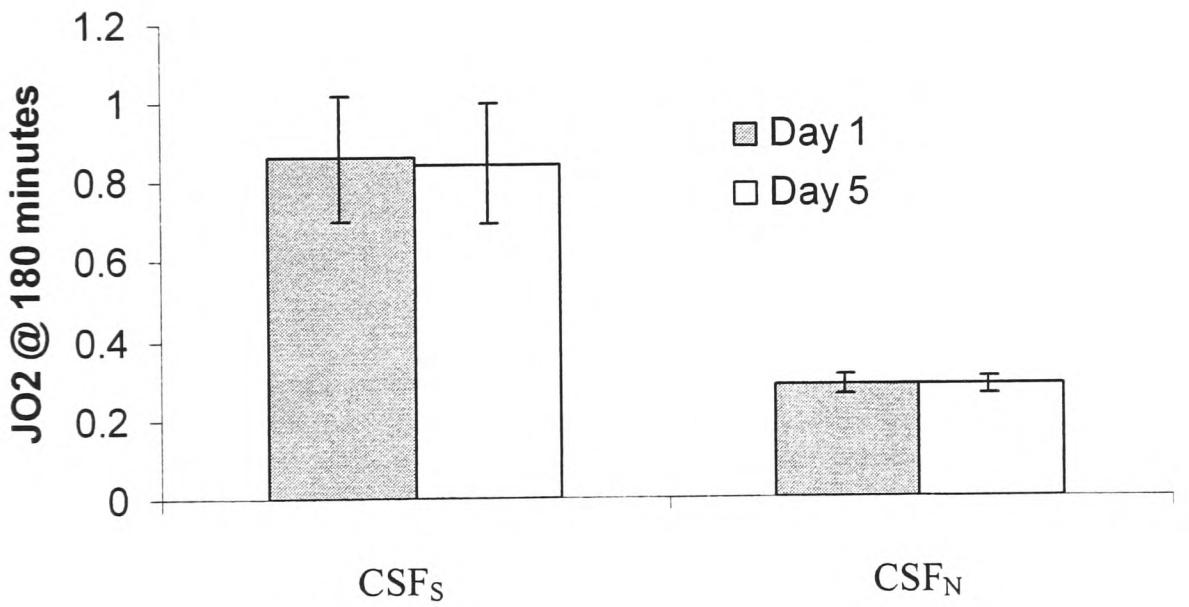

Figure 3.1. Each bar represents the rate of O_2 consumption 180 minutes after addition of a 1 in 30 dilution of CSF in μmoles min^{-1} g dwt^{-1} . CSF was collected at 24 hours or 5 days after haemorrhage. CSF_S n=5 (different patients) , CSF_N n=3 (different patients). Each sample is tested using a different carotid. Each day one and day 5 collection patient sample is run once. Errors are standard deviations of the between patient data.

Experiments were carried out in order to determine a suitable concentration of CSF to use in the model. Dose response curves were constructed for several CSF_S samples and a one in thirty dilution was found to cause a maximum stimulation in all cases. This was used in all subsequent O_2 consumption experiments unless otherwise stated. Figure 3.2 shows a typical dose response curve with rate of O_2 consumption at 180 minutes plotted against dilution of CSF_S.

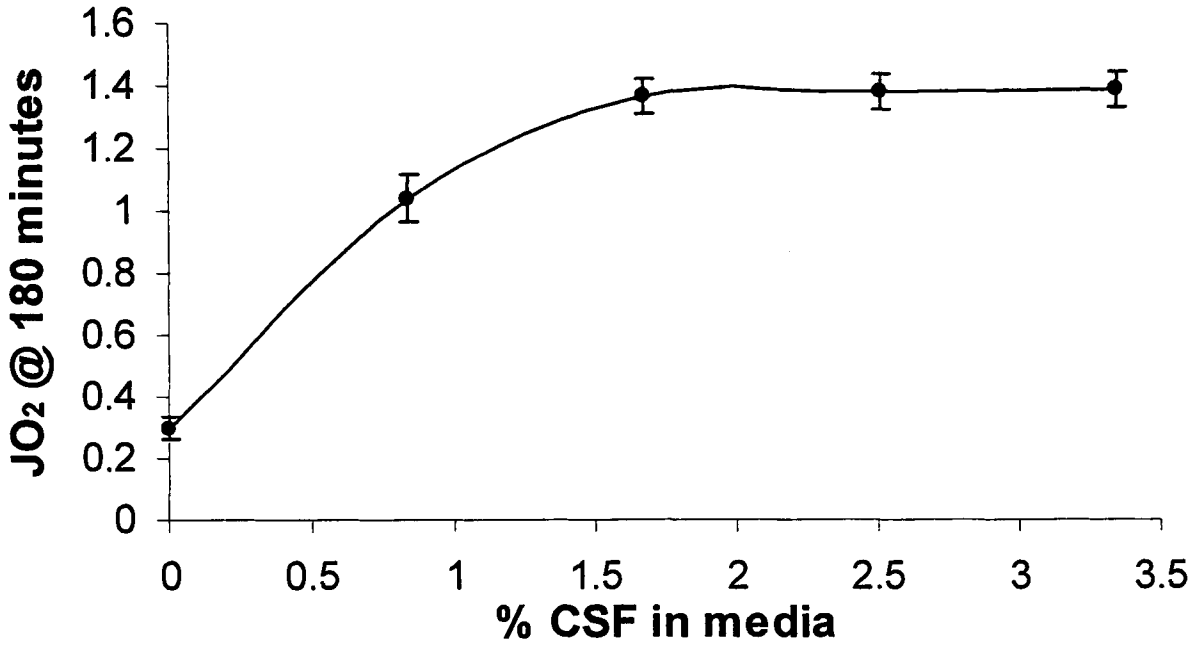

Figure 3.2: A single patient CSF_S sample stimulating JO_2 (μmol $O_2.min^{-1}.g\ dwt^{-1}$ at 4 different dilutions. Each point is taken at 180 minutes after addition of CSF_S to the porcine carotid, n=4 for each point, and errors are standard deviations. Each sample is a different patient CSF tested on a different carotid.

The tissue used in this model, the porcine carotid artery, although similar to the human basilar artery, has some key differences. The wall of the porcine carotid is thicker, comprising much more connective tissue than the human basilar artery. The human basilar artery also has many small branches, whereas the porcine carotid is not as branched.

In order to check that the same stimulation would be seen in the human basilar artery, human samples were obtained (with post mortem consent from the next of kin) and the O_2 consumption experiments carried out using the human basilar artery. Figure 3.3 shows that stimulation is clearly obtained in human tissue as well as porcine tissue, but that rat tissue has a smaller range over which it can be stimulated by CSF_S. A similar response was seen with guinea pig aorta and porcine cerebral arteries.

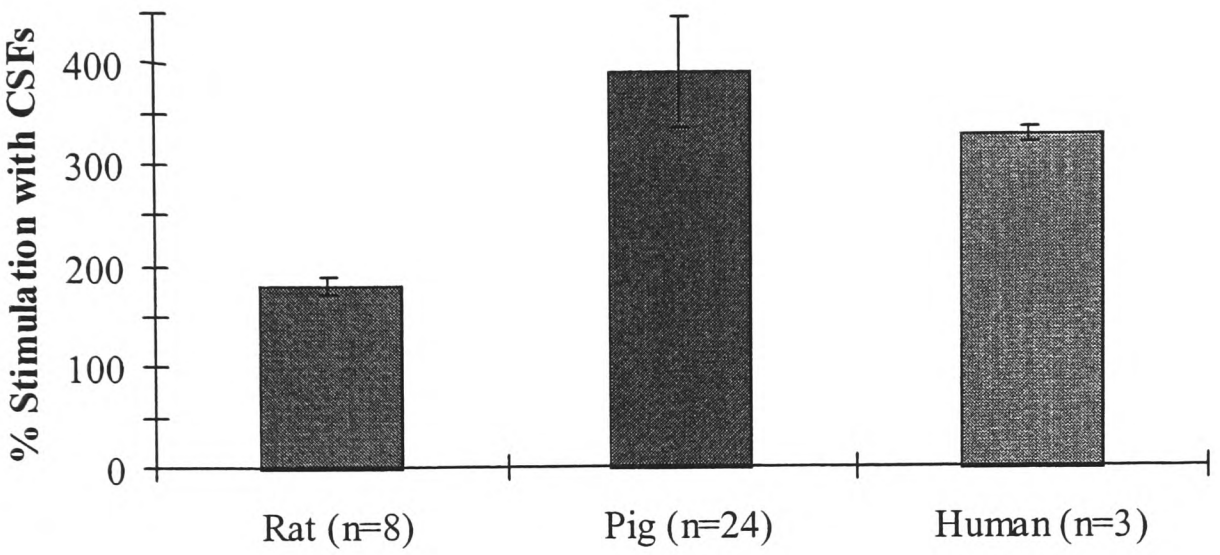

Figure 3.3: A comparison of the effect of CSF_S on porcine carotid arteries (n=24) human basilar arteries (n=2) and rat thoracic aortae (n=8). Error bars are σ_{n-1}. % stimulation with CSF_S is calculated by dividing the CSF_S stimulated rate of O_2 consumption by the basal rate and multiplying by 100.

3.3.3 Comparison to traditional model

The accepted method, *in vitro*, of determining whether a CSF sample is from a vasospastic patient or not is to measure the tension generated when it is added to smooth muscle preparations[32, 35]. In order to make a direct comparison in this way, a number of CSF samples were used in concomitant measurements and the results reported in Figure 3.4.

These data were gathered at 37°C using perchloric acid extracted freeze-dried CSF_S added to the chamber so that the final concentration is approximately equal to undiluted CSF.

There is a trend between the level of stimulation of O_2 consumption and the maximum tension generation. The gradient of the part of the relationship that is linear (between 0.75 and 1.25 μmoles O_2 min^{-1} g dwt^{-1}) is 15.766 Nm^{-2} for every increase in rate of O_2 consumption of 0.1 μmol min^{-1} g dwt^{-1}. The increase of tension from untreated, CSF free baseline levels was an average of 8 fold, whereas the increase in the rate of O_2 consumption from a similar baseline was 5 fold.

3.3.4 Comparison to clinical findings

Dr. Zayne Domingo carried out a statistical analysis correlating the classification of the CSF using the stimulation of O_2 consumption and the occurrence of vasospasm in the

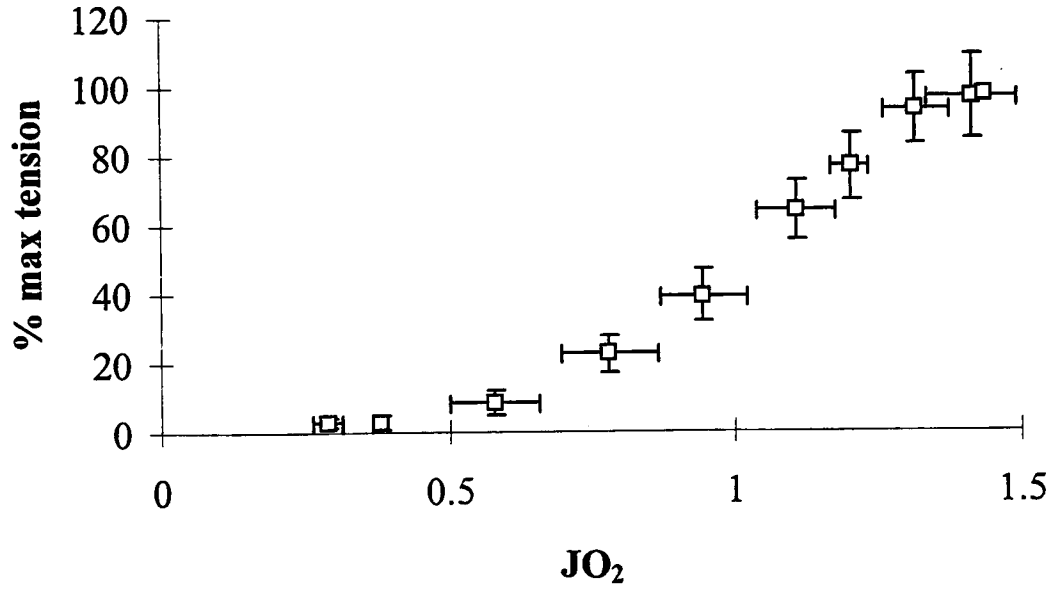

Figure 3.4: Each point represents one pair of data points for O_2 consumption (μmol min^{-1} g dwt^{-1}) and tension generation (N m^{-2}) for a single CSF_S sample. Each sample was run 3 times, and errors are standard deviations. This relationship appears again as Figure 4.7.

patients whose CSF was tested. He found that 89 ± 9% of the patients that yielded CSF_S classified using stimulation of O_2 consumption developed angiographically evident vasospasm. Of the remaining 11%, some died, and others were aggressively treated with non-typical therapies.

3.4 Discussion

3.4.1 Existing models

When designing an experimental model, there are several factors to be taken into consideration. First, is there already a model in existence that can be used? In the case of cerebral vasospasm after subarachnoid haemorrhage, the answer to that question is none that are appropriate for the purposes of this thesis. The two haemorrhage model has become the established *in vivo* model, but there are, as yet, no adequate *in vitro* models of vasospasm. All the *in vitro* methods that have been reported utilise tension measurement as a way of evaluating vasospasm and the way that the vasospasm is induced makes them unsuitable models for cerebral vasospasm[295]. The vasospasm in existing models is induced by some chemical or mechanical stimulation of the tissue. Clearly, this is unsatisfactory and non-physiological. The main criticism of these methods is that the vasospasm induced is of an acute nature, whereas cerebral vasospasm after subarachnoid haemorrhage in humans may take anywhere between 3 and 12 days[294]. The most reproducible *in vitro* simulation of cerebral vasospasm is found in those studies that use cerebral vessels taken from animals subjected to the two-haemorrhage protocol[163, 165, 283]. This, however, involves two complex, invasive procedures and a week of waiting as well as care of the animals in order to achieve vasospasm.

3.4.2 Temperature effects

The decision to carry out O_2 consumption measurements at 30°C and the tension measurements at 37°C required careful consideration. Running the O_2 electrode at 37°C resulted in a reduced range of response to both CSF_S and 1nM okadaic acid (Table 3.2). The baseline respiration was higher, but the stimulated rate, in both cases, was little higher than at 30°C. This may be due to the myosin MgATPase reaching a temperature-dependent V_{max}, preventing the same range of response to CSF_S stimulation at 37°C as at 30°C. There were also problems with bacterial growth in the chambers at 37°C. Non-tissue respiration

started to interfere with experimental results at 300 minutes, 60 minutes earlier than at 30°C. This was tested by measuring the oxygen consumption of chambers containing buffer alone, or buffer and CSF at a dilution of 1 in 30. A rather simplistic explanation could be that the tissue simply cannot respire any faster, it may have reached its maximum.

It has also been reported that *in vitro* experiments involving O_2 consumption run at 37°C may compromise mitochondrial function[254, 255] and so many experiments involving O_2 consumption measurements were carried out at 30°C. In order to allow comparison between these data and previously published data, O_2 consumption measurements were carried out at 30°C, with some specific experiments carried out at 37°C.

The force measurements, however, were carried out at 37°C, as the changes in contractile function with temperature are not fully characterised. Current research suggests that the rate of isometric force development and maximal shortening velocity are temperature dependent[130]. There may be a rate limiting effect of temperature on the transition of the contractile proteins into force generating states[230]. The temperature dependence of the maximal shortening velocity indicates effects of temperature on the reactions associated with cross bridge detachment and there is also a small temperature dependence of steady state force maintenance that is not seen in skeletal muscle[36, 230]. This means that force measurement data has been obtained at 37°C.

3.4.3 Suitability of the model

The model that has been described in this chapter overcomes some of the problems of reproducibility and reliability of the existing models described previously (3.1.1). The tissue used in the model, the porcine carotid artery, is freely available and homologous to the human basilar artery with respect to load *in vivo* and structure. The strain of pigs from which the carotids are obtained (Large White Land pig) are reasonably homogeneous, which also aids reproducibility. The substance used to induce the vasospasm is the same substance that is thought to induce vasospasm *in vivo*, namely CSF_S. The problem of the

discrepancy in the time course between the *in vitro* model and what happens in humans in eliminated by using CSF from patients who are at risk from vasospasm. That is, the incubation of the blood and CSF mixture for the appropriate length of time is carried out in entirely physiological conditions, i.e. inside the patient.

Statistically, this model is robust. The O_2 consumption measurements gave a classification of vasospastic for all the CSF_S samples that stimulated tension development that were tested (n=8) and similarly, all the CSF_N samples that did not stimulate tension generation were classified as non-stimulatory using O_2 consumption measurements (n=7). The coefficients of variation calculated for the conditions described in Table 3.1 indicate the reproducibility and reliability of the model. These values have been minimised by using a method of detection that is reliable and reproducible in itself and the dry mass of the tissue to calculate the rates of O_2 consumption.

The relationship between tension and O_2 consumption shown in Figure 3.4 indicates that the model is as accurate as the previous method of evaluation (tension generation). It may also be more sensitive, as the O_2 consumption rises before any response is seen in terms of tension generation (see Figure 3.4) although tension generation is stimulated over a greater range than O_2 consumption. These results, in terms of characterisation of the pathology of vasospasm, are discussed at length in Chapter 4, section 4.4.

3.4.4 Practical considerations

The model must be practicable in a laboratory setting. The equipment required to measure O_2 consumption is a standard piece of laboratory equipment, the Clark type oxygen electrode, whereas force measurement apparatus is somewhat specialised, only usually found in muscle research laboratories. Problems arising from dealing with human body fluids must also be taken into consideration. The CSF used for force measurements has to be lyophilised and PCA extracted before use and the volume of contaminated waste

is around 30-150ml per assay. In contrast, the CSF is injected untreated into the O_2 electrode chambers and the waste is limited to between 1 and 6ml per assay. In addition to this, the O_2 electrode chambers are sealed, thus containing any hazard.

3.4.5 Conclusions

The model described in this chapter is more suitable and more practical than force generation measurements with regard to the research presented here. For the purposes of this investigation, CSF_S stimulation of JO_2 in the porcine carotid artery is a good model for cerebral vasospasm after subarachnoid haemorrhage, allowing the investigation of the mechanism of this pathology.

O_2 consumption measurements appear to be more sensitive to stimulation by CSF_S than force measurements, indicating that changes in oxidative metabolism occur at lower CSF_S levels than in contractile function. This allows investigation of possible therapeutic intervention.

Limitations of the model include the variation between carotids from different pigs and inter-patient variation. The difference between responses elicited by CSF_S at the two test temperatures (30°C and 37°C) is also not fully understood and so the temperature sensitivity of the experiments is an unknown quantity. Other, as yet, uncharacterised vasoactive compounds may also be present in the CSF.

4.Characterisation of CSF_S stimulation of O_2 consumption and tension

4.1 Introduction

This chapter contains the results of experiments performed in order to examine the mechanism of action of the active constituent of the CSF_S. Various inhibitors and agonists were employed to dissect out a possible pathway of action. The suitability of this model of cerebral vasospasm after subarachnoid haemorrhage was discussed in the last chapter including a statistical assessment.

4.1.1 Intracellular signalling in smooth muscle.

4.1.1.1 Protein kinase A (cAMP dependent protein kinase).

PKA is involved in the control of ion channels in smooth muscle as well as other functions. Through the control of these channels PKA and raised intracellular cAMP levels can influence contractility and energy metabolism. Other effects on contractility can also be mediated by PKA, although these functions are less numerous than the ion channel effects.

It was suggested by a number of authors[178, 234] that PKA may phosphorylate MLCK and thus decrease the affinity of the kinase for calmodulin. In effect, this reduces the sensitivity of the contractile system to calcium. Cornwell *et al*[50] found that nitric oxide (NO) effects which had previously been attributed to cGMP dependent protein kinase were in fact due to PKA. They showed that [NO] greater than 1μM raised the levels of intracellular cGMP so much that PKA was activated.

It was previously thought that the L-type voltage dependent calcium channels of smooth muscle were controlled by phosphorylation by cAMP dependent protein kinase[170]. In cardiac muscle, the main point of control of the L-type voltage dependent calcium channels (LVDCC) is via phosphorylation by PKA. A PKA inhibitor was used to determine any involvement of this kinase in the ætiology of vasospasm.

4.1.1.2 Calcium regulation of smooth muscle contraction

Calcium concentration is possibly the most important determinant of smooth muscle contractility[243] (1.4). Here, I will describe, in brief, the role of protein kinase C and intracellular calcium concentration in smooth muscle contractile function. This information will aid the interpretation of results obtained using staurosporine (PKC inhibitor) and the calcium channel blockers nimodipine and nifedipine.

Currently, Nimodipine® is the therapy of choice administered to subarachnoid haemorrhage patients as a preventative measure against the development of vasospasm[107]. Other calcium channel blockers such as nifedipine and nicardipine have been utilised, but without the same effect[107]. There have been a number of studies examining the effects of administration of nimodipine to patients after subarachnoid haemorrhage and there are conflicting results. Some reports show that outcome is improved when nimodipine is used[8, 14, 30, 81, 193, 309]. Others show that there is less ischaemic change in the patient's brain[15, 34, 78, 91, 153, 224]. With the exception of the experiments of Grotenhuis[81] nimodipine significantly improves neurological outcome without altering the lumenal diameter of the vessels. For nimodipine to be effective against development of cerebral vasospasm, the ætiology of vasospasm must be assumed to be due to a rise in intracellular calcium concentration. This may not be the mechanism, however, because the prevention of calcium influx into neurones may be the cause of the improved neurological outcome seen in patients treated with nimodipine. An increase in lumenal diameter is not seen concomitant with this

increase in neurological outcome. Thus, nimodipine may not have equivalent effects on neurones and vessels.

Intracellular free calcium acts as a second messenger in smooth muscle contraction (section 1.4). Like all second messengers, its intracellular concentration is strictly regulated. Although there is an extracellular calcium concentration ($[Ca^{2+}]_O$) of around 1-2 $\times 10^{-3}$ M, the intracellular free calcium concentration ($[Ca^{2+}]_i$) is kept to sub-micromolar levels.

4.1.1.3 Protein kinase C

The classification, distribution and specificity of protein kinase C are introduced in 1.5.4.2. Unlike protein phosphatases, protein kinases are the products of a small related family of genes[47]. There is much evidence to suggest that PKC has an important role in smooth muscle contraction[149, 165, 238, 289]. Several smooth muscle preparations have been shown to develop tension in response to phorbol esters and diacyl glycerol analogues[52]. In addition, sustained, elevated levels of diacyl glycerol production are observed in smooth muscle in response to agonists which are known to cause sustained contraction such as angiotensin II[80] and carbachol [276]. The source of this diacyl glycerol was found to be the phospholipase D (PLD) mediated cleavage of phosphatidyl choline (PC)[150] which produces DAG but not inositol triphosphate (IP_3). It has been reported that PKC is translocated from the cytosolic to the membrane fractions transiently in response to stimulation[87]. This means that during sustained contraction, PKC is activated, but intracellular calcium stores are not opened by IP_3, consistent with the low levels of intracellular calcium seen in sustained contractions. Walsh *et al*[289] postulates the mechanism for the calcium-independent PKC-mediated stimulation of sustained smooth muscle contraction as shown in Figure 4.1. Protein kinase C activation has been implicated in the ætiology of cerebral vasospasm after subarachnoid haemorrhage. Ohta *et al*[201] report that there is 12-hydroxyeicosotetranoic acid (12-HETE) production from the platelets in the subarachnoid clot. The time course of the

increase in 12-HETE concentration corresponds to the time course of development of vasospasm after subarachnoid haemorrhage in man[294]. They postulate that 12-HETE causes an accumulation of DAG in the basilar artery by inhibition of DAG-kinase. This leads to a sustained activation of protein kinase C and a concomitant sustained contraction. DAG is produced from non-IP_3 forming reactions as described previously using PLD. This DAG then activates the isoenzyme PKCε, which phosphorylates calponin[269, 305]. This phosphorylation would result in the release of calponin from the thin filaments and the relief of inhibition of cross bridge cycling. A slow, sustained contraction then results as the level of baseline phosphorylation is low in this kind of stimulation[304]. These observations are consistent with the hypothesis that PKC plays a role in the sustained contraction of smooth muscle. Since vasospasm is a chronic contraction, it is feasible to suggest that a chronic activation of PKCε may lead to a pathological vasoconstriction.

4.1.1.4 Endothelin and smooth muscle.

Endothelin is widely believed to be involved in the ætiology of cerebral vasospasm after subarachnoid haemorrhage[240, 245, 299, 310, 318-320]. Clinical trials using the endothelin antagonists Bosentan and BQ123 have however proven inconclusive[245] and evidence for the involvement of endothelin is contested[166].

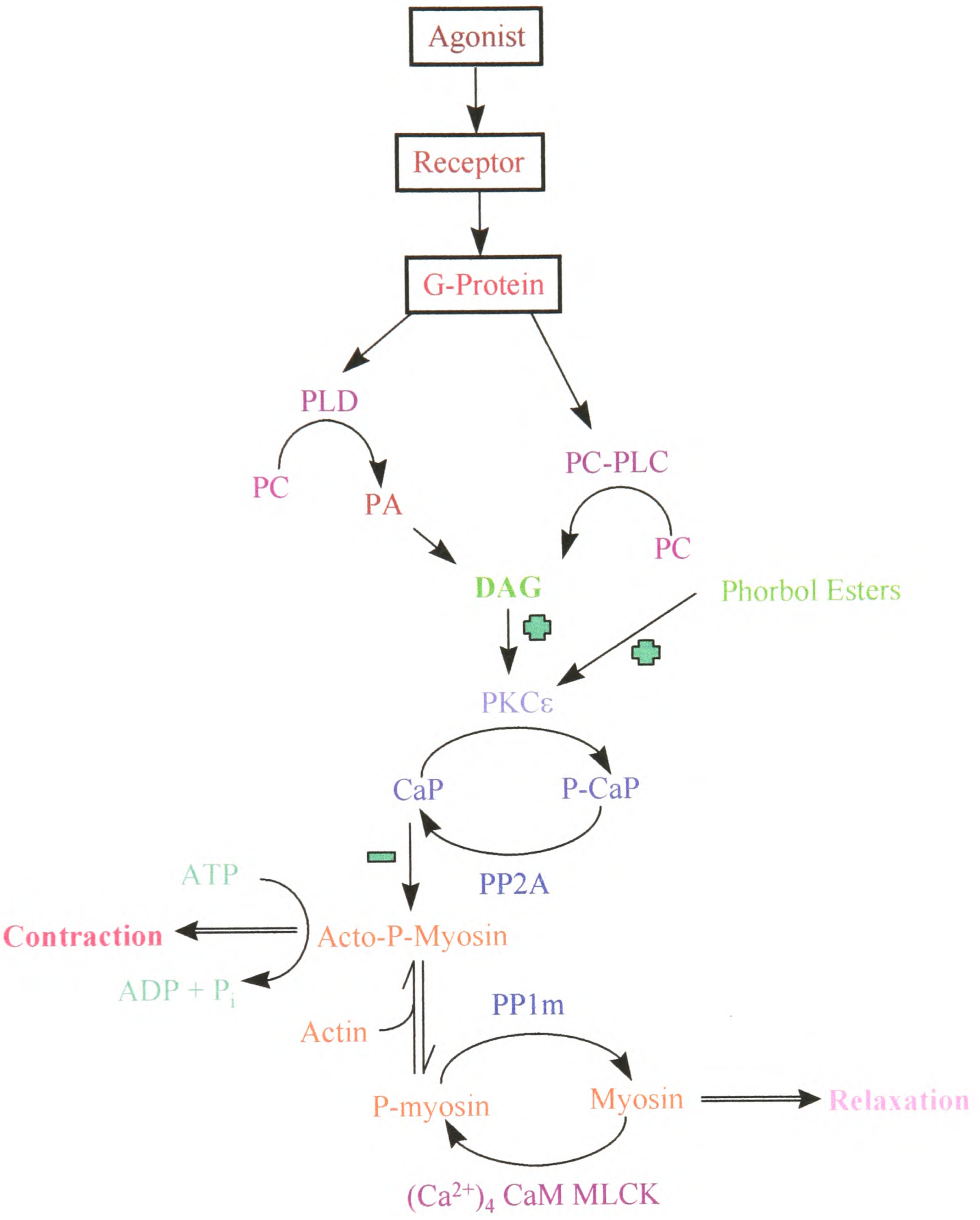

Figure 4.1: The-calcium independent PKC-dependent contraction of smooth muscle possibly implicated in cerebral vasospasm after subarachnoid haemorrhage. CaM, calmodulin; CaP, calponin; DAG, *sn*-1,2-diacylglycerol; MLCK, myosin light chain kinase; PA, phosphatidic acid; PA-PHA, phosphatidate phosphohydrolase; PC, phosphatidylcholine; PC-PLC, phosphatidylcholine specific phispholipase C; PKC, protein kinase C; PLD, phospholipase D; $PP1_M$, myosin light chain phosphatase (myosin-associated type 1 protein phosphatase); PP2A, type 2A protein phosphatase.

The vasoactive peptide secreted by endothelial cells was first described as endothelin (ET, later ET1) by Yanisagawa et al in 1988[311]. So far, there are three functionally similar proteins in the endothelin family (ET1, ET2 and ET3) and the related peptides, sarafotoxins (S6a, S6b, S6c and S6d) in the family of structurally and functionally related peptides. They are all composed of 21 amino acids and contain two disulphide bridges. There have, so far, been two ET receptors characterised in smooth muscle, the ET_A and ET_B receptors. The endothelin inhibitor used in this investigation is called PD142893 and is an analogue of endothelin, blocking both the ET_A and ET_B receptors.

4.1.1.5 α_1-Adrenergic receptor agonist effects on smooth muscle.

α_1-Adrenergic receptor agonists induce contraction in smooth muscle via a G-protein coupled signal transduction process. Phospholipase C is activated by conformational changes in the receptor, which is coupled, to a stimulatory G protein. Phosphatidylinositol bisphosphate is then hydrolysed to inositol triphosphate (IP_3) which allows intracellular calcium release by opening intracellular IP_3 gated calcium stores and liberates diacyl glycerol, which activates PKC. The rise in intracellular calcium induces a contraction by binding to calmodulin and activating MLCK.

4.1.2 Force-function relationship in smooth muscle.

This subject in introduced in 1.3.3. Lynch and Paul described the evidence which supported the postulation that glycolytic and oxidative metabolism may be compartmented in smooth muscle[156]. Since then, there has been a volume of literature which describes and investigates this compartmentation[44, 122, 124, 125, 156, 216, 219, 220]. There are a number of experimental observations that support the compartmentation theory. It was observed that the Ca^{2+}ATPase and membrane pumps were more efficient when utilising ATP produced

from glycolysis than from oxidative metabolism[156, 220], indicating that this ATP source is more accessible to the membrane related energy utilising functions than the oxidatively produced ATP. Ouabain was found to abolish lactate production, further supporting the coupling of glycolytic metabolism to membrane pumps[124]. A coupling of energy supply and utilisation, or an energy shuttle was also suggested[218]. These findings were substantiated by ^{14}C labelling experiments which proved that 90% of glucose taken up by the tissue appears as lactate[126]. It was found that 20% of the ATP production in resting smooth muscle was glycolytic[124], which accounts for the well known characteristic of vascular smooth muscle having aerobic lactate production. Localisation of the glycolytic enzymes in smooth muscle appears to be with the thin filaments of actin, the sarcoplasmic reticulum and the plasma membrane, all sites of energy utilisation[124].

The role of ATP produced by oxidative metabolism is now discussed because of its functional link to contractility. Vascular smooth muscle depends upon oxidative ATP for contractile work which accounts for around 70% of its ATP demands[124]. Arnqvist *et al* reported that glycogen was depleted and lactate produced at O_2 tensions less than 20% indicating increased glucose mobilisation and metabolism compensating for the reduced O_2 consumption contribution to the ATP[10]. This effect can also work in reverse. Incubating resting tissue with octanoate, a known inhibitor of aerobic glycolysis[26], inhibits the lactate production of the vessels by 64% and increases oxygen consumption presumably in order to compensate for the loss of ATP production from glycolysis[24]

The functional coupling of tension generation and oxygen consumption is such that oxygen consumption measurements can be used to estimate activation processes in smooth muscle. Wingard, Paul and Murphy[307] correlated the O_2 consumption of the porcine carotid artery with activation energy (J_A), by varying the length under constant activation and varying activation at long (1.8 times L_O) length. They found that the relationship was linear. In our model of cerebral vasospasm, the rate of oxygen consumption is stimulated

without increase in lactate production (see 4.2.2), indicating a specific stimulation of oxygen consumption, not of glycolysis.

4.2 Methods

The methods used to gather the data presented in this chapter are detailed in Chapter 2. Concentrations of pharmaceutical agents used and conditions for individual incubations are given in 2.3.6.

4.2.1 Force measurements

The haemorrhagic CSF resulting from the SAH used in these experiments contained a large amount of protein, which, when gassed, caused foaming. The foaming of un-extracted CSF when aerated with a sintered glass aerator constituted an unnecessary biohazard. To decrease this, the CSF was PCA extracted before application to tissue in an organ bath on the force measurement apparatus. The PCA extracted CSF was freeze-dried and added to the organ bath so that the final concentration was approximately equal to undiluted CSF. This concentration of CSF has been used previously in the literature[33, 35] and allowed comparison of our results with literature values. This concentration was also used because a 1 in 30 dilution, as used in the oxygen consumption experiments, elicited no increase in tension. This observation is discussed in 7.1.5.

As okadaic acid becomes a non-specific phosphatase inhibitor above 5 nM and toxic at 10 nM (Figure 4.3), it was used at a concentration of 1 nM for force measurement experiments. Okadaic acid was also used at concentrations of 1nM for force measurements as increasing this to 30 nM for the force measurements (in proportion to the increase in CSF_S concentration between these two protocols) would elicit non-specific phosphatase inhibition and toxicity.

4.2.2 Lactate production

The method used to measure the lactate in the buffer is given in 2.3.5, as are the incubation conditions for the analysis of lactate production in response to CSF_S.

4.3 Results

4.3.1 Oxygen consumption measurements

The initial observation that CSF from patients at risk of vasospasm (see Chapter 3) when applied to vascular smooth muscle *in vitro* stimulated the rate of oxygen consumption was made by Joseph F. Clark. It was found that adding CSF at a 1 in 30 dilution to porcine carotid arteries in the oxygen electrode elicited an up to 5 fold increase in the rate of oxygen consumption. This stimulation was not observed when CSF from patients without risk of vasospasm was used. The results of this and further experiments are shown in Figure 4.2. Following the preliminary observations, CSF was separated into CSF_S and CSF_N on the basis of their stimulation or lack of stimulation of the rate of O_2 consumption of the porcine carotid artery as determined using O_2 consumption measurements and not on the basis of clinical observation.

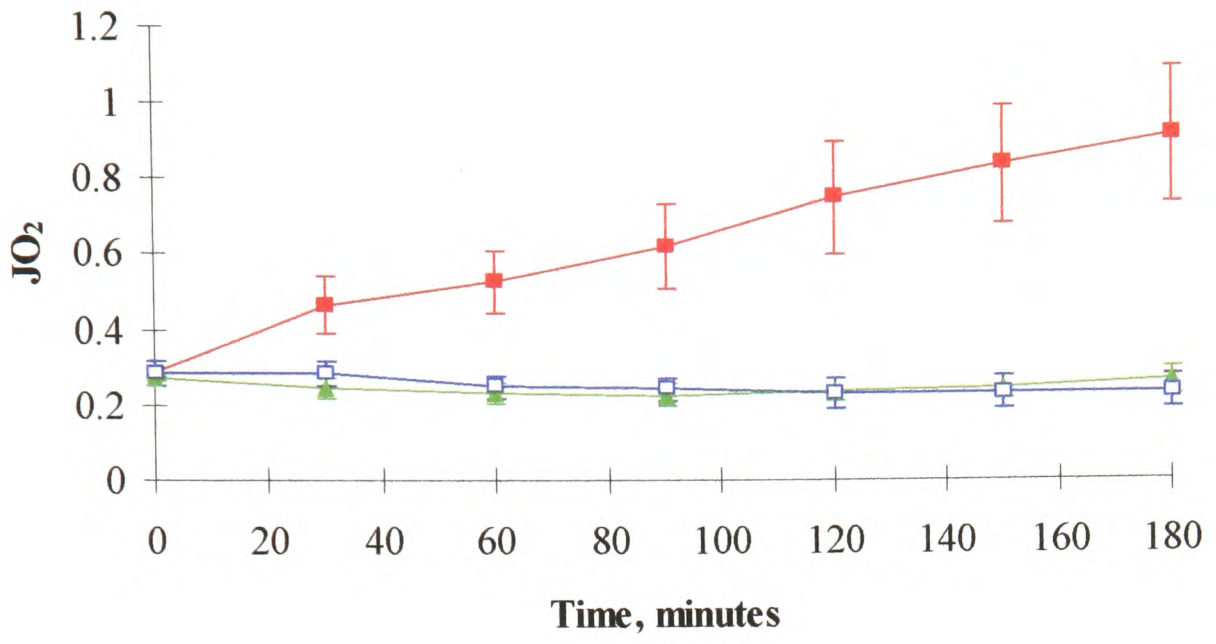

Figure 4.2: The stimulation of oxygen consumption by CSF_S, but not CSF_N at 30°C. CSF_N (open squares, n=8) did not stimulate the rate of oxygen consumption above control basal levels (filled triangles, n=34). However, the CSF_S (filled squares, n=24) stimulated respiration significantly. JO_2 is the rate of O_2 consumption in μmol min^{-1} g dwt^{-1}. Errors are SEM values.

The effect of each agent alone on the tissue (null effect) is given, as well as any effect of each agent on CSF_S induced stimulation. The tissue was pre-incubated in the agent at the concentrations given in Table 2.2. for 30 minutes before exposure to a 1 in 30 dilution of CSF_S. A number of inhibitors were employed in order to characterise the mechanism of the CSF_S stimulation of O_2 consumption in the porcine carotid artery.

Agent	Null effect	n	% Change	n
Dobutamine	+8±0.9%	4	−53±6%	3*
Endothelin	+185±21%	8*	-	-
Histamine	+75±8%	4*	−53±5%	3*
Noradrenaline	+5±0.4%	4	−48±6%	3*
Okadaic Acid	+279±22%	8*	-	-
PD142893	+12±2%	3	+11±2%	6
PKA Inhibitor	+79±9%	3*	+26±4%	3
Staurosporine	+45±5%	3*	+23±3%	3

Table 4.1: The null effect is given as the % increase (+) or decrease (-) in rate of oxygen consumption elicited by the agent alone at 180 minutes from baseline JO_2. The effect of the agent on the CSF_S induced stimulation of JO_2 is given as the percentage increase (+) or decrease (-) in rate of CSF_S stimulated oxygen consumption. The number of times the experiment was performed on different carotid arteries is given in the column titled **n** to the right of each parameter. * denotes a significant difference ($p \leq 0.05$) between the effect of CSF_S with and without the agent.

The addition of okadaic acid to the tissue on the force measurement apparatus elicited no response, even though a significant stimulation of oxygen consumption was observed with the same concentration of okadaic acid (1 nM). Observed stimulations of force generation by okadaic acid in the literature have only been achieved with toxic doses of the inhibitor. A dose response curve for okadaic acid stimulation can be seen in Figure 4.3.

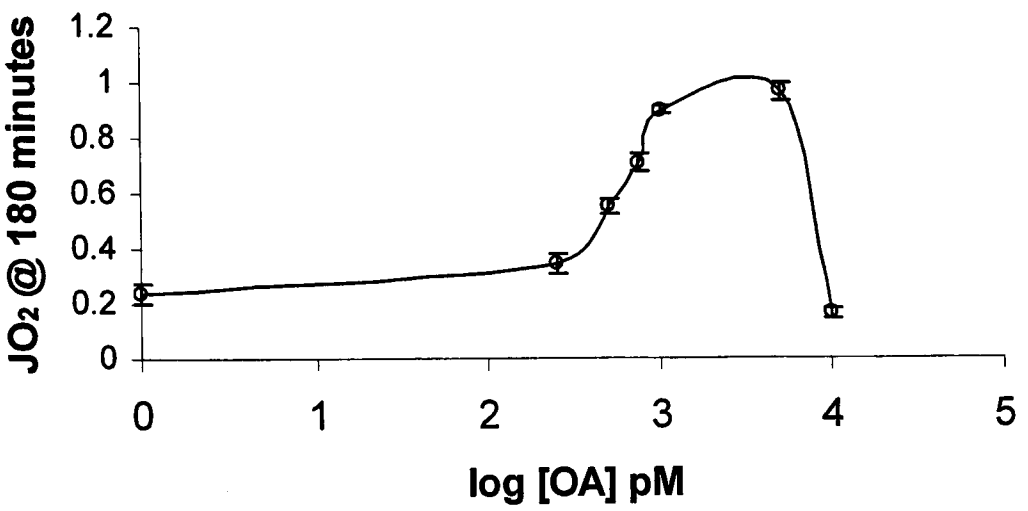

Figure 4.3: Dose response curve of okadaic acid in terms of rate of O_2 consumption at 180 minutes under 6 different concentrations of okadaic acid. For each point, n=8 and errors are standard deviations. The first 5 points of this graph appear again as Figure 6.2.

It was found that the endothelin A and B receptor antagonist PD142893 did not inhibit significantly the CSF_S stimulation of oxygen consumption (Figure 4.4 open squares). This was surprising because the involvement of endothelin in cerebral vasospasm after subarachnoid haemorrhage has been extensively cited in the literature[240, 245, 318-320] and endothelin antagonists such as bosentan[245] and BQ 123[320] have reached the stage of clinical trials in humans, although with no significant improvement in outcome[104]. From Figure 4.4, it can be seen that the CSF_S stimulated rate of O_2 consumption of the PD142893 pre-treated tissue is depressed significantly compared to CSF_S treated tissues for the first 120 minutes. The rate then increases to above (but not significantly) the CSF_S stimulated tissue.

In order to investigate the possible involvement of endothelin in our model of vasospasm, control tissue and tissue pre-incubated with 1 μM PD142893 (an endothelin inhibitor that acts extracellularly) was exposed to CSF_S or 10^{-5} M endothelin. The results of this can be seen in Figure 4.4. It can be seen that the inhibitor has a significant action against the endothelin induced stimulation (open circles) of oxygen consumption in these vessels, but the CSF_S induced stimulation was not significantly reduced (open squares). The null effect of PD142893 is discussed in 4.4.2.

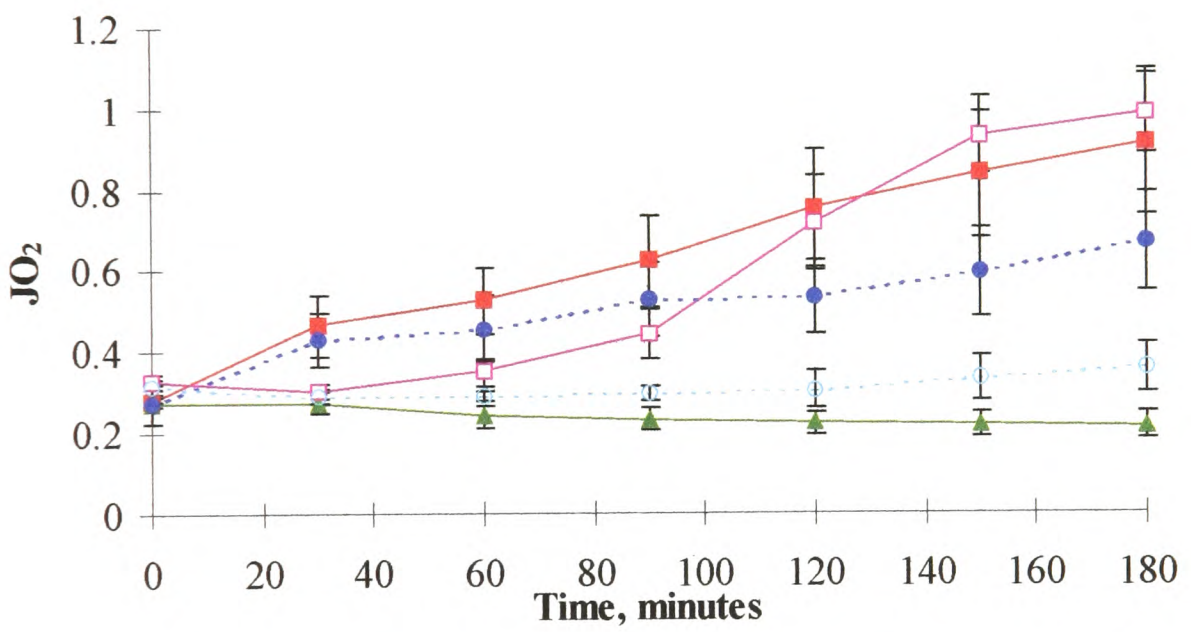

Figure 4.4: Effect of PD142893 on CSF_S and endothelin induced stimulation. Tissue was pre-treated with PD142893 and then exposed to either CSF_S (open squares, n=5) or endothelin (open circles, n=6). The effect of CSF_S alone (filled squares, n=34) and endothelin alone (filled circles, n=8) are also shown for comparison. Control, basal respiration is also shown (filled triangles, n=34). JO_2 is the rate of O_2 consumption in μmol min^{-1} g dwt^{-1}. Errors are SEM values.

It was also found that the α_1-adrenergic receptor agonists, noradrenaline and dobutamine showed a significant level of protection against the CSF_S induced stimulation of oxygen consumption (see Table 4.2). Such a protective role was first observed when patient samples were obtained from a vasospastic patient before and after treatment with dobutamine and noradrenaline. The vasospastic patients were placed on this combinational therapy subsequent to subarachnoid haemorrhage to treat a concomitant heart condition. There was a remarkable decrease in activity of the patient's plasma following a combination of dobutamine and noradrenaline treatment.

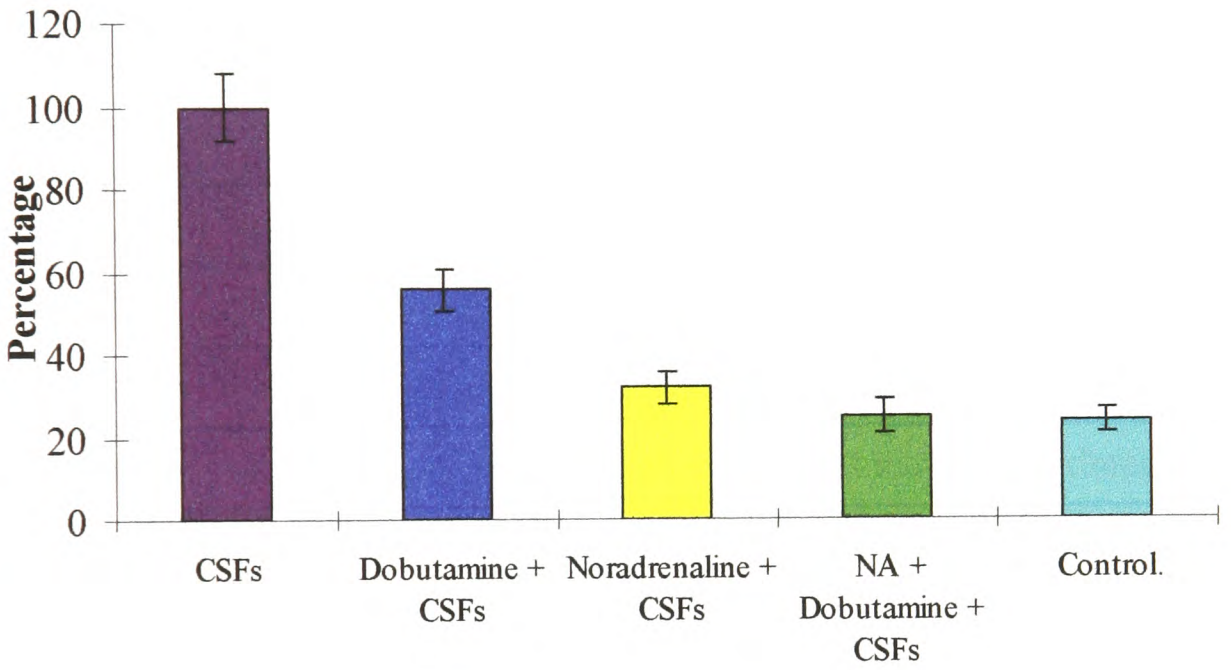

Figure 4.5: The protective effects of different α_1-adrenergic receptor agonists. The average stimulation of respiration by CSF_S (n=5) was assigned a value of 100% and the stimulation elicited by the CSF_S after pre-treatment with dobutamine (n=5) and noradrenaline (n=5) are expressed as a percentage of this. The effect of a combination of noradrenaline and dobutamine (n=5) is also shown. Control respiration is also shown (n=34). Errors are SD values.

In order to investigate this protection in more detail, histamine, noradrenaline and dobutamine were all used in the concentrations shown in Table 2.2 to pre-treat the tissue for 30 minutes prior to exposure to a number of different CSF_S samples. Figure 4.5 shows the relative protection afforded by each of the agents and a combination of noradrenaline and dobutamine as was administered to the patient.

4.3.2 Force and simultaneous force and O_2 consumption measurements.

It has been shown previously that CSF from vasospastic patients is able to elicit tension generation[33, 35]. We set out to determine if the tension generation in question is an acute or a chronic effect. We also set out to correlate the extent of contractile response to the stimulation of oxygen consumption using the adapted oxygen electrode plunger described in 2.3.3.

CSF was PCA extracted, freeze dried and added to the organ baths so that the final concentration was equivalent to undiluted CSF for these experiments. Both CSF_S and CSF_N added to porcine carotid arteries mounted on a force measurement apparatus as described in 2.3.2 elicited an acute contraction. CSF_N added to the tissue elicited an increase in tension of 38.9 ± 5 % (n=8) of the 70 mM KCl induced maximum. This initial contraction was increased to 73.9 ± 8% by the use of CSF_S (n=8) and 1nM okadaic acid had little effect, the tissue only reaching 6.14 ± 0.7 % (n=8) of the maximum. Control tissue was at a resting level of 4.91 ± 0.32 % (n=8) of the maximum tension. This was followed, in the case of the CSF_N, by relaxation back to a tension approaching control levels 6 hours after addition of the CSF (5.1 ± 0.3 %). In the CSF_S treated tissue, however, a chronic contraction (6 hours post-CSF addition 79 ± 9 %) was then observed which lasted over 16 hours and was irreversible by rinsing as seen in Figure 5.5 (except after addition of 12 mM Mg^{2+} followed by rinsing as described in 5.3.2.2). A representative trace can be seen in Figure 4.6.

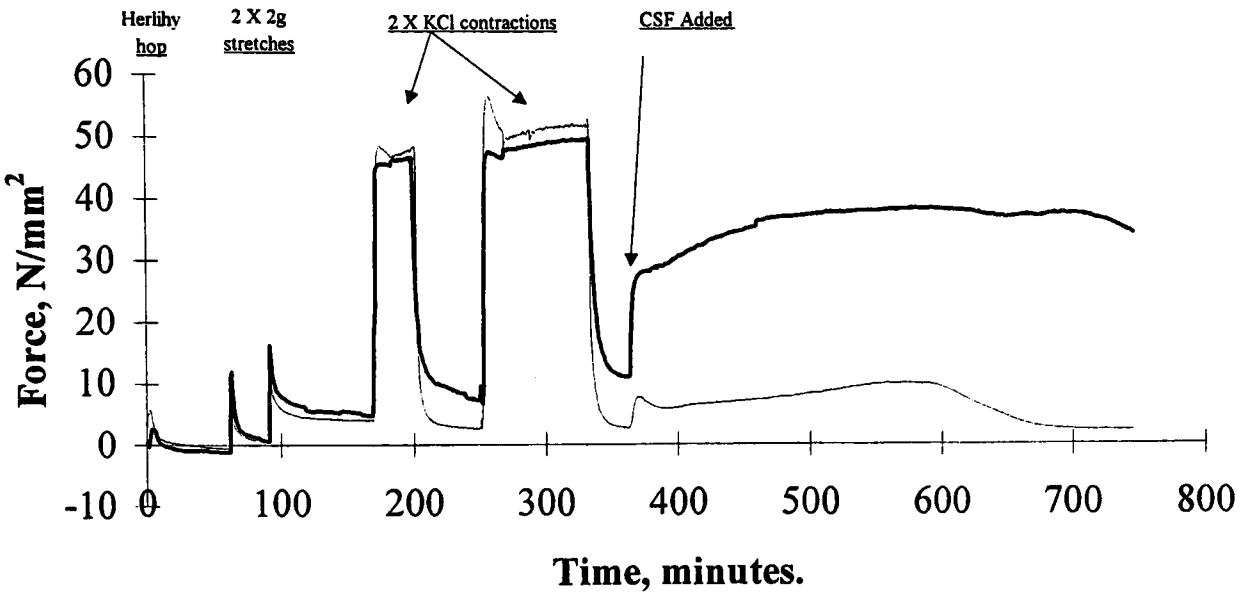

Figure 4.6: Representative trace of the response of the porcine carotid to CSF_S and CSF_N. The pale grey line is the response elicited by CSF_N and the black line, CSF_S. These experiments are carried out at 37°C. Concentrated, PCA extracted CSF was used so that the final concentration that the tissue is exposed to is approximately equal to undiluted CSF. KCl was used at a concentration of 70mM. This trace is representative of an n of 8 of each CSF.

The addition of freeze dried, PCA extracted CSF to an organ bath posed a potential problem regarding hyperosmolarity. This effect was shown to be insignificant by rinsing the CSF treated tissue (Figure 5.5). Any artifactual contraction elicited by hyperosmolarity would have been reversed upon incubation in CSF free solution.

When the tissue is mounted on the concomitant force and oxygen consumption apparatus, force generation and oxygen consumption data can be obtained simultaneously and oxygen consumption can be correlated to development of force on the same timescale and under the same conditions. Carotids were exposed to PCA extracted, freeze dried and reconstituted (to undiluted CSF concentration) CSF and the relationship compared to the

tissue response to increasing concentrations of calcium. Figure 4.7 shows the relationship between force generation and oxygen consumption when induced by CSF_S and Calcium.

The protocol for obtaining the calcium data can be found in 2.3.3. From the linear portion of each graph in Figure 4.7 a rate of oxygen consumption per unit tension generation can be obtained. The rate can be given as the amount of increase in rate of oxygen consumption correlating to an increase in tension of 1 percent of the maximum tension generated. The units for this value would be $\mu Mol\ min^{-1} g\ dwt^{-1}$ % increase in $tension^{-1}$.

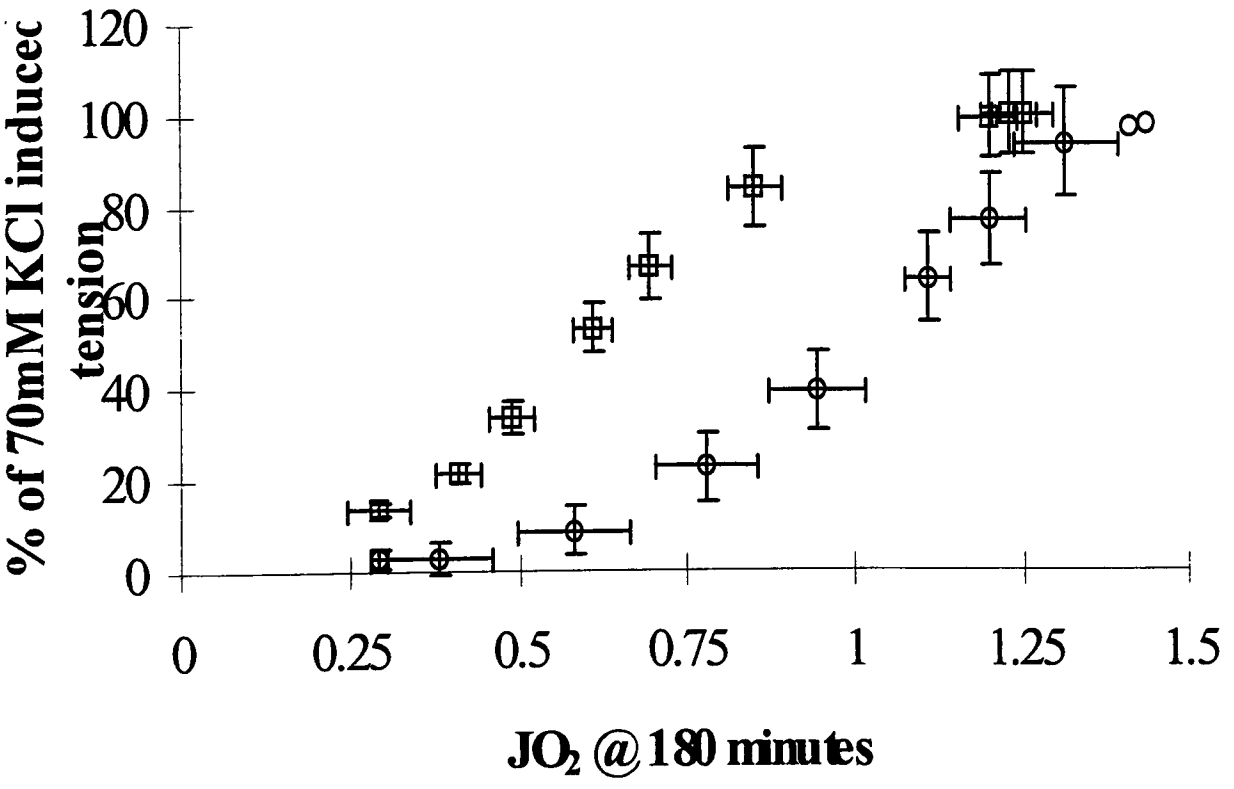

Figure 4.7: Concomitant increase in oxygen consumption with force development. The graph shows the relationships between Ca^{2+} (open squares, n=3) and CSF_S (open circles, n=3) stimulated rate of O_2 consumption @ 180 minutes and force. x and y errors are standard deviations.

Agonist	rate (μMol $min^{-1}g$ dwt^{-1} % increase in $tension^{-1}$)
CSF_S	$6.47 \times 10^{-3} \pm 2.9 \times 10^{-4}$
Calcium	$6.86 \times 10^{-3} \pm 5.7 \times 10^{-4}$

Table 4.2: Data determined from Figure 4.7. The increase in JO_2 required to support an increase in tension of 1% of the 70mM KCl induced maximum is given. Errors are standard deviations.

4.3.3 Lactate production

The lactate production of the porcine carotid artery was determined in order to assess whether the stimulation of O_2 consumption was accompanied by a stimulation of lactate production. It was found that neither resting nor working (slipped over a length of glass 1.5 times the internal diameter of the vessel) carotid arteries produced significantly different rates of lactate production from control when treated with CSF_S or CSF_N. The rates of lactate production are given in Table 4.3.

Condition	Lactate Production, μmol min^{-1} g^{-1}	
	resting	isometric load
Control	0.109 ± 0.009	0.203 ± 0.012
1 in 30 CSF_N	0.112 ± 0.013	0.215 ± 0.019
1 in 30 CSF_S	0.116 ± 0.014	0.210 ± 0.015
1 μM Okadaic acid	0.108 ± 0.011	0.216 ± 0.018

Table 4.3: Each value is the average of 5 experiments ± the standard deviation.

The incubation conditions are described in 2.3.9. In all cases, the glucose concentration in the incubation medium was 11 mM and the lactate added in the CSF samples was taken into account. These rates of lactate release in resting and contracting tissue are comparable to literature values[126].

4.3.4 Cholesterol esterase depletion of activity.

It is known that human cerebral spinal fluid contains a cholesterol ester hydrolase that specifically cleaves oleic acid from cholesterol oleate[131]. It was proposed that an excess of this cleavage could result in an increased concentration of oleate in the CSF, which may stimulate oxygen consumption. Adding cholesterol esterase to CSF and observing changes in its ability to stimulate oxygen consumption tested this theory. The findings were that incubating the CSF with different concentrations of cholesterol esterase for 1 minute at 37°C and then quenching with 12% perchloric acid yielded an extract which had lost activity in a dose dependent manner, depending on the activity of cholesterol esterase in the incubation. Figure 4.8 illustrates this effect.

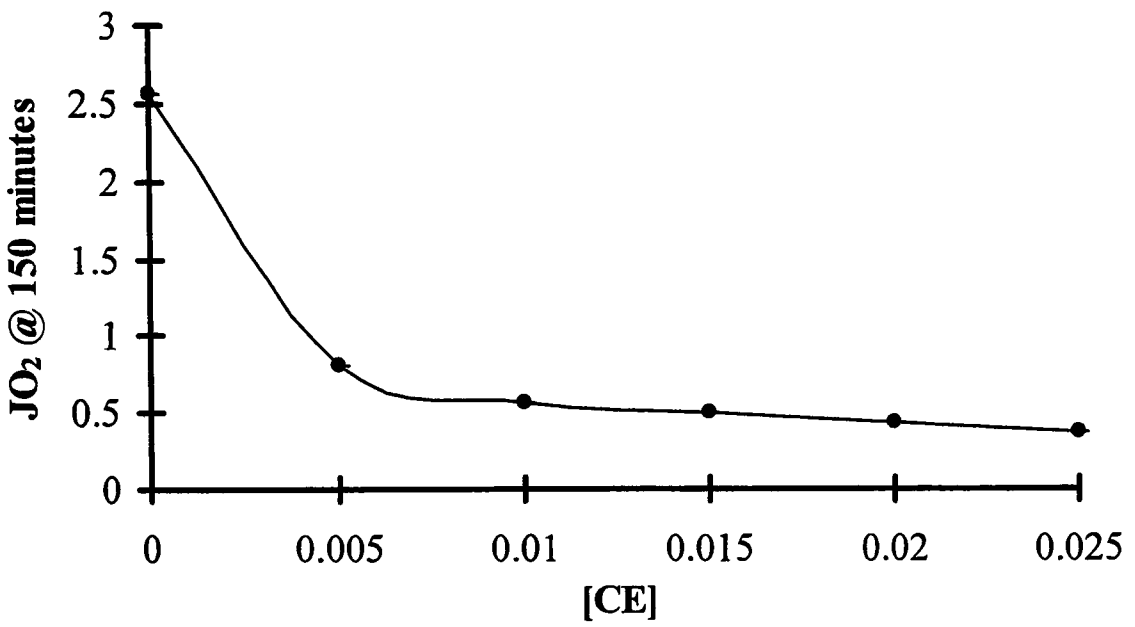

Figure 4.8: Effect of cholesterol esterase incubation on the activity of CSF_S. Errors are S.E.M. Rate of oxygen consumption @ 180 minutes is in μmol min^{-1} g dwt^{-1}. Concentration of cholesterol esterase is expressed as IU ml^{-1}.

The activity of the CSF_S estimated using its capacity to stimulate O_2 consumption is reduced by 81% with just 0.005 IU of the enzyme and this is further reduced using 0.025 IU by 85% of the CSF_S induced stimulation. The EC_{50} for this inhibition is 0.0041 $IUml^{-1}$.

This may give some indication of the structure of the vasoactive molecule in CSF_S. Non-specific cleavage of a hydrophobic molecule from a cholesterol-like molecule linked by an ester bond may lead to the inactivation of the vasoactive molecule. Another possibility is that a protective molecule or inhibitor is formed by the action of cholesterol esterase which prevents the CSF_S from stimulating respiration. Since the inhibition of vasoactivity is related to the concentration of cholesterol esterase the CSF is exposed to (see Figure 4.8), it would seem that the interaction is of a specific nature. This would be expected to result in a quantitative inhibition of the CSF_S stimulation unlike a non-specific quenching or binding of the enzyme protein.

4.4 Discussion

4.4.1 Stimulation of O_2 consumption and tension generation by CSF_S, but not CSF_N.

In vascular smooth muscle, the coupling of oxidative metabolism to contractile function is such that inferences about myosin ATPase activity can be made from observations of O_2 consumption[306, 308]. Our model of cerebral vasospasm after subarachnoid haemorrhage utilises this relationship by measuring rates of O_2 consumption in order to investigate the effect of pharmacological agents such as inhibitors and receptor antagonists. This helps to elucidate the nature of the stimulation of tension generation and rate of O_2 consumption seen with CSF_S. We have shown that this is a relevant strategy by correlating elevation of O_2 consumption with tension generation in response to CSF_S.

It can be seen in Figure 4.7 that the greater the elevation of O_2 consumption, the greater the tension developed. This is not a novel observation. The relationship between tension generation and rate of O_2 consumption is different, though, between calcium induced and CSF_S induced stimulations. This relationship is significant and some quantitation of the amount of tension development induced per increase in rate of O_2 consumption is possible from the linear part of the relationship. The actual rate obtained from the linear part of the relationship is not significantly different between the two agonists. An increase in O_2 consumption of $6.47 \times 10^{-3} \pm 2.9 \times 10^{-4}$ μmol min^{-1} g dwt^{-1} was elicited for each increase in tension of 1% of the maximum induced by calcium. This value was similar for CSF_S induced tension and O_2 consumption, at $6.87\times 10^{-3} \pm 5.7 \times 10^{-4}$ μmol min^{-1} g dwt^{-1} $\%^{-1}$ (see Table 4.2). There is, however, a right shift of the CSF_S induced relationship with respect to the calcium induced relationship. This indicates that the smooth muscle is more sensitive to calcium than to CSF_S.

In other words, O_2 is required to be consumed at a faster rate in order to initially fuel CSF_S induced contraction than calcium induced contraction, but the increase in rate of

O_2 consumption correlated to an increase in tension on the linear part of the relationship is similar. It appears, from this data, that CSF_S induces tension by a mechanism other than the direct increase in intracellular calcium concentrations of the tissue. The right shift of the relationship without change in efficiency after initiation of contraction may indicate a mediating step that requires a threshold level of stimulation which may well be the activation of an enzyme that results in the increase of intracellular calcium concentration such as protein kinase C.

4.4.2 Ineffectiveness of endothelin inhibition.

Endothelin has long been implicated as a causative molecule in the ætiology of cerebral vasospasm after subarachnoid haemorrhage[225, 319, 320]. Various inhibitors, both receptor subtype-specific[264, 299] and non-specific[177, 245, 320] have been used to investigate the possible involvement of endothelin. Endothelin is used as a model for cerebral vasospasm in some *in vivo* models, but the involvement of endothelin has not been shown in this pathology in humans[166, 245]. The non-specific endothelin antagonist, PD142893 was used to examine its effect on our model. Endothelin was also tested to compare it with the CSF_S response. It was found that endothelin did indeed stimulate O_2 consumption, but this stimulation was, on average, 185 ± 21% (n=8) above control respiration, whereas CSF_S stimulation was in the region of 280 ± 31% (n=24). A similar stimulation could not be achieved by adding a greater concentration of endothelin and the endothelin stimulation was reversible by rinsing, unlike the CSF_S stimulation. In addition to these dissimilarities, the effect of pre-treatment of the tissue with PD142893 was different on each stimulation. PD142893 inhibited the endothelin induced stimulation by a significant amount ($P=<0.05$), but had little effect on the CSF_S stimulation, increasing it by only 11 ± 2% which is within the variation expected when a random sample of 6 CSF_S samples are taken from the population. The slight decrease in carotid O_2 consumption when exposed to PD142893 may be due to the inhibition of endogenous endothelin. These results indicate that endothelin is not involved in the ætiology of cerebral vasospasm in this model and this is

corroborated by clinical trials of endothelin antagonists and other investigations in the literature[166, 225, 245].

Although no significant change in CSF_S stimulated rate of O_2 consumption is seen at 180 minutes when the tissue is pre-treated with PD142893, some effect is seen earlier in the timecourse. Up to 120 minutes, the pre-treated tissue stimulated with CSF_S has a significantly lower JO_2 than that of CSF_S stimulated tissue alone. The shape of the increase in JO_2 changes from hyperbolic (CSF_S stimulated tissue) to sigmoidal (CSF_S stimulated, PD142893 pre-treated tissue). This may possibly indicate some involvement of endothelin in the acute stimulation of O_2 consumption and perhaps tension as well.

Interestingly, PD142893 increased both basal O_2 consumption (by 12 ± 2 %) and CSF_S stimulated O_2 consumption (by 11 ± 2 %). This would indicate an additive effect of ET receptor stimulation on CSF_S stimulation, further confirming that ET is not the primary cause of vasospasm.

4.4.3 Inhibition of phosphatases

The very similar stimulation of O_2 consumption by okadaic acid and CSF_S may provide a valuable clue as to the cause of the CSF_S induced stimulation. Inhibition of phosphatase would force the cross bridges to remain phosphorylated and therefore actively cycling and consuming ATP. This ATP is provided, in vascular smooth muscle, by oxidative metabolism and therefore oxygen is consumed[44]. This rather simplistic explanation also provides an explanation for a number of other observations. Okadaic acid does not, however, stimulate tension at 1 nM concentrations (4.3.2) and the loss of specificity of phosphatase inhibition at increased concentrations (>5 nM) prevents conclusions being drawn from the use of concentrations of okadaic acid capable of producing contraction in the porcine carotid artery. Okadaic acid actually inhibits O_2 consumption at 10nM and above (see Figure 4.3) as its inhibition of type 2A phosphatase becomes non-specific and it starts to inhibit type 1 phospshatases. The similar attenuation

of relaxation by 1 nM okadaic acid and a 1 in 30 dilution of CSF_S (see Chapter 6) also indicates an involvement of phosphatase inhibition and reinforces the similarity of actions of CSF_S and the predominately type 2A phosphatase inhibitor, okadaic acid. There is, however, still one unanswered question regarding the role of the phosphatase. If cerebral vasospasm is caused by an inhibition of phosphatase activity, why does okadaic acid not elicit an increase in tension generation? The answer to this question may be that there are two events occurring during vasospasm; a stimulation of contraction along with an inhibition of myosin light chain phosphatase which would not allow the tissue to relax from the contraction. This is addressed more fully in the next section (4.4.4).

The postulated stimulation of contraction and concomitant phosphatase inhibition could be due to the same molecule. If one considers the intracellular signalling that is thought to control smooth muscle function, several suggestions became apparent. The activation of PKC suggested in 4.4.4 could also be responsible for the inhibition of the phosphatase. An inhibitory subunit of smooth muscle myosin light chain phosphatase, thought to be a PP1[215] has recently been found in vascular smooth muscle[68]. Eto *et al*[68] report that this inhibitory protein is potentiated by PKC-mediated phosphorylation. Although the isoform of PKC responsible for this inhibitory potentiation has not yet been elucidated, this may be a mechanism by which activation of PKC by a molecule or molecules in the CSF_S both stimulated contraction and inhibited relaxation concomitantly.

4.4.4 Possible involvement of protein kinase C in cerebral vasospasm

Although staurosporine did not attenuate the stimulation of O_2 consumption, this may be because sustained PKC activation is not what causes the stimulation, but the phosphatase inhibition. The possibility of protein kinase C activation being involved in cerebral vasospasm was introduced in 4.1.1.3. Briefly, Ohta and colleagues[201] determined that levels of 12-hydroxyeicosotetranoic acid (12-HETE) were elevated in patients with subarachnoid haemorrhage over a time course comparable to that

of onset of vasospasm in man[294]. 12-HETE then causes a chronic accumulation of diacylglycerol (PKC activator) by inhibition of DAG kinase, thus preventing its metabolism. Other groups have suggested that DAG lipase is the enzyme inhibited[76, 291]. The source of the DAG has been reported to be the phospholipase D cleavage of phosphatidyl choline, without IP_3 production. This PKC activation is likely to be Ca^{2+} independent[150]. This is another indication that endothelin is not involved, as calcium is required for endothelin receptor-mediated stimulation. In turn, DAG production without Ca^{2+} release is known to be responsible for a sustained, PKCε mediated contraction in smooth muscle[276]. PKCε phosphorylates and inactivates calponin, removing its inhibitory actions so that cross bridge cycling resumes. Results from experiments carried out recently by myself outlined briefly below seem to uphold this theory. It was found that vasospastic CSF could be formed by adding whole blood to control CSF (CSF from patients without haemorrhage, usually communicating hydrocephalus) and pieces of Pia mater from pigs. I separated the blood into several fractions using Ficoll gradients and mixed the individual fractions with CSF and Pia to see which blood component is likely to be involved in vasospasm. It was found that all the fractions containing platelets stimulated oxygen consumption significantly, whereas mixtures containing no platelets did not stimulate respiration at all. The respiration of the platelets alone did not account for the suprabasal respiration observed. As 12-HETE is produced by the platelets, the sustained activation of PKC would seem to be a feasible explanation for the tension increase seen with native CSF, but not with okadaic acid alone.

4.4.5 Attenuation of CSF_S stimulation by α_1-adrenergic receptor agonists

Dobutamine and noradrenaline both significantly ($P = < 0.05$) protected the tissue from the CSF_S stimulation of O_2 consumption (Table 4.2) and tension development (data not shown). This protection was only afforded if the tissue was pre-treated with the agonist; addition after the CSF_S had no effect. These agonists are known to induce an acute

translocation of PKC to the plasma membrane[208] which is associated with stimulation of both oxidative metabolism and tension development.

So, why, then should they protect smooth muscle against a sustained PKC induced tension? There are two possible theories. Danthuluri and co-workers[52] reported that phorbol ester-induced PKC activation (DAG analogue, sustained contraction) inhibited α_1-adrenergic receptor agonist induced PKC activation and concomitant rise in intracellular calcium. If this inhibition could work in both directions, so that the activation of a sustained contraction by PKCε somehow inhibits acute tension activation by another PKC isoform at the same time, the acute PKC activation by α_1-adrenergic receptor agonists may, conversely, prevent the sustained PKCε activation by the increased DAG levels in vasospasm.

The second option is that the α_1-adrenergic receptor agonists somehow enable the cross bridges to enter the "latch state", that is, the attached cross bridges are dephosphorylated and enable the tissue to relax, even with phosphatase inhibition. There is no direct evidence to support this latter theory, but determinants of the latch state include inhibition of myosin light chain kinase or activation of myosin light chain phosphatase[86, 182, 185]. If the phosphatase is activated in advance of exposure to CSF_S, a conformational change may make the site of action of the putative phosphatase inhibitor molecule unavailable. It seems feasible that both PKC activation and phosphatase inhibition are involved in the ætiology of cerebral vasospasm.

4.4.6 Lactate production

Table 4.3 shows that neither CSF_S nor okadaic acid stimulated lactate production in either resting or working tissue. This corroborates the theory that the stimulation elicited by CSF_S is specifically of oxidative origin and the lack of increase in lactate production in CSF_S stimulated tissue shows that this process is pathological and not an exaggerated physiological response.

4.4.7 Cholesterol esterase action

The dose dependent decrease of CSF_S stimulation of O_2 consumption (Figure 4.7) possibly indicates the nature of the molecule responsible for the phosphatase inhibition part of the phenomenon. One possible explanation is the production of substances in the CSF, which induce acute PKC responses in the tissue, by cleavage from cholesterol and subsequent enhancement of phosphatase activity. Alternatively, the cholesterol esterase may break down the molecule responsible for the phosphatase inhibition directly. This would imply that the pathogenic molecule might contain an ester linkage between a planar, multi-cyclic compound and a fatty acid type compound.

From the dose dependent manner of the depletion of CSF_S activity, it can be ascertained that cholesterol esterases effect on CSF_S is probably not non-specific, such as binding of the active molecule(s) to the enzyme. Removing the enzyme with perchloric acid extraction does not restore the activity of the CSF_S, indicating an irreversible change in the active constituent. This also shows that the enzyme is acting on the CSF_S, not the tissue.

4.5 Conclusions

From the data presented in this chapter, several conclusions can be drawn;

- The stimulation of tension development by CSF_S is likely to be due to a sustained activation of protein kinase C arising from platelet-derived 12-HETE inhibition of DAG kinase allowing an accumulation of DAG. The PKC would then phosphorylate calponin alleviating the inhibition of cross bridge cycling. This is corroborated by the observation that platelet-containing blood fractions simulate CSF_S action when mixed with non-haemorrhagic CSF and porcine pia. The activation of the sustained contraction-inducing form of PKC may also explain the attenuation of the CSF_S response by α_1-adrenergic receptor agonists, as the activation of the sustained and acute contraction related protein kinase C isoforms is thought to be mutually exclusive[87].

- The stimulation of oxygen consumption is probably due to inhibition of myosin light chain phosphatase, but there may also be a contribution from PKC. The non-significant reduction in CSF_S induced stimulation when the tissue was pre-treated with staurosporine (1 nM) suggests the involvement of PKC in conjunction with another factor. The similarity of response of tissue to okadaic acid and CSF_S may also be indicative of this.

- The initial stimulation of contraction is likely to be due to PKC activation as it is seen in both CSF_S and CSF_N treated tissue (see Figure 4.6), however, the putative phosphatase inhibitor in CSF_S results in the tissue being unable to relax from this stimulus, giving the insidious, slow onset of tension characteristic of vasospasm.

5.Effects of manipulating magnesium

5.1 Introduction

Magnesium is the second most abundant soft tissue divalent cation in the human body[285]. It is absorbed into the blood stream from the entire length of the small intestine, in contrast to calcium, which is taken up through the duodenum only[285]. In the adult male human, there is between 21 and 28g of magnesium, 60% of which is essentially fixed in bone. Only 2 or 3% is in a biologically active form, as free Mg^{2+} ions inside cells. It is the properties of the free ion that is of interest in this chapter.

5.1.1 Physiological requirement for magnesium

There are many homeostatic systems in smooth muscle that absolutely require the presence of magnesium ions, such as myosin light chain kinase[222] and the myosin ATPase[261]. It has been found that it is not possible to reduce the intracellular magnesium concentration to below 4 μmoles/g protein[235] by incubation of tissue in magnesium-free conditions with EDTA, which suggests that the maintenance of intracellular magnesium is tightly controlled[263]. This is further suggested by the difficulty with which intracellular magnesium concentrations are manipulated *in vitro*[72, 189, 191, 192].

The apparent dependence of MLCK on magnesium may actually be due to the control of myosin ATPase by magnesium[222, 262]. Russell [235] reported that magnesium (and other divalent cations) may play a role in the control of the conformation of the arterial myosin ATPase. He postulated that the presence of magnesium and calcium increases the myosin ATPase activity over that when calcium alone is present because the conformation of the myosin is shifted from the dissociated to the associated state. The activity of the myosin ATPase under different magnesium concentrations was also investigated by Moreland and Ford[176]. They found that an intermediate magnesium concentration (3-5mM)

provided optimum conditions for calcium activation of ATPase. The maximum activity obtained was in the presence of 5mM extracellular free magnesium and pCa^{2+} of 4.5. Ikebe *et al.* clarified these observations by showing that low magnesium (1mM extracellular free magnesium) favours the 10s (folded, less active) myosin conformation and raised magnesium (11-15mM extracellular free magnesium) favours the 6s (extended, more active) myosin which is more susceptible to phosphorylation. These studies were[118] all carried out on skinned fibre preparations. The exact mechanism of conformational change between the 10s and 6s species is not yet known, but is thought to be a point of control of the myosin ATPase cycle regulating cross bridge cycling. If the susceptibility of the myosin light chains could be controlled by an external factor, such as magnesium or calcium, another level of control would be introduced into the cross bridge cycle. The intracellular free magnesium concentration not only affects the level of phosphorylation of the ATPase, but also the rate at which maximal calcium-sensitive phosphorylation is achieved through conformational change of the regulatory light chains[176].

Paul and Ruegg[222] reported that magnesium is a requirement for the activity of myosin light chain kinase, although not for the phosphatase. They found that magnesium-free solutions actually inhibited the kinase. It was proposed that any calcium-dependent mechanisms for the regulation of smooth muscle contractility that are independent of myosin phosphorylation/ dephosphorylation must then be magnesium-dependent[191, 315].

Alternatively, the requirement of MLCK for Mg^{2+} could be due to some involvement of magnesium-dependent protein phosphatase (PP2C). This is a type-2 phosphatase, the α isoform of which is known to be expressed in smooth muscle and to dephosphorylate phosphorylated myosin light chains *in vitro*. Its *in vivo* activity towards myosin light chains has not been verified, although it is known that the enzyme requires an intracellular free Mg^{2+} concentration of around 1mM which is around twice that normally found in smooth muscle[189]. A more detailed description of this enzyme can be found in section 1.4.4.

If PP2C was involved in a dephosphorylation event leading to the activation of MLCK, this may confer a magnesium dependence on MLCK activity. MLCK has a pseudosubstrate region which is open to autophosphorylation, leading to inhibition[120, 263]. This region is not available for autophosphorylation when calmodulin is bound, but perhaps PP2C is able to dephosphorylate the autophosphorylated pseudosubstrate domain and allow calmodulin binding.

5.1.2 Effect of magnesium on calcium homeostasis

There appears to be a link between the levels of intracellular magnesium and calcium concentrations because in order to load or deplete tissue of magnesium effectively, extracellular calcium concentration must be at a minimum[99, 210, 211]. Ideal loading or depleting conditions for smooth muscle are calcium-free buffer containing 0.1mM EGTA[191]. Why this should be the case has been extensively investigated[9, 39, 188, 189, 191, 192, 282], but is still not fully understood. It is known that magnesium plays important roles in calcium homeostasis. At very low intracellular free magnesium concentrations, below 0.1mM, the ability of the sarcoplasmic reticulum of smooth muscle to retain calcium is impaired, whereas high free magnesium concentrations, above 5 mM, induced rapid calcium uptake and inhibition of release from the sarcoplasmic reticulum[95].

Magnesium has been postulated to antagonise calcium in multiple ways. It was thought to directly displace calcium from the myofibrils[176], but subsequently, Weber *et al* concluded that the concentration of MgATP defined the activation of the ATPase, but MgATP concentration was not directly responsible for inhibition of the ATPase[292]. Yu et al. reported an increase in spontaneous contraction of smooth muscle upon the removal of extracellular magnesium[314]. It has also been described that spontaneous contractions of smooth muscle are abolished upon the addition of magnesium[98]. It was also seen that removal of extracellular magnesium results in an increase in the total exchangeable (free) and intracellular (stored) calcium fraction. However, increasing extracellular magnesium

results in a decrease in the membrane bound and exchangeable free calcium, leaving the intracellular store fraction unchanged[95, 253, 282]. Some reports have suggested competition between magnesium and calcium ions for binding sites on the MLCK regulatory protein calmodulin[261]. Since magnesium bound to calmodulin is not able to activate myosin light chain kinase, competition of this nature would result in a lower activity (therefore lower tension) of myosin light chain kinase in the presence of increased concentrations of magnesium.

5.1.3 Transport of magnesium across the plasma membrane

Smooth muscle cells, like all other cells, maintain intracellular free magnesium concentrations at levels lower than that of the external concentration[273]. This gradient is effectively maintained, via pumps and/ or channels facilitating the extrusion of magnesium. Varying extracellular magnesium alone has very little effect on the intracellular concentration[195]. Removing glucose, which in smooth muscle is thought to power membrane pumps[122, 220], still yields little change in intracellular free magnesium concentration. This may be because oxidative metabolism, usually fuelling contractile function, is diverted in the absence of glycolytic substrate[280]. Without glycolytic substrate and under anaerobic conditions, significant losses of magnesium were observed[195, 274] whilst the tissue was still viable. This may indicate the magnesium is lost in preference to calcium (which may be more crucial in smooth muscle function) when metabolic disturbance results in loss of function of membrane pumps. Loss of calcium would render smooth muscle unable to respond to contractile stimuli and so the intracellular calcium concentration is maintained at the expense of magnesium.

Most evidence for the transport of magnesium into cells indicates the presence of membrane channels and carriers for other divalent cations (e.g. Ca^{2+}) that do not completely exclude Mg^{2+}[281]. Mg^{2+} currents have been measured in prokaryotic and eukaryotic cells[282] which suggests the presence of channels able to allow magnesium

movement. If this is the case, the magnitude of the transmembrane Mg^{2+} concentration difference (small) suggests that the influx of magnesium through channels is likely to be membrane voltage driven[281, 282].

Magnesium efflux has been of great interest to researchers investigating the significance in the drop in brain intracellular magnesium seen after brain injury and stroke[96, 265, 278, 286]. Both passive and secondary active mechanisms have been reported for the efflux of magnesium[211]. Results from studies using the inhibitors amiloride and ouabain suggest magnesium is extruded in exchange for the influx of sodium (secondary active transport). Inhibition of the sodium-magnesium exchanger by amiloride and treatment with ouabain prevented magnesium efflux by dissipating the transmembrane sodium gradient[188, 280]. A passive transporter which is less sensitive to, or insensitive to amiloride, has also been postulated in smooth muscle[188]. It has also been reported that the sodium dependent extrusion of magnesium may be ATP driven, which is primary active transport[280]. The physiological extracellular concentration (1.2 mM) of magnesium in vascular smooth muscle is approximately 3 fold higher than the intracellular concentration (0.4 mM[189]). It appears that magnesium plays an important role in smooth muscle function, which may be disrupted by an excess or deficit of magnesium.

Both magnesium influx and efflux have been linked to hormonal stimuli[232, 256]. Adrenergic stimulation of cardiac and hepatic cells results in significant magnesium efflux, whereas activation of protein kinase C by carbachol, vasopressin, phorbol esters or diacylglycerol analogues induces a small magnesium accumulation in the cell[232]. It was reported that the cAMP induced efflux was mainly from intracellular stores held in the mitochondria via the mitochondrial adenine nucleotide translocase[256]. Magnesium influx, however, appeared to be related to the sarcoplasmic reticulum[232]. As the intracellular calcium concentration rose in response to protein kinase C activation, an influx of extracellular magnesium was observed[232]. This may indicate either that magnesium is a physiological calcium antagonist and modulates intracellular calcium responses, or that

magnesium enters cells in a non-specific manner whenever calcium channels are open and the control of the intracellular concentration of magnesium is by the rate of extrusion.

5.1.4 Measuring intracellular magnesium

Until recently, it has been difficult to measure intracellular magnesium pools with any degree of precision. Various methods have been employed to estimate intracellular magnesium, both *in vivo* and *in vitro*. A metallochrome, eriochrome blue[239], was used to detect free magnesium efflux from mitochondria in vitro[256], but this is not suited to whole animal studies. Atomic absorption spectroscopy (flame photometry) has also been used to measure the magnesium content of a sample[210, 211]. For measuring magnesium levels in intact systems, the method most used is Nuclear Magnetic Resonance (NMR)[9, 83, 88, 278, 286].

The intracellular free magnesium concentration was first measured using this method in 1978 by Gupta et al[83]. ^{31}P NMR was used to obtain spectra of red blood cells. The frequency separation between the αP and βP of ATP and the α-β and β-γ ^{31}P spin-spin coupling constants of the intracellular ATP, along with prior knowledge of the interaction of magnesium with other phosphorylated substrates allows calculation of intracellular free magnesium concentrations[84].

The oldest currently used therapeutic use of magnesium is for the condition known as eclampsia[110]. This strikes pregnant women and involves hypertension and cerebral vasospasm. It may progress to seizures and sometimes stroke, including subarachnoid haemorrhage which are serious complications. This condition is preceded by preeclampsia, which is characterised by proteinuria, oedema and a rise in blood pressure. Its treatment with magnesium was first reported in 1906[110] and still proves to be the safest and most reliable treatment for eclampsia[231].

Recent advances in non-invasive measurement of intracellular magnesium have led to therapeutic studies involving a range of pathologies. Magnesium therapy was

investigated for use in the treatment of coronary artery spasm, with no observed benefits[169]. Spectroscopy of brain tumours led to a report outlining improved patient condition when magnesium deficiency was overcome[278]. A relatively new application of magnesium therapy is for head injury[96, 100, 265]. It was noted that patients with low plasma magnesium displayed impaired recovery compared to those with normal or high magnesium. Raising the patients' magnesium levels has proven to be beneficial, with human and animal studies corroborating this observation[96, 265]. It has not yet however been established whether the hypomagnesaemia is a result of the injury, or a potentiating factor for poor recovery. Another recent observation is that of treating patients who have suffered strokes with magnesium[100, 179]. Reports are restricted to improvement in neurological outcome, but other studies to investigate the potential prevention of vasospasm after subarachnoid haemorrhage using magnesium may have clinical implications.

The aim of the experiments detailed in this chapter is to determine the effect of manipulating the intracellular magnesium on the porcine carotids used in our model of cerebral vasospasm after SAH. The effect of magnesium manipulation is investigated with respect to oxidative metabolism and contractile function, as well as concomitant measurements. The effect of acute elevation of magnesium on CSF_S induced contraction is also investigated and reported.

5.2 Methods

5.2.1 Introduction

All the methods used to obtain the results presented in this chapter are described in full in Chapter 2. Oxygen consumption measurements (2.3.1) were used to investigate the effect of manipulating the intracellular magnesium content of smooth muscle on the oxidative metabolism of the tissue. This may give some indications as to what pathological mechanisms may be acting on the contractile apparatus. The response of the tissue to 70mM KCl was used to assess the effect of magnesium loading and depletion (2.2.11) on

isometric tension development. A further insight into the changes occurring in the contractile apparatus was gained by carrying out stretch-release experiments (2.3.2.1), which allow characterisation of effects of magnesium on the ability of the tissue to regenerate tension after a stretch, followed by a rapid release. As myosin light chains are phosphorylated in response to stretching[61], the subsequent return of the tissue towards its pre-stretch length shortly after the stretch results in a regeneration of tension correlating to the amount of phosphorylated light chains[61]. Analysing the rate of regeneration of tension and the maximum tension regained after a stretch and release gives us an idea of the effect of certain agents on the contractile function of the tissue. The development of the concomitant oxygen consumption and tension measurement apparatus allowed investigation of any effect of magnesium depletion or loading on hypoxia induced relaxation (2.3.3). Acute effects of magnesium on CSF_S and 70mM KCl induced tension were also investigated. The actual intracellular magnesium concentrations were not measured, but can be estimated from literature values (see 2.3.11).

5.2.2 Oxygen electrode experiments

The porcine carotid arteries were prepared by incubation in Ca^{2+} free HEPES buffer containing 0 mM Mg^{2+} + 0.1 mM EDTA, 1.2 mM Mg^{2+} or 12 mM Mg^{2+} as described in 2.2.11. The tissue was then prepared for oxygen consumption measurements as described in 2.3.1. Control experiments were run in 1.2 mM magnesium HEPES to measure the baseline rate of respiration under each magnesium condition. The tissue was first allowed to respire in the oxygen electrode untreated. Unextracted CSF_S was then added to the tissue under each condition in order to assess the possible benefits of manipulating magnesium with respect to vasospasm and CSF_N was added in a separate experiment as a control. CSF was added to a final dilution of 1:30 and the oxygen consumption of the tissue was recorded for at least 120 minutes. In all experiments, all tissue was placed in 1.2mM magnesium (control) HEPES before measurements were taken.

5.2.3 Force measurements

A number of different measurements were made using the force measurement apparatus: the effect of 70 mM KCl induced isometric tension on the tissue under different magnesium states, the response of the tissue under different magnesium states to PCA extracted CSF_S and the acute effect of magnesium on the effect of PCA extracted CSF_S or 70 mM KCl induced tension. Stretch-release experiments were carried out on the tissue under control and loaded magnesium conditions.

5.2.3.1 70 mM KCl induced isometric tension

Tissue was prepared with respect to magnesium loading and depletion as described in 2.2.11 and with respect to force measurements as described in 2.3.2. The tissue was mounted between the clamps and allowed to equilibrate for 1 hour. This was the initial length (L_i) of the tissue. It was then stretched to 1.5 times its initial length (to L_O for porcine carotid) and allowed to equilibrate for a further 30 minutes. 70mM KCl buffer (2.2.3) which had been pre-equilibrated to 37°C and aerated with 95% O_2/ 5% CO_2 was used to replace the buffer in the organ bath and tension allowed to develop for at least 3 hours. The rate at which tension developed and the maximum tension reached were obtained using a curve fitting program which fitted the data to the equation for a rectangular hyperbola, allowing calculation of the rate of tension generation and the maximum tension obtained.

5.2.3.2 Acute effects of magnesium

Tension was induced in control tissue using 70 mM KCl as described in 2.3.2. When a steady tension was achieved, increasing amounts of magnesium (from 0 to 27 mM in 3 mM increments) was added and the relaxation observed until a plateau was reached. This was then repeated until no more relaxation could be observed upon the addition of further magnesium. The effect of acute magnesium incubation on CSF_S induced tension was also determined using these methods.

5.2.3.3 Stretch-release measurements

Magnesium loaded tissue was stretched as described above and allowed to equilibrate for 30 minutes. Stretch release experiments were carried out to see if there was any conformational change in the contractile apparatus of the muscle. Tissue was stretched to 1.5 times its resting length and then released within 4 seconds to the resting length again. These methods are in 2.3.2.1.

5.2.3.4 Concomitant measurements

Treated tissue was prepared as described in 2.3.3. The tissue was allowed to equilibrate at 37°C for 30 minutes and then stretched and allowed to respire until oxygen was depleted. Tension was measured over the same period.

5.3 Results

5.3.1 Oxygen consumption measurements

From the baseline oxygen consumption of the tissue under different magnesium conditions, it can be seen in Figure 5.1 that the baseline rate of O_2 consumption in the tissue that had been depleted of magnesium is not different from that under control conditions (1.2 mM Mg^{2+}). The baseline consumption of oxygen by the tissue that had been loaded with magnesium is significantly lower than that of control.

Upon the addition of CSF_S to tissue depleted of magnesium, stimulation of the rate of O_2 consumption occurred to 90% of the stimulation seen in control tissue (1.2 mM Mg^{2+}) at 120 minutes. The difference between the stimulation seen in control tissue (0.70 ± 0.12 μmol/min/g dwt) and the magnesium-depleted tissue (0.63 ± 0.11 μmol/min/g dwt) was not significant as can be seen in Figure 5.2.

It can also be seen from Figure 5.2 that loading the tissue had a significant ($P = < 0.05$) effect on the maximum rate of the response to CSF_S (stimulated from 0.267 ± 0.06 to

0.46 ± 0.1 μmol/min/g dwt) but not the magnitude of the response. The increase in rate in response to CSF_S in control tissue was by 204 ± 41%, in magnesium depleted tissue 165.9 ± 24% and in magnesium loaded tissue, 192 ± 30%, none of these values are significantly different.

5.3.2 Force measurements

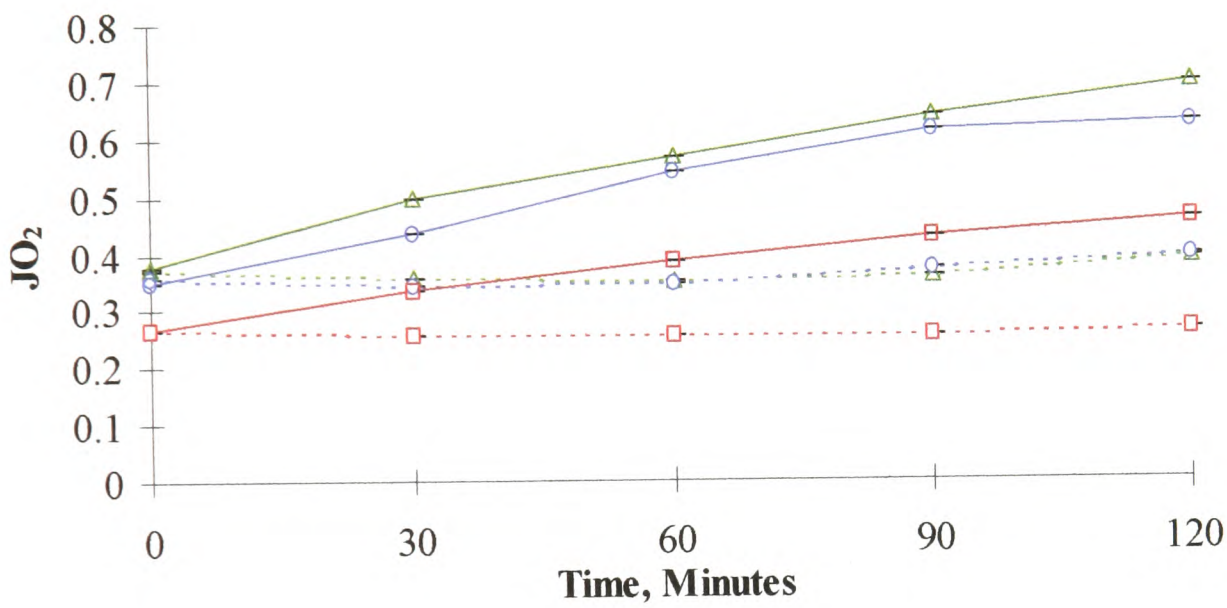

Figure 5.2: Control tissue (triangles), magnesium loaded tissue (squares) and magnesium depleted tissue (circles) baseline respiration are all shown (dashed lines) as well as the CSF_S stimulated rates of O_2 consumption (solid lines) JO_2 is rate of O_2 consumption in μmol min^{-1} g dwt^{-1}. Error bars are omitted for clarity.

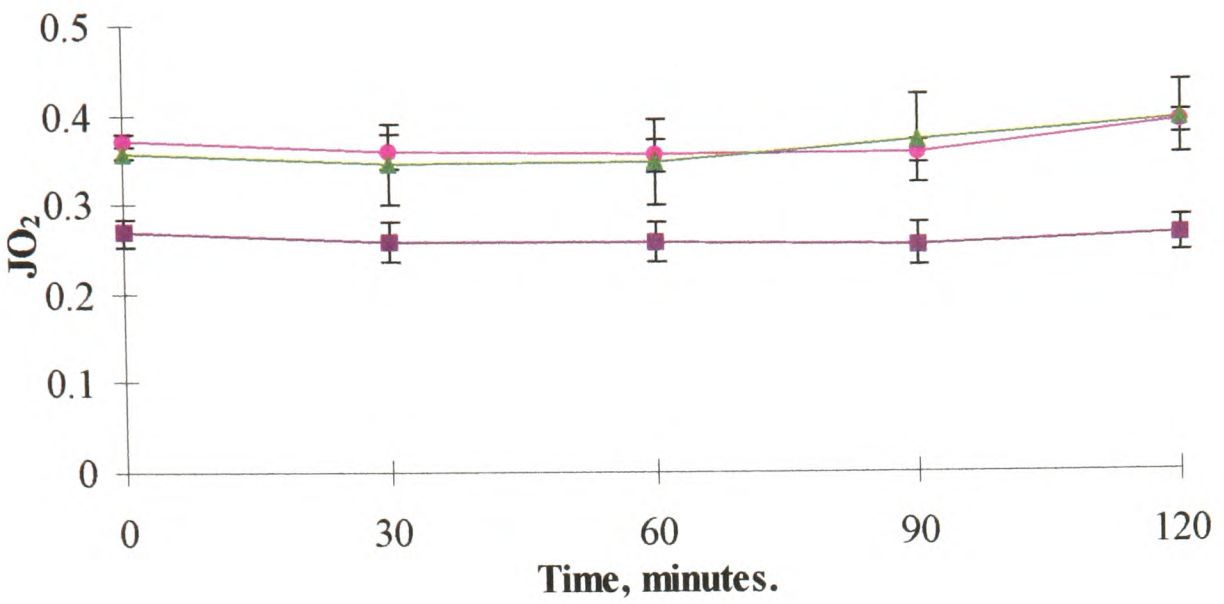

Figure 5.1: The baseline rate of respiration of magnesium loaded (closed squares), magnesium depleted (closed circles) as compared to control tissue (closed triangles). n=6 for each data set and error bars are $\pm \sigma_{n-1}$.

5.3.2.1 70mM KCl induced isometric tension

The effect of magnesium manipulation on the isometric tension induced by 70 mM KCl has been shown previously[243]. The results are very similar here, but the rate of increase has been calculated using a curve-fitting program, which fitted each set of data to the equation for a rectangular hyperbola. Figure 5.3 shows the response of the three differently treated tissues to 70 mM KCl.

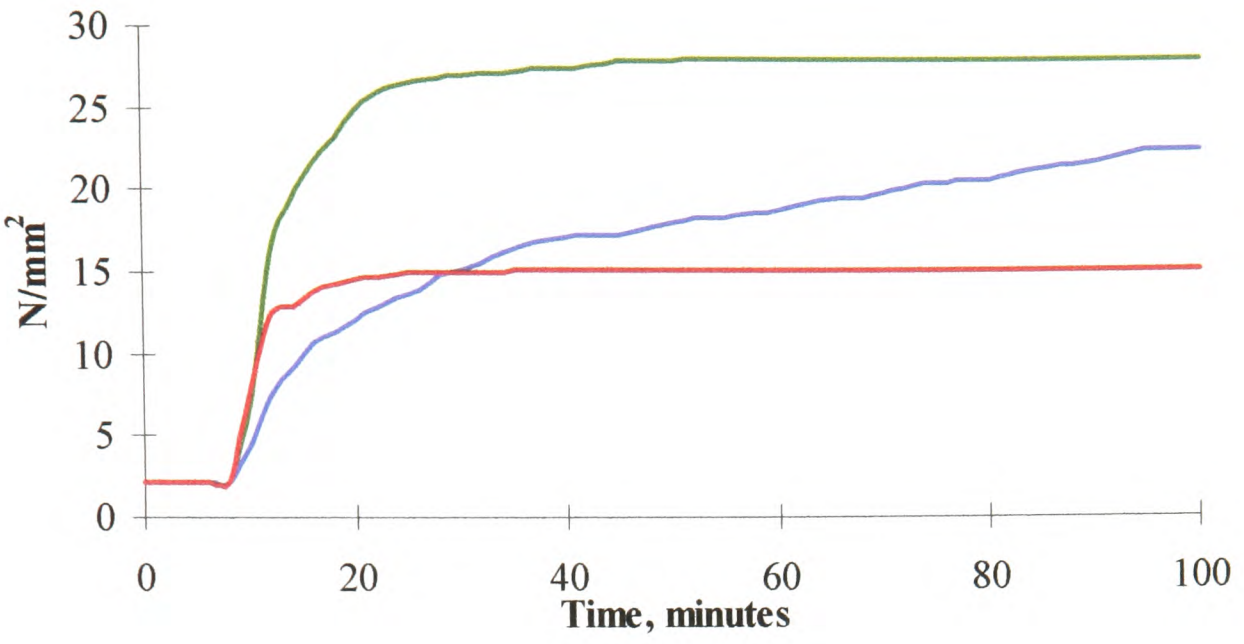

Figure 5.3: Effect of magnesium manipulation on the response to 70mM KCl. Control tissue has the highest maximum tension, followed slowly by magnesium depleted tissue and by magnesium loaded tissue . Each line represents an n of 3 and error bars are omitted for clarity.

It can be seen in Table 5.1 that the loaded tissue response is 2 fold faster than control tissue, but reaches a lower maximum. The depleted tissue, on the other hand, shows both a lower maximum tension and a markedly slower rate of tension generation (k_{TG}).

$[Mg^{2+}]_E$	k_{TG} (Nmm^{-2}sec^{-1})	Max. tension (Nmm^{-2})
0 mM + 0.1mM EDTA	0.059 ± 0.0024	19.07 ± 1.1
1.2 mM	0.162 ± 0.0099	26.60 ± 2.0
12 mM	0.3206 ± 0.007	13.24 ± 1.6

Table 5.1: Rate of tension generation and maximum tension generated by 70 mM KCl under three different magnesium conditions. Tissue was pre-loaded/ depleted in the appropriate HEPES buffer (Table 2.3) and the experiment was carried out in normal (1.2 mM Mg^{2+}) HEPES.

5.3.2.2 Acute magnesium effects

The phenomenon of magnesium-induced relaxation has been well documented[72, 282, 292]. Similar experiments were carried out here as shown in Figure 5.4.

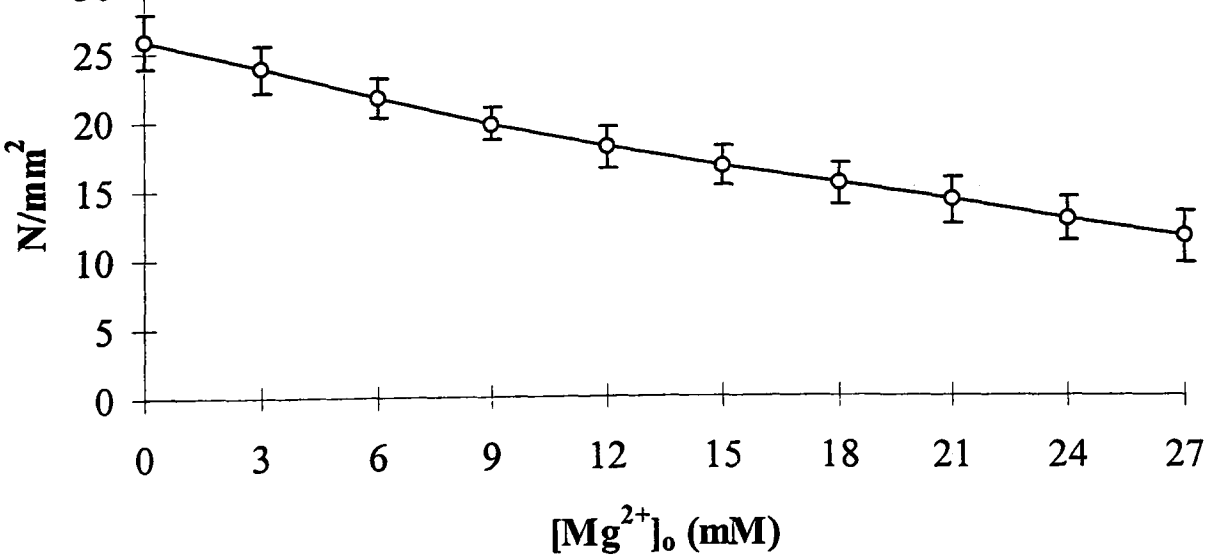

Figure 5.4: Tissue was equilibrated in magnesium free buffer and tension induced using 70 mM KCl. Magnesium was added in a stepwise fashion so that the concentration that the tissue was exposed to rose by 3 mM each time. Calcium was present throughout the experiment and no appreciable magnesium loading or depletion would be expected to occur. Each point represents an average of 5 experiments and error bars are standard deviations (σ_{n-1}).

Figure 5.4 shows the clear relationship between concentration of magnesium in the organ bath and relaxation of tissue contracted with 70 mM KCl. The average of 6 separate dose response curves carried out on tissue from 6 different pigs yielded a dose response curve with a y intercept of 26.67 ± 1.96 Nmm^{-2} (70 mM KCl induced maximum for these tissues).

The effect of adding magnesium to CSF_S contracted tissue was also studied. Figure 5.5 shows the effect of adding 12mM magnesium to tissue that had been contracted with CSF_S as well as the lack of effect of rinsing tissue treated with CSF_S.

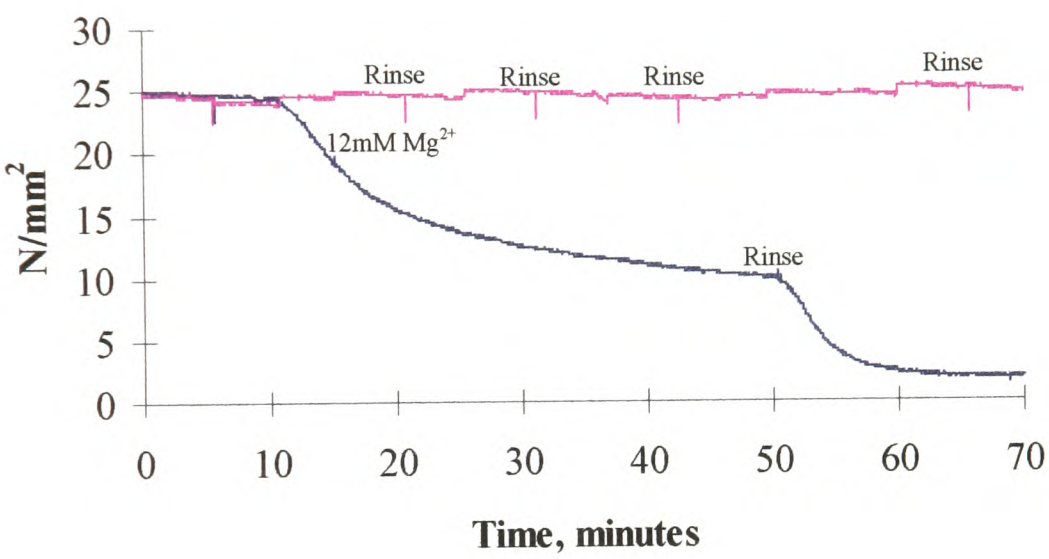

Figure 5.5: A representative trace of the acute effect of magnesium on CSF_S induced tension. A similar result was obtained with 2 other CSF samples. Tension is induced with CSF (freeze dried, PCA extracted and reconstituted to approximately 1:1 concentration) acute addition of 12 mM magnesium, followed by a rinse with fresh buffer was then done. A graph of CSF_S induced tension without addition of magnesium is also shown as a representative graph of and n of 6. Text above this line applies to this data, text below the line applies to the magnesium treated tissue.

The reduction in tension upon the addition of 12 mM magnesium during CSF_S induced tension is 16.55 ± 1.5 Nmm^{-2} (n=3) whereas the reduction of tension upon the addition of 12 mM Mg^{2+} to tissue contracted with 70 mM KCl was a lot less at just 5.49 ± 0.41 Nmm^{-2} (n=6). The difference between the reduction from a 70 mM KCl induced

contraction and a CSF_S induced contraction elicited by 12 mM magnesium is significant (P= <0.05).

An interesting finding in this set of results was that following exposure of CSF_S pre-contracted tissue to magnesium (12 mM) acutely, the effect became reversible by rinsing, and contractile function was restored (Table 6.1). Contractile function was examined by measuring the rate of relaxation after a stretch (methods in 2.3.2.1 and Figure 2.4). In tissue treated with CSF_S, the fast phase of relaxation (phase a, as defined by me) was found to be 2.698 ± .705 $Nm^{-2}s^{-1}$ which was significantly (P=<0.05) less than control tissue (16.094 ± 4.848 $Nm^{-2}s^{-1}$) which are shown in Table 6.1. If the CSF_S contracted tissue was exposed to 12 mM magnesium and then rinsed, the rate of relaxation returned to near control levels, at 15.820 ± 4.196 $Nm^{-2}s^{-1}$, indicating a reversal of the effect of CSF_S on the tissue.

5.3.2.3 Stretch-release experiments

Stretch release experiments (see 2.3.2.1) were carried out on control and magnesium loaded tissue in control HEPES solution. The regeneration of tension was fitted to the equation for a rectangular hyperbola using ModelMaker®, a curve-fitting programme. It was found that the rate of regeneration of tension after a stretch and release in magnesium-loaded tissue was not significantly different to that of control tissue. In magnesium loaded tissue, the rate was 0.056 ± 0.013 $Nm^{-2}s^{-1}$ and the rate in control tissue was 0.061 ± 0.007 $Nm^{-2}s^{-1}$.

The maximum tension regenerated was also measured. Expressed as a percentage of the maximum tension obtained during the stretch, the values for loaded and control tissues were significantly different. Magnesium loaded tissue regenerated tension to 8.06 ± 1.41% of the stretch tension, whereas control tissue regenerated tension to 15.98 ± 3.3% of the stretch tension.

5.3.3 Concomitant measurements

Figure 5.6 shows the effect of loading tissue with magnesium on hypoxia-induced relaxation.

Normal and magnesium-depleted tissues begin to relax at an O_2 concentration of 20μM, the depleted tissue showing a slight tendency to relax more slowly than the normal tissue. The magnesium-loaded tissue relaxes at the much higher O_2 concentration of 50μM and is significantly different to control and depleted tissue at 30μM. At 30μM O_2 concentration, the tension of depleted tissue(22.392 ± 0.013 Nmm^{-2}) is not significantly different to that of control tissue (22.396 ± 0.017 Nmm^{-2}).

Magnesium loaded tissue has, however, relaxed significantly at the same oxygen concentration, with a tension of 22.286 ± 0.024 Nmm^{-2}. The capacity of the tissue to recover with addition of oxygen was not tested due to the limitations of the apparatus.

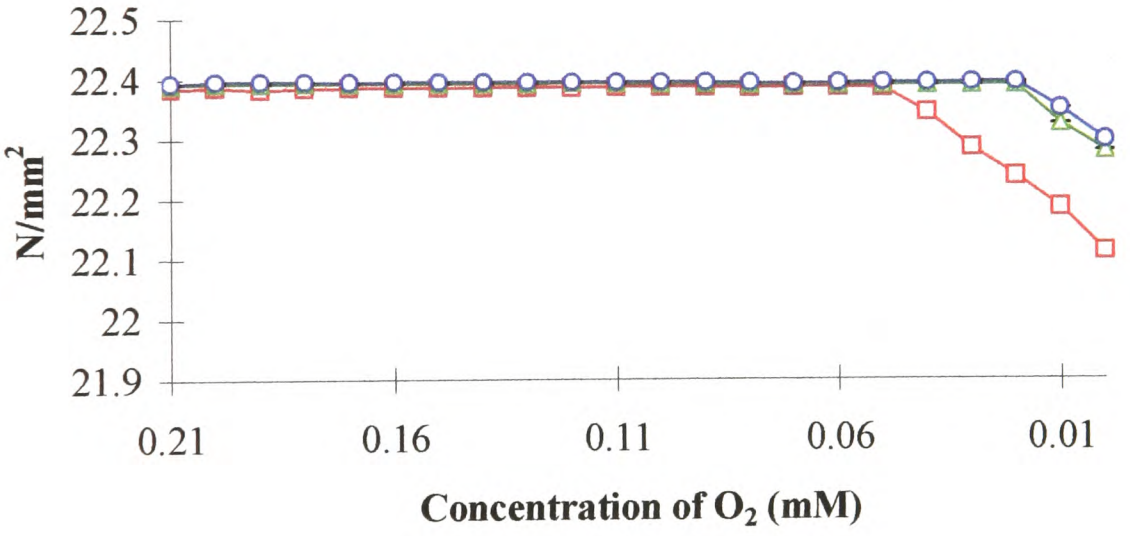

Figure 5.6: Concomitant force and oxygen consumption measurements. Initial tension was achieved by adding 70mM KCl to induce isometric contraction. The tissue was incubated in the oxygen electrode, allowing the depletion of O_2 by the tissue. Each point represents an average of 3 experiments and error bars are omitted for clarity. Magnesium loaded tissue (open squares), magnesium depleted tissue (open circles) and control tissue (open triangles) are shown.

5.4 Discussion

5.4.1 Introduction

The aim of the experiments reported in this chapter is to examine the effects of manipulating magnesium in the smooth muscle on the stimulation of tension generation by CSF_S. The results obtained give insight into the mechanism by which tension is induced by CSF_S, while at the same time assessing the suitability of magnesium as a possible therapy for vasospasm.

The results presented here show that magnesium manipulation affects the tissue in a number of ways: 1. metabolically, as measured using oxygen consumption measurements; 2. functionally, as ascertained from the results of several tension generation experiments and; 3. signalling pathways, which can be seen in the alteration of the tissue response to hypoxia in loaded conditions and the calcium antagonistic properties that may account for many of the observations.

There is much that could be discussed regarding the putative use of magnesium as a therapy for vasospasm and its current usage in the clinical setting, but in this thesis, I am primarily studying the biochemical changes and mechanisms of vasospasm so the clinical aspect of this work should be discussed elsewhere.

5.4.2 Oxygen consumption

The main observations made using O_2 consumption measurements are that loading with magnesium lowers the baseline respiration of the porcine carotid artery and the rate of O_2 consumption of the CSF_S stimulated magnesium loaded tissue was consequently lower, although the magnitude of the response to CSF_S in the loaded, control and depleted tissue remained unchanged. These will be discussed below with regard to the possible mechanism as well as metabolic implications.

The lowered baseline rate of O_2 consumption in magnesium loaded resting smooth muscle may be accounted for in various ways. A straightforward calcium antagonism event would result in such a lowered respiration. Calcium is known to stimulate mitochondrial respiration[226] and so antagonism of this calcium effect by inhibition of calcium channels would be expected to slow respiration significantly. Another possibility (suggested by Sloane *et al*[256]) is that the mitochondria need a low magnesium concentration to function normally. They noted that there was an efflux of magnesium from vascular smooth muscle mitochondria with concomitant ATP hydrolysis[256]. When mitochondrial respiration was inhibited using cyanide, no efflux of magnesium was observed. This efflux may be an essential part of the control of respiration. A high intracellular magnesium concentration may prevent this efflux, thus compromising mitochondrial function resulting in a lowered baseline rate of O_2 consumption.

It seems that the magnesium antagonism of calcium is more likely than mitochondrial impairment because the size of the tissue response to CSF_S remained constant despite magnesium manipulation. One might expect that impairment of mitochondrial function would also decrease the magnitude of a stimulation of the rate of O_2 consumption. The range of the response to CSF_S is not statistically different in control tissue increasing by 216 ±39% from baseline to CSF_S stimulated rate to that of magnesium loaded tissue (216 ± 24%). This would suggest that loading vascular smooth muscle with magnesium does not impair mitochondrial function.

The magnitude of the depleted tissue response (when calculated from matched experiments, same tissue, control and stimulated) was not significantly lower than that of control response. From Figure 5.3, no significant difference between the depleted tissue (159 ± 15%) and control tissue response (216 ± 39%) can be seen, however there is a downward trend in the depleted tissue.

5.4.3 Force measurements

Using force measurements to assess the contractile function of the tissue, three important observations were made. The rate and maximum tension of a 70 mM KCl induced contraction was profoundly altered both in the loaded and the depleted tissue, as reported in Table 5.1. The addition of 12 mM magnesium acutely not only partially relaxed tissue pre-contracted with CSF_S, but rendered the effect reversible by rinsing and the magnitude, but not the rate of tension regeneration after a stretch and release protocol was significantly different between control and magnesium loaded tissue.

5.4.3.1 Effect of magnesium on 70mM KCl induced contractions.

There are conflicting reports in the literature concerning the effect of magnesium loading and depletion on smooth muscle response to potassium depolarization. Carrier *et al.* found that magnesium loaded tissue reached a higher maximum tension in the presence of 2.5mM Ca^{2+} and 60mM KCl than did the depleted tissue[39]. This experiment yielded different results when reported by Ford and Driska ten years later. They found that the loaded tissue had a lower maximum tension in response to 60mM KCl than either control or depleted tissue[72]. The results that I obtained agree with those of Ford and Driska[72]. The KCl depolarised magnesium depleted tissue, although much slower to reach a maximum, plateaued at a tension between that of control and magnesium loaded tissue (Figure 5.6). Again, there may be more than one mechanism involved in this phenomenon.

One mechanism that could account for the low maximal tension of the loaded tissue is calcium antagonism as mentioned in 5.1.2. Magnesium is thought to displace calcium from actomyosin ATPase and therefore reduce its activity[292]. In the presence of residual magnesium concentrations, the myosin ATPase activity is 0.1μmole/min/mg protein, twice that of when there is higher than normal (5.4mM) levels of magnesium when the ATPase activity was 0.045 μmole/min/mg protein in the presence of 0.6μmoles of calcium bound per g of myofibrillar protein[292]. In addition to this the ATPase requires a higher level of

calcium to activate it in the presence of high magnesium (>0.8mM intracellularly)[176]. High magnesium (>5mM extracellularly) has also been reported to elicit a rapid uptake and inhibition of release of calcium from the sarcoplasmic reticulum[95, 253]. In heart muscle, magnesium has been found to bind to calcium channels and prevent efflux[12]. These factors would result in the accumulation of calcium in the sarcoplasmic reticulum, which would be unavailable to stimulate contraction.

Magnesium loaded tissue gave a rate of tension generation (0.32 ± 0.007 $Nmm^{-2}s^{-1}$ approximately twice that of control tissue (0.162 ± 0.01 $Nmm^{-2}s^{-1}$). Ikebe *et al.* described a phenomenon that may explain this result. They reported that the level of magnesium affects the proportion of myosin fibres adopting the folded conformation or the extended conformation. They found that increasing the magnesium concentration favoured the extended form of myosin which is susceptible to phosphorylation compared with the folded conformation[118]. This would support the observation that the rate of tension development in response to 70 mM KCl is around 2 fold faster in the magnesium loaded tissue than in the control magnesium group (Table 5.1)

The propensity for myosin to adopt the less active folded conformation in the absence of magnesium would also agree with my data in that the rate of tension generation in magnesium depleted tissue, at 0.059 ± 0.0024 $Nmm^{-2}s^{-1}$, was approximately half that of control tissue. However, there are also other factors involved in the diminished response of magnesium-depleted tissue to 70mM KCl. Some of the reactions occurring during smooth muscle contraction have been shown to have a significant requirement for magnesium[176, 222, 235, 292]. In these cases, the level of magnesium does not control the enzymes involved, rather the magnesium level controls the level of calcium that is required to activate/ inhibit them. In particular, myosin light chain kinase has been found to require magnesium for normal activity[222]. Magnesium free solutions were found to clearly inhibit myosin light chain kinase. In combination, adoption of the less phosphorylatable conformation of

myosin and the inhibition of myosin light chain kinase produced a slow contraction with a lower maximal tension[298]. This corroborates the results reported in Figure 5.3.

5.4.3.2 Acute magnesium effects

The relaxation achieved in pre-contracted smooth muscle may be caused by the calcium antagonist activity of magnesium. More precisely, magnesium induced relaxation is thought to be due to conformational changes in the actomyosin ATPase as described in 5.1, rendering it less active in a dose dependent manner[176, 292]. It has been shown that neither adenylate cyclase nor guanylate cyclase are involved in magnesium induced relaxation[300]. Though not yet confirmed, magnesium may activate a phosphatase activity in smooth muscle (5.1.1). There is a magnesium-activated phosphatase known (PP2C, see 1.4.4), but it has not yet been isolated from smooth muscle.

As previously discussed (Chapter 4), the stimulation of a slow, insidious onset of pathological constriction/ failure to relax by CSF_S has so far proven to be irreversible clinically. Neither rinsing, nor the addition of vasorelaxants produced a total restoration of normal contractile function in our model of cerebral vasospasm after subarachnoid haemorrhage (4.3.2). Whilst investigating the effect of acute magnesium application on CSF_S stimulated contraction, it was found that exposure of tissue pre-contracted with CSF_S to 12mM magnesium caused a 66.5 ± 6% decrease in tension (Figure 5.5). This effect yields several clues as to the mechanism of the pathology of vasospasm, as well as to the potential therapeutic mechanism of magnesium. As well as continued use of magnesium to prevent the onset of eclampsia in preeclamptic women, raising the plasma magnesium levels of patients with subarachnoid haemorrhage may help prevent onset of vasospasm.

The irreversible nature of the CSF_S induced contraction suggests that a conformational change in the contractile proteins of the smooth muscle has taken place, resulting in the inability of the tissue to relax. It seems, then, that magnesium may reverse

the conformational change and relieve the inhibition of relaxation in some way. The involvement of magnesium in calcium antagonism is not likely to be the sole explanation.

As we have already seen, pre-treating the vessels with substances thought to induce the latch state protects the tissue against CSF_S induced contraction and stimulation of the rate of oxygen consumption (4.3.1 and Figure 4.5). Where might magnesium be able to act in order to achieve this after exposure of the tissue to CSF_S? The latch state has already been discussed in some depth in Chapter 1. In brief, attached phosphorylated cross bridges may become dephosphorylated when still attached, thus becoming latch bridges which are approximately five times slower than cross bridges at entering the relaxation (A + M) state[184]. ATPase activity, $[Ca^{2+}]_i$, shortening velocity and phosphorylation of myosin are all near levels associated with relaxation during the latch state[22]. The latch state is controlled by the calcium dependent phosphorylation of myosin by myosin light chain kinase and dephosphorylation by myosin light chain phosphatase[22]. How these phosphorylation and dephosphorylation events are controlled and co-ordinated is not understood.

The entry of actively contracting smooth muscle, such as tissue exposed to CSF_S, into the latch state depends on the dephosphorylation of attached cross bridges. The way that magnesium relieves the tension in the smooth muscle and enables the effect to become reversible depends on the way that the tension is induced by the CSF_S. An inhibition of phosphatase activity is a possible way that this may be achieved and this is discussed in the next chapter. Without a more detailed knowledge of exactly how the CSF_S renders the tissue to be unable to relax, it is very difficult to hypothesise on the way that magnesium is acting here.

It is possible that the CSF_S causes the myosin to enter a state that allows MLCK to act, but not the phosphatase. The magnesium would relieve this by pushing the myosin into the extended state, allowing dephosphorylation. The CSF_S may act directly upon the phosphatase, inhibiting it in a way that is reversible by conformational change or phosphatase activation induced by magnesium. It is also possible that the myosin ATPase

may be constitutively active in the presence of CSF_S. The high magnesium, which has been shown to inhibit the ATPase by increasing the calcium requirement, may relieve the pathology in this manner.

Magnesium-dependent protein phosphatase 2C (introduced in 1.4.4 and 5.1.2) may also play a part in magnesium reversal of *in vitro* vasospasm. If PP2C (which is known to be present in a number of smooth muscles[120]) is not active at basal Mg^{2+} concentrations, then perhaps it is activated in the presence of elevated intracellular free magnesium such as after loading or acute addition of 12 mM Mg^{2+}. Could this phosphatase then dephosphorylate the myosin light chains thus allowing relaxation? This hypothesis is discussed more fully in section 7.1.4.

5.4.3.3 Stretch release experiments

Barany *et al.* showed that stretching arterial smooth muscle to 1.7 times its resting length results in maximal phosphorylation of myosin light chains even in the absence of any stimulus[19]. This phosphorylation of light chains results in the regeneration of tension when the tissue is released to the resting length again. The regeneration of tension depends on the extent of the phosphorylation that occurred during the stretch phase. This level of phosphorylation can change according to the conditions applied to the tissue[19]. Please see Figure 2.4 for an idealised stretch-release trace.

Currently there is much debate as to the correlation between MLC_{20} phosphorylation and tension or velocity[38, 63, 67]. The experiments described here were carried out in order to determine the effect of high magnesium on the contractile function of the tissue. Although the rate of regeneration of tension was not significantly different in the two states, the magnitude of the tension regenerated in the magnesium treated tissue was half that of control. This would suggest that the integrity of the tissue has been maintained and the decrease in tension regeneration is a well characterised, reproducible and dose dependent effect of magnesium.

From these results, it may be implied that magnesium affects the level of the phosphorylation of myosin light chains during the stretch phase of the stretch/release, which is consistent with the findings of Moreland *et al*[176]. Calcium in the cells of the magnesium-loaded tissue will have been tightly sequestered by the sarcoplasmic reticulum. It is then unable to stimulate myosin light chain kinase and so the level of phosphorylation (and therefore the magnitude of the regeneration of tension) is decreased in magnesium-loaded tissue.

5.4.4 Concomitant measurements: Hypoxia induced relaxation

The phenomenon of hypoxia induced relaxation, although thoroughly investigated, is still not fully understood[267]. The relaxation of vascular smooth muscle[6] in response to hypoxia is a protective mechanism. It enables the conservation of ATP in times of metabolic stress and allows a greater blood supply to hypoxic regions[121].

There are currently two theories applicable to tonic smooth muscle for the mechanism of hypoxia-induced relaxation. Both theories ultimately depend on the blockage of calcium channels and depletion of intracellular calcium, which leads to relaxation. The existence of hypoxia sensitive calcium channels is postulated in the first explanation. This would mean that calcium channels become impermeable to calcium during hypoxia and the subsequent fall in intracellular calcium concentration leads to relaxation[202, 203]. A second explanation could be that as ATP, which usually exists in the cell as MgATP, is used up below normal intracellular levels during hypoxia. The intracellular magnesium concentration would cause relaxation in the ways previously described[308].

---

[6] except some respiratory tract smooth muscle, which contracts in response to hypoxia.

The second theory would explain the early relaxation of the magnesium-loaded tissue, but does not explain why the depleted tissue relaxed at the same [O_2] as the control tissue. If this were the case, the depleted tissue would be expected to relax at a higher [O_2] if at all. Considering the results presented here, it seems that a combination of the two theories would explain them very well. The reduction of intracellular Ca^{2+}, which in itself would cause relaxation, in combination with a reduced ATP demand, could result in the observations that have been reported.

5.5 Conclusion

The data presented in this chapter all indicate that a lack of magnesium may be detrimental to the contractile function and metabolic integrity of the smooth muscle. Loading with magnesium demonstrated no observable undesirable effects *in vitro* assessed using oxygen consumption measurements and force measurements. In fact, it seems that the loading of vascular smooth muscle with magnesium is beneficial, because it has been the first intervention to be found effective in reversing cerebral vasospasm after subarachnoid haemorrhage in our model. This reversal of the CSF_S effect by rinsing after acute application of magnesium suggests that extracellular magnesium has a protective role to play.

The possibility of using magnesium as a treatment for vasospasm *in vivo* has yet to be evaluated through clinical trials and further animal studies. I believe that these data offer substantial encouragement to researchers pursuing the development of one of the first effective therapy for cerebral vasospasm after subarachnoid haemorrhage.

6.Myosin Light Chain Phosphatase

6.1 Introduction

The control of smooth muscle contraction by phosphorylation of contractile proteins has been reviewed in detail[21]. It has been known since 1963 that covalent modification, including phosphorylation, of proteins regulates numerous cellular processes[145]. New control mechanisms involving phosphorylation and dephosphorylation of proteins have been continuously under investigation[1, 51, 108, 251, 270, 275]. The examination of the phosphorylation patterns of the contractile proteins in smooth muscle yields valuable information when investigating pathologies. The mechanism by which smooth muscle contraction is controlled by phosphorylation and dephosphorylation events has been discussed in Chapter 1 (see 1.4.2 and 1.4.4). An abridged reiteration of the major events pertinent to the results presented in this chapter follows.

Figure 6.1 shows a simplified four state model of smooth muscle contraction[86]. Myosin, with Mg-ATP bound, is phosphorylated by myosin light chain kinase using ATP leaving ADP. Actin and Myosin phosphate with bound Mg-ATP then become attached, forming a cross bridge. This interaction can be broken with Mg-ATP hydrolysis by the actomyosin ATPase activity of the myosin head and the binding of a new Mg-ATP molecule. The right hand pair of reactions constitutes the part of the cycle where tension is actively generated. The myosin molecule must be phosphorylated for tension to be developed. Dephosphorylation of the attached cross bridge can take place using myosin light chain phosphatase[79]. If this occurs, dephosphorylated, attached cross bridges, or latch bridges, result[182, 185]. Rephosphorylation by myosin light chain kinase can occur, allowing fast cycling of the cross bridges and tension generation once again. Dephosphorylated myosin and actin can attach and detach without hydrolysis of ATP, resulting in a low energy cost tension maintenance state known as the latch state, where tension is maintained

maintained at little energetic cost with a lowering of [Ca^{2+}] and phosphorylation levels. This allows prolonged, economical tension maintenance, such as is required of vascular smooth muscle for maintenance of blood pressure.

6.1.1 Phosphorylation of contractile proteins

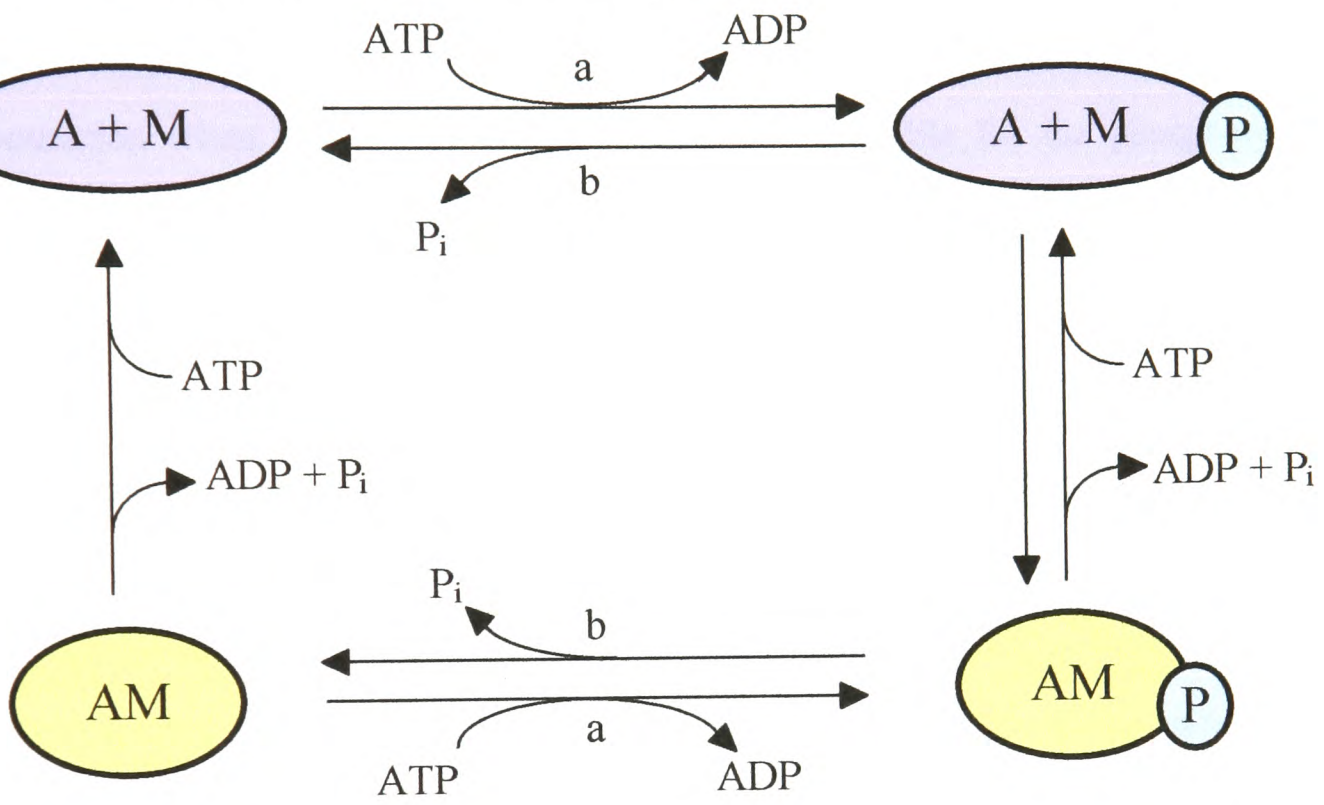

Figure 6.1: A simplified diagram of the four-state model of smooth muscle contraction. A is Actin and it can either be attached to M (myosin) or not. In addition, myosin may be phosphorylated or unphosphorylated. Myosin phosphorylation is effected by enzyme a, myosin light chain kinase. Dephosphorylation is achieved with enzyme b, myosin light chain phosphatase. See text for a fuller explanation.

Other contractile proteins are also phosphorylated during the contractile cycle. A 28 kDa protein with similar properties to the heat shock protein Hsp27 has been suggested to be phosphorylated in various smooth muscles[22, 54]. Its structure bears a resemblance to the protein named α-crystallin[103] which stabilizes myofibrils[13]. It has been found to mediate the long-term contraction of vascular smooth muscle[28]. It is postulated that the

phosphorylation of this 28kDa protein may activate it to bind to myofibrils and induce a conformational change in the contractile proteins[21].

Caldesmon was found to be phosphorylated during the contractile cycle in 1989[3]. It was then found to slow cross bridge detachment during sustained smooth muscle contraction when phosphorylated. The enzyme responsible for the phosphorylation of caldesmon was not elucidated until much later[2, 5] when mitogen activated kinase (MAP kinase) was found to be one of the kinases attributable.

In 1990, Stromer and Bendayan[262] reported the existence of a network of proteins in the cytosol of smooth muscle cells linking the nuclei with the mitochondria which may be responsible for vascular tone in a mechanism separate to cross bridges. They reported that the proteins involved included the phosphorylatable protein desmin. Park and Rasmussen had previously found that desmin was phosphorylated in smooth muscle during sustained contraction[212]. The existence of a tone maintenance system separate to cross bridge formation involving desmin had been postulated already[257]. That more than one system of control of smooth muscle contractility by phosphorylation appears to exist has to be taken into account when postulating theories as to the æ tiology of diseases though to involve perturbation of phosphatase activity, as here. The question is, is desmin phosphorylated as a result of sustained contraction, or is the phosphorylation of desmin the mechanism to allow sustained contraction? The answer to this question has not yet been resolved, but it could go some way to explaining the effect of CSFs on smooth muscle that we observe.

6.1.2 Myosin light chain phosphatase

In order for myosin light chain kinase to be activated, intracellular calcium must be raised, either via mechanical or chemical stimuli. The calcium then binds to calmodulin in a 4:1 ratio forming $CamCa^{2+}_4$. This complex binds to and activates myosin light chain kinase. This in turn activates myosin light chains allowing contraction. Myosin light chain

phosphatase dephosphorylates and inactivates the myosin ATPase activity of the myosin light chains thus leading to relaxation of the smooth muscle.

Many different phosphatases have been attributed with the role of the specific myosin light chain phosphatase[66]. It is now generally accepted that it is a form of PP1 but an absolute determination has not yet been made and several publications report evidence of the phosphatase being type 2A[59, 205, 297], which shares characteristics with type 1[47].

Very little is known about the regulation of myosin light chain phosphatase activity. The trimeric phosphatase thought to be involved in the relaxation of smooth muscle is composed of three subunits of 130, 38 and 20kDa[115, 168, 281]. The 38kDa subunit is the catalytic subunit. It has been proposed that the 130kDa subunit is able to bind to myosin, enabling targeting and that the affinity of this subunit for myosin is higher when the myosin is phosphorylated that dephosphorylated[7, 68, 77, 115]. It has been found that the isolated catalytic subunit has a much higher affinity for myosin than the assembled trimer, leading to suggestion that disassembly could be a form of regulation[66]. These theories of regulation are supposition, as the actual mechanism has yet to be elucidated.

As we postulated that cerebral vasospasm after subarachnoid haemorrhage was not a pathological constriction, but a pathological failure to relax[228], the experiments described in this chapter were carried out to determine the extent, if any, of the involvement of phosphatase inhibition in the ætiology of vasospasm in our model.

6.2 Methods

All the general methods used in this chapter are detailed in Chapter 2. Items specific to these experiments are detailed below.

6.2.1 Okadaic Acid

Okadaic acid requires careful handling, as it is a known tumour promoter, irritant and is easily absorbed through the skin and mucous membranes. Safety glasses, laboratory coats and gloves were worn at all times whilst handling this hazardous substance. The acid was dissolved in 100% methanol and aliquots of this were used to treat tissue in experiments.

6.2.1.1 Oxygen consumption measurements

Okadaic acid was added to porcine carotid arteries in the oxygen electrode at a final concentration of 1 nM, which gives the maximum inhibition of PP2A without inhibiting PP1 (PP2A>>>PP1) whilst still retaining specificity[47]. Above around 5nM, okadaic acid starts to inhibit PP1 as well as PP2A. At 10 nM, okadaic acid appears to have become inhibitory and this can be seen in 4.3.1 and Figure 4.3.

A dose response curve was constructed to determine whether the stimulation of O_2 consumption by okadaic acid is dose dependent, or an all or nothing response. Okadaic acid was added to final concentrations of 250 pM, 500 pM, 750 pM, 1 nM and 5 nM. The rate of O_2 consumption at 180 minutes was taken to construct the dose response graph. The full graph, with the inhibitory 10 nM point can be seen in Figure 4.3.

6.2.1.2 Stretch-release experiments

Tissue was loaded onto the force measurement machine and incubated for 180 minutes in buffer, 1 nM okadaic acid or a 1 in 30 dilution of CSF_S before stretch release experiments were carried out. A resting tension was obtained before the addition of okadaic acid. This time, instead of the rate of regeneration of tension being calculated, the rate of relaxation after the stretch was calculated.

6.2.2 Phosphatase assay

This assay was developed for this thesis to enable the measurement of phosphatase activity in a crude preparation of porcine carotid. The details of the development of the assay are described in section 2.3.9. Commercially available smooth muscle substrate (Alexis Corporation) and small pre-packed ion exchange columns (Whatman) meant that the assay, similar to a protocol utilized by Pato and Kerc[215] to purify smooth muscle myosin phosphatase, could be simplified and shortened considerably.

6.3 Results

6.3.1 Stimulation of O_2 consumption by okadaic acid

The addition of 1 nM okadaic acid to porcine carotid artery stimulated the rate of oxygen consumption in a very similar manner to that of CSF_S. Figure 6 shows the okadaic acid stimulation and the CSF_S stimulation for comparison.

In order to determine whether this response to okadaic acid is dose dependent or not, tissue was exposed to several concentrations of okadaic acid and the rate of O_2 consumption at 180 minutes was plotted against the concentration. The results of this can be seen in Figure 6.2.

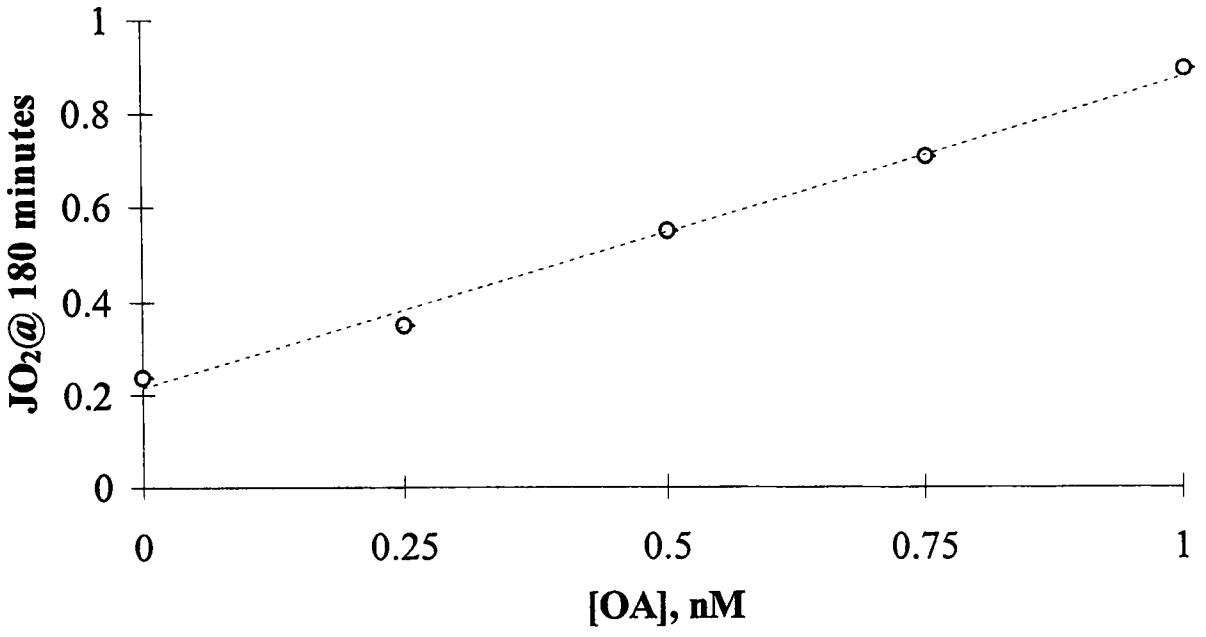

Figure 6.2. Each point is the average of 4 experiments. Rate of O_2 consumption (JO_2) is expressed in units of μmol min^{-1} g dwt^{-1}. The dotted line is the result of a linear regression calculation. Error bars are SEM values and are within the data markers in some cases.

This relationship between okadaic acid concentration and stimulation of O_2 consumption can be fitted using linear regression. The R^2 value obtained was 0.99. indicating a good linear relationship. The gradient of the line indicates an increase of rate of O_2 consumption of 0.168 μmol min^{-1}g dwt^{-1} for every increase in okadaic acid concentration of 250 pM. This relationship ceases to be linear above 1 nM (Figure 4.3) until, at okadaic acid concentrations above 5 nM, the rate of O_2 consumption is significantly inhibited.

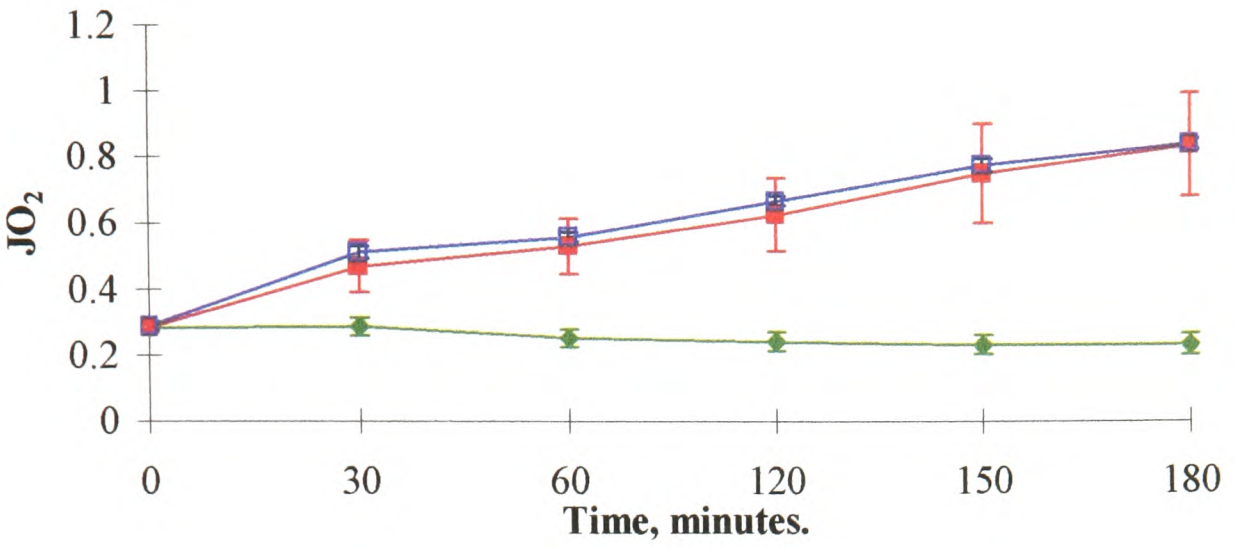

Figure 6.3. Control tissue (diamonds) data points represent the average of 34 data points. CSF_S stimulated tissue (closed squares) data points represent the average of 24 different CSF_S samples. 1 nM okadaic acid stimulated tissue (open squares) data points represent the average of 8 different experiments. Error bars are $\pm \sigma_{n-1}$. The rate of O_2 consumption (JO_2) is expressed in units of $\mu mol\ min^{-1}\ g\ dwt^{-1}$.

6.3.2 Stretch release measurements

There is a noticeable effect of 1nM okadaic acid and a 1 in 30 dilution of CSF_S on the relaxation of the carotid arteries after a stretch. Four control (not exposed to okadaic acid) experiments were carried out, three okadaic acid experiments and three CSF_S experiments, each with a different CSF sample. The relaxation was observed to have two phases; a fast relaxation (termed phase a) and a slower second phase (phase b). The rates were calculated for each phase on each piece of tissue and the data is shown in Table 6.1.

rate in units $Nm^{-2}s^{-1}$	**Phase a relaxation**	**Phase b relaxation**
Control	16094 ± 4848	259 ± 82
CSF_S 1 in 30	2698 ± 705	161 ± 59
1nM okadaic acid	2716 ± 712	156 ± 43

Table 6.1: The fast and slow phase relaxation after a stretch under various conditions. Phase a and phase b relaxation are defined in 2.3.2.1 and Figure 2.4.

The phase a, or fast relaxation is significantly slower in okadaic acid treated tissue and CSF_S treated tissue than in control tissue. The phase b relaxation is also slower in okadaic acid treated tissue and CSF_S treated tissue than in control, although not significantly.

6.3.3 Phosphatase assay

As introduced in 2.3.13.3 a number of control experiments were carried out in order to assess the assay. It was found that carrying out the assay in the absence of substrate resulted in a fractional phosphorylation of just 0.015 ± 0.002, amounting to just 3.8% of the control fractional phosphorylation. This could be due to non-specific radiolabelled-ATP binding to proteins in the mixture, or incomplete MLCK inhibition by ML-9 HCl. This was not considered to be a major source of error.

The effect of temperature on non-specific cleavage of radiolabelled phosphate from the substrate was also assessed. It was found that in the absence of phosphatase preparation the fractional phosphorylation at 22°C was 0.994 ± 0.086 and at 37°C, 0.879 ± 0.089. These values are not significantly different and the advantages of running the experiment at physiological temperatures (37°C) were considered to outweigh the slightly lower level of non-specific cleavage seen at 22°C.

The optimum time to quench the reaction and measure the phosphate released was determined by plotting the fractional phosphorylation of a control preparation against time. A time that gave a fractional phosphorylation on the linear part of the relationship was chosen, 10 minutes. The relationship is shown below in Figure 6.4.

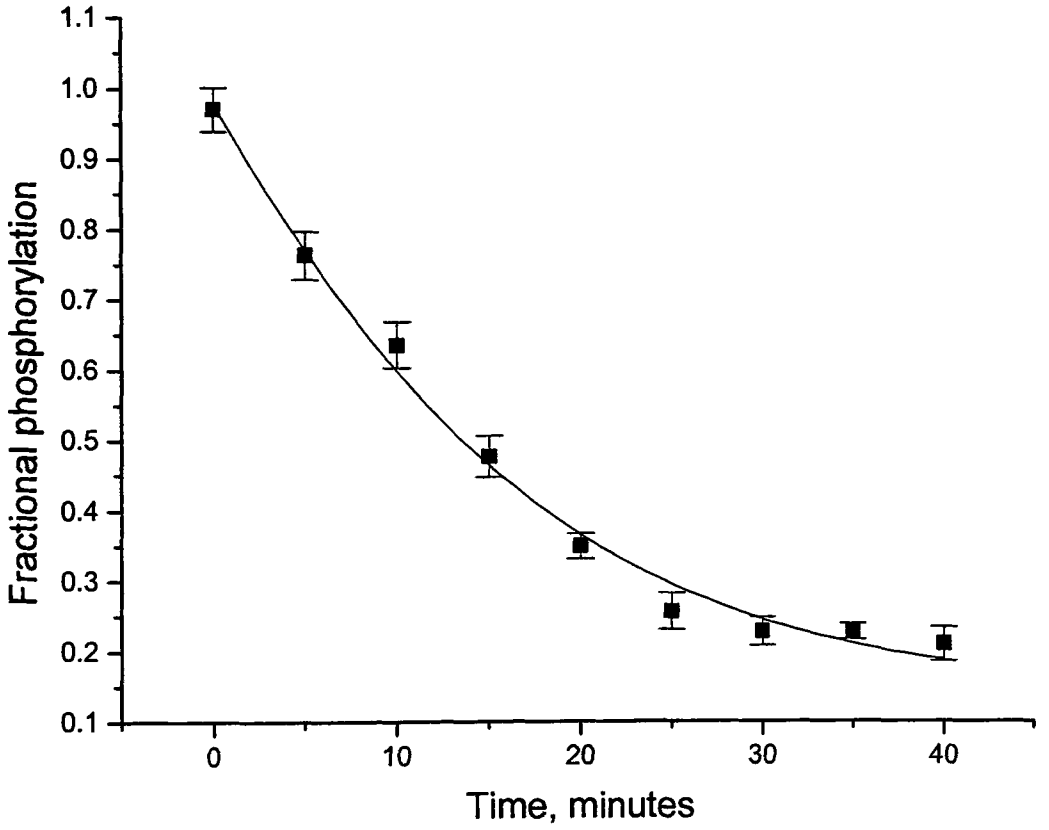

Figure 6.4. The relationship between fractional phosphorylation of a control preparation and time of incubation with the phosphatase preparation. n=4 for each data point, errors are standard deviations.

The results of the phosphatase assay can be reported in several ways. Results are obtained in the form of moles of phosphate released and so, knowing the concentrations of all the components of the assay there are several relevant ways to present the data. The most appropriate way in this case is to express the results as fraction of total available phosphorylatable sites phosphorylated under different conditions, as can be seen in Figure 6.5. This is known as fractional phosphorylation.

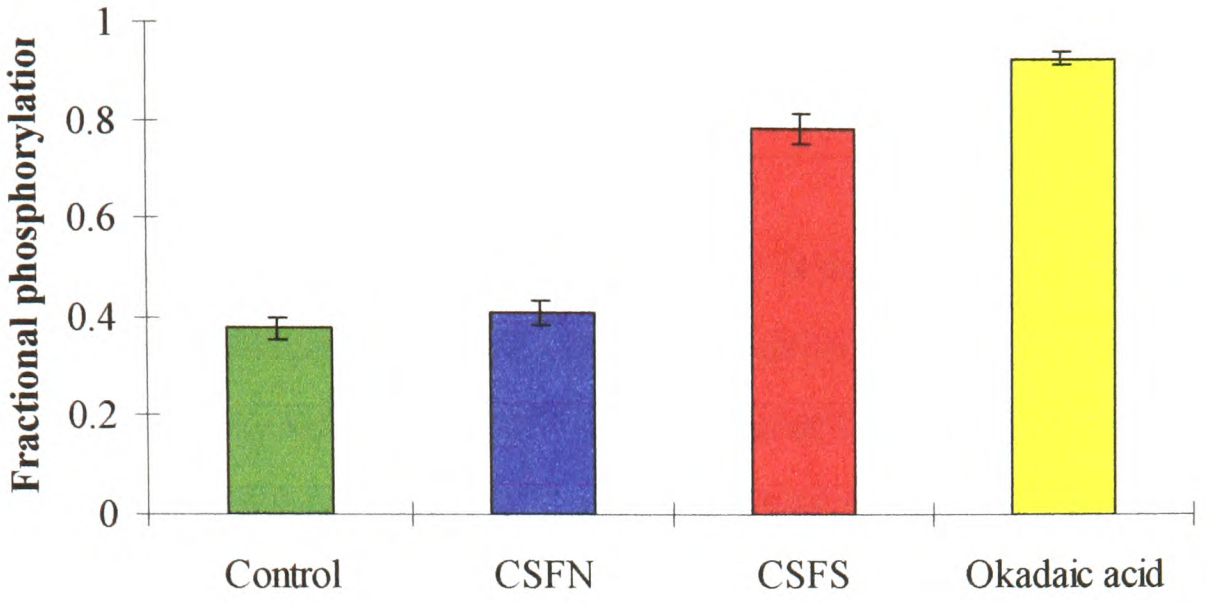

Figure 6.5: Each bar represents the average of 5 measurements. The error bars are $\pm \sigma_{n-1}$. Okadaic acid was used at a concentration of 1 nM. Extracted CSF samples were used at a concentration approximating to undiluted CSF.

Fractional phosphorylation was determined by calculating the number of phosphorylatable sites of myosin light chain kinase substrate present in each tube. This is known, since each molecule of substrate contained only one phosphorylatable site and the amount of substrate used was known. The phosphate released must have come from the substrate and so the number of moles of phosphate released divided by the total number of moles of sites available for phosphorylation subtracted from 1 gives the fractional phosphorylation. Figure 6.4 shows the fraction of phosphate still bound to the substrate. Thus, in Figure 6.5, the greater the fractional phosphorylation, the less active, or more inhibited, the phosphatase.

6.4 Discussion

The role of phosphorylation and dephosphorylation events in the regulation of smooth muscle contractility has been discussed, both in Chapter 1 and in section 6.1. The results presented in this chapter show that the energy metabolism of the muscle is also perturbed significantly. That the contractile function and energy metabolism of vascular smooth muscle is unbalanced by an inhibitor of phosphatase activity, okadaic acid, is well

documented, here and elsewhere[21, 22, 129, 135, 317]. It is not these observations that are of interest, but the similarity of the effects of a concentration of okadaic acid known to inhibit PP2A specifically but not PP1 (1 nM) [47] to the effect of CSF_S treatment. We hypothesized that a pathological failure to relax that may be involved in vasospasm could either be due to a constitutively active MLCK, no longer dependent on calcium or inhibition of MLCP activity. It appears, with reference to the results presented here that the latter is more likely. This could indicate that the phosphatase responsible for the dephosphorylation of smooth muscle myosin light chains is either an okadaic acid sensitive type 1 phosphatase, or, more likely, a type 2A phosphatase. It is also possible that okadaic acid prevents the dephosphorylation and inhibition of the PP1 inhibiting protein CPI17 by a type 2A phosphatase.

The stimulation of oxygen consumption by a non-toxic dose of okadaic acid can be explained by the inhibition of a type 2A myosin light chain phosphatase. At any one time in tonic smooth muscle, a certain population of cross bridges will be attached. Others will be phosphorylated and the rest will be unattached. These populations cycle, with the net result of a constant tone known as myogenic tone. Disturbing the proportion of cross bridges in each state results in a net imbalance and relaxation or contraction. This disturbance can be effected in several ways. Action of an agonist such as nitric oxide or calcium antagonists lead to relaxation via decreased phosphorylation of the cross bridges, but increasing the population of the phosphorylated cross bridges with an agonist such as noradrenaline, calcium, or CSF_S results in contraction. Inhibition of the phosphatase by okadaic acid means that the cross bridges remain phosphorylated and therefore actively creating tension(6.1.1) which consumes ATP. The compartmentation of glycolytic and oxidative metabolism in vascular smooth muscle[216] means that this ATP demand is met by an increase in oxygen consumption. The similarity between the stimulation by 1nM okadaic acid and a 1 in 30 dilution of CSF_S may suggest that a similar level of inhibition of MLCP is reached with 1 nM okadaic acid and the average of 5 CSF_S samples.

If the phosphatase inhibition is directly responsible for the stimulation of O_2 consumption, the okadaic acid induced stimulation should be dose dependent, as is shown in Figure 6.2. The relationship between okadaic acid concentration and rate of O_2 consumption is linear up to 1nM. Above this, up to 5 nM, a plateau is reached and above 5nM okadaic acid becomes toxic and inhibition of O_2 consumption is observed (Figure 4.3).

The relaxation of vascular smooth muscle is profoundly affected by the phosphatase inhibition or CSF_S. Again, the results are similar between 1 nM okadaic acid and a 1 in 30 dilution of CSF. This lower concentration of CSF_S was used so that energy metabolism was affected, but no active force was being generated. This was done in order to ensure that the contractile proteins were at the same stage of the contractile cycle as control before the stretch took place. Both phases of relaxation, the fast phase termed a and the slow phase termed b, are slowed. The slowing of phase b relaxation is not statistically significant, however the downward trend is clear. This effect is again a direct result of phosphatase inhibition. Other researchers have reported similar effects from inhibiting phosphatase activity in smooth muscle[21, 22]. This reinforces the postulation that phosphatase inhibition is a part of, if not the sole cause of cerebral vasospasm after subarachnoid haemorrhage.

This hypothesis can be tested further by directly measuring the activity of the MLCP under various conditions. The fractional phosphorylation of control samples was similar to literature values[21, 22, 38, 129, 137]. The CSF_N samples had a fractional phosphorylation not significantly different from control, but the CSF_S and okadaic acid treated samples showed a significant increase in fractional phosphorylation and therefore a significantly inhibited phosphatase (see Figure 6.5).

The mechanism by which okadaic acid inhibits PP2A is not known. It is difficult to postulate a mechanism considering the lack of knowledge of how the phosphatase is regulated normally. The most likely mechanisms of inhibition are straightforward binding

to the active site of the catalytic subunit of the phosphatase, although a level of dose dependence suggests a more subtle form of inhibition possibly involved in a control mechanism that has not yet been elucidated. As such, it is also very difficult to try and postulate which component of CSF_S is having the inhibitory effect and how such a substance or combination of substances might come to be in CSF from patients at risk of vasospasm and not those with no signs of vasospasm.

6.5 Conclusion

CSF_S has a very similar effect with respect to phosphatase activity and related indicators of phosphorylation level such as rate of O_2 consumption and relaxation rates to okadaic acid, a known inhibitor of type 1 and type 2A protein phosphatases. Okadaic acid did not stimulate tension generation at levels specific to PP2A inhibition (<5 nM). Relaxation is slowed in both phases, rate of oxygen consumption is increased and phosphatase activity is decreased similarly in CSF_S treated tissue and okadaic acid treated tissue, suggesting a role for myosin light chain phosphatase inhibition in the etiology of cerebral vasospasm after subarachnoid haemorrhage in this model.

7.Discussion

7.1 General discussion

There are many theories as to the ætiology of cerebral vasospasm[49], but none have yet been generally accepted in the scientific community. The aim of the research presented in this thesis is to try to determine the biochemical processes occurring in vascular smooth muscle during cerebral vasospasm after subarachnoid haemorrhage. In order to achieve this, a number of novel research modalities needed to be developed. These, along with established methods, have allowed me to study the nature of this significant pathology. This has obvious implications for the development of more appropriate therapies for managing this condition and elucidating the mechanism by which vasospasm exerts its actions.

7.1.1 Intervention studies. What do they all actually say?

As can be seen from Table 1.2, there are a number of intervention studies that report apparently effective prevention of vasospasm. On closer inspection, however, a number of these "successful" outcomes were achieved by treating the animal with the agent before the induction of the subarachnoid haemorrhage. Few papers report reversal of vasospasm after it has manifested. Those that did appear to reverse vasospasm were the calcium antagonists of the HA type[273, 274]. The HA type calcium antagonists are modified calmodulin antagonist molecules and act intracellularly to block the Ca^{2+} activation of tension generation, as well as promoting the inhibition of tension. The authors do not postulate a mechanism for cerebral vasospasm, merely state that calcium antagonists reverse spasm regardless of the cause[273, 274]. Unfortunately, a reversal of the spasm was only seen with intracisternal infusion of the drugs, intravenous administration only eliciting a 10% dilation of the cerebral vessels.

There have been numerous trials, in animal models and patients, using the calcium channel blocker, Nimodipine® (Bayer)[301]. Out of the 16 trials described in Table 1.2, just 3 report some small reversal of the spasm in humans. The reason that nimodipine is the treatment given to subarachnoid haemorrhage patients is that it does seem to produce a significantly improved neurological outcome (21%)[224]. This may be due to the suppression of excess neurological activity in the traumatised brain, allowing it to recover more function. Reducing the fluctuations in calcium levels by blocking the channels may help to stabilise the neuronal activity in the damaged areas of the brain, thus aiding neurological recovery without the need for an increased blood flow facilitated by the relief of vasospasm.

7.1.2 An *in vitro* model of cerebral vasospasm after subarachnoid haemorrhage

Development and verification of a model of cerebral vasospasm after subarachnoid haemorrhage was an essential step in the investigation of this phenomenon. The analysis of the model parameters is presented and discussed in detail in Chapter 2. The dearth of "user-friendly" models of cerebral vasospasm led to the development of a method by Drs. Joe Clark and Zayne Domingo. Dr. Zayne Domingo examined the stimulation of oxygen consumption of porcine carotid arteries by CSF_S but not CSF_N. In this study, the CSF was characterised using established clinical parameters. CSF from patients with a high risk of vasospasm and/ or angiographically visible vasospasm was categorised as CSF_S. It was found that 89% of the CSF from patients at risk of vasospasm that stimulated O_2 consumption to levels above 0.4μmol min^{-1} g dwt^{-1} came from patients who subsequently developed clinically relevant vasospasm. For the purposes of this thesis, it was taken that CSF that stimulated O_2 consumption was in fact CSF_S and the biochemical mechanisms underlying this stimulation investigated (see Chapter 3).

The results presented in Chapter 3 indicate the robustness of the model. The coefficients of variation (Table 3.1) for all the parameters that could introduce error into

the model are acceptably low and indicate the reproducibility of the stimulation by CSF_S. The extraction of the CSF samples also presented in Chapter 3 was developed in order to eliminate a number of known vasoactive substances so that this variation could be kept to a minimum. That the stimulation of O_2 consumption by CSF_S correlates well to the stimulation of tension generation again indicates the suitability of the model to the investigations presented in this thesis. Figure 3.4 shows that there is a clear correlation between the stimulation of oxygen consumption and tension generation when stimulated with CSF_S. The rate of O_2 consumption increases upon addition of CSF_S that elicits little or no tension development, indicating the sensitivity of O_2 consumption as an indicator of the presence of a vasospastic substance in the CSF. This *in vitro* model allows elimination of a large part of the error due to variation between patients/ animals seen in animal models and clinical studies. Overall, the model proved to be a reliable and reproducible source of data from which I could be confident in drawing conclusions.

7.1.3 Metabolic studies

The lack of increase in lactate production shown in 4.3.3 has several implications. Firstly, it suggests that the CSF_S stimulation of metabolism is only of the oxidative metabolism. It also shows that neither the CSF_S induced stimulation, nor the okadaic acid induced stimulation of oxidative metabolism is the result of mitochondrial uncoupling, which would result in an increased lactate production because of decreased mitochondrial ATP production.

The protective effects of magnesium on both the stimulation of tension generation and O_2 consumption may simply be due to the calcium antagonistic activity of magnesium. Calcium antagonism could also account for the lowered regeneration of tension after a stretch (5.3.2.3) and the potentiation of hypoxia induced relaxation seen in magnesium loaded tissue (Figure 5.6). The reversibility of contractile stimulation following acute magnesium administration (Figure 5.5), however, may be a more complex mechanism.

There appear to be three possibilities that may explain this phenomenon. If the failure of the vessels to relax is due to some conformational change in the contractile proteins, (perhaps the regulatory light chains becoming unavailable to myosin light chain phosphatase), magnesium may allow the normal MLC_{20} conformation to be adopted, thus allowing normal dephosphorylation and relaxation.

Calcium antagonism by magnesium may also result in a threshold level of myosin light chain kinase activity being reached, whereby the net result of the cross bridge cycling is shifted from maintenance of tension to relaxation when calcium antagonism by magnesium inhibits MLCK, thus preventing attachment. Another alternative is that magnesium activates the MLCP[172] such that the MLC_{20} become dephosphorylated at a faster rate. This suggests the involvement of a magnesium-activated protein phosphatase.

The magnesium dependent PP2C (see 1.4.4 & 5.1.2) may play a role in this reversal of *in vitro* vasospasm. As introduced in 5.1.2, the basal concentration of intracellular free Mg^{2+} in smooth muscle is not considered high enough to allow activation of PP2C. When this is raised to around 1mM, however, PP2C has been shown (*in vitro*) to dephosphorylate phosphorylated myosin light chains[46]. Interestingly, PP2C has also been shown to be essentially okadaic acid insensitive[75]. This leads to a question; in the absence of PP2A activity, the native phosphatase that is responsible for dephosphorylation of myosin light chains in smooth muscle, could PP2C compensate in the presence of high intracellular free Mg^{2+} concentrations? If, as postulated in 6.4, there is a component of the CSF_S that inhibits PP2A in a similar fashion to okadaic acid, then PP2C may also be insensitive to CSF_S. In the presence of physiological intracellular free Mg^{2+} concentrations and the CSF_S derived phosphatase inhibitor, neither PP2A nor PP2C are able to dephosphorylate the myosin light chains and allow relaxation. Raising the Mg^{2+} concentration may then activate the CSF_S insensitive PP2C, resulting in myosin light chain dephosphorylation and relaxation.

Whichever way the magnesium acts, the relaxation of CSF_S induced tension upon acute addition of 12 mM (10 × physiological) magnesium seems to suggest that there must

be a stimulus to contract in the CSF, even if the putative ætiology of vasospasm is inhibition of phosphatase activity. If this were not true, the addition of magnesium prior to that of CSF_S would prevent the stimulation both with respect to tension generation and O_2 consumption, but the stimulation is of the same magnitude, although the maximum is lower (Figure 5.2). As magnesium has been used as a therapy for preeclampsia for some years[110], magnesium as a therapy for patients with cerebral vasospasm after subarachnoid haemorrhage is a likely candidate, if the appropriate clinical protocol can be determined.

7.1.4 Phosphatase inhibition

The stimulation of O_2 consumption by okadaic acid which, at the concentrations used in this thesis is specific to PP2A, is most likely due to the inhibition of myosin light chain phosphatase, as discussed in 6.4. The same concentration of okadaic acid did not, however, stimulate tension development (data not shown). This pattern of results bears a striking resemblance to the data obtained using CSF_S, where the 1 in 30 dilution produced up to 5 fold stimulation of O_2 consumption, but tension generation was only stimulated by using concentrated, reconstituted CSF at a concentration approximately equal to undiluted CSF (4.3.2). Could there be phosphatase inhibitory action in the CSF? The phosphatase assay designed for that very purpose (2.2.3) showed that there is and that CSF_S at a 1 in 30 dilution, elicited an inhibition of myosin light chain phosphatase similar to that of 1 nM okadaic acid (Figure 6.5). Thus it is indeed quite possible that CSF_S contains some phosphatase inhibitory activity. Moreover, the possibility that an alteration in phosphatase activity may play a role in the pathogenesis of SAH induced cerebral vasospasm is also likely.

What would inhibiting myosin light chain phosphatase do to the contractile function of the smooth muscle? Dephosphorylation of MLC_{20} is a requirement for the majority of the population of cross bridges to change from the tension generating, ATP utilising, cycling state to the tension maintenance, attached, dephosphorylated cross bridge

(latch) state of vascular smooth muscle. From this state, cross bridges are more likely to detach and the muscle is able to relax. This prediction is consistent with the data presented in Table 6.1 where the rate of relaxation was significantly slowed in the presence of CSF_S and okadaic acid. Whilst the myosin is phosphorylated, active tension is generated and only dephosphorylation can lead to formation of "latch" bridges and relaxation. Therefore, phosphatase inhibitors that act on the phosphatase responsible for dephosphorylating MLC_{20} either from attached myosin and actin or detached phosphorylated myosin would render the muscle unable to relax. They do not, however, appear to elicit contraction in themselves. That okadaic acid affects the ability of the porcine carotid artery to relax is shown in Table 6.1. Both the initial, fast phase and the second, slower phase of relaxation are slowed by okadaic acid, perhaps indicating that the myosin light chain phosphatase is type 2A. Again, CSF_S mimics the results obtained using okadaic acid, as both phases of relaxation are slowed in response to a 1 in 30 dilution in a very similar fashion to the action of 1 nM okadaic acid (Table 6.1).

It is possible that any phosphatase inhibition is not acting directly on the myosin light chain phosphatase, but rather "above" MLCP in the signalling cascade. A likely candidate is the recently discovered inhibitory subunit of smooth muscle PP1. It is phosphorylated and inhibited by PKC, although which isoenzyme is involved is not yet known. The dephosphorylation of this subunit and therefore reactivation of MLCP, is believed to be by a PP2A, which may explain the similarity between okadaic acid (PP2A inhibitor) and CSF_S responses.

7.1.5 Stimulation of contraction by CSF_S

What, then, is causing the muscle to contract? In absence of a contractile signal, what pathology could arise from the inability of the tissue to relax? It seems that the stimulatory action of CSF_S is therefore twofold: a contraction is stimulated which would normally be dealt with by intrinsic control mechanisms (i.e. relaxation upon removal of the

stimulus) and a second, phosphatase inhibition activity prevents the tissue from relaxing appropriately. Reports that protein kinase C is implicated in the ætiology of vasospasm, are discussed in Chapter 4 and discussed below. PKC activity may therefore cause the stimulation of contraction from which the tissue is unable to relax *in vivo*. Though this thesis did not study the mechanisms of PKC stimulated constriction a proposal is made below outlining how these data may be able to explain the generation and maintenance of tension seen in this disease.

Could this pathology be explained by sustained activation of protein kinase C in the cerebral vessels? If we take sustained and acute PKC induced contraction to be separate events and possibly mutually exclusive events, then I believe so. A number of papers implicate PKC in the ætiology and sustained activation of PKC could certainly explain the phenomena that we have seen. The absence of contraction with low doses of CSF_S and PP2A specific doses of a pure phosphatase inhibitor show that phosphatase inhibition cannot be the sole cause of vasospasm (Figure 4.6). The small and transient, but significant, stimulation of tension generation by CSF_N (Figure 4.6) and the protection afforded by agonists of an alternative protein kinase C isoform support this hypothesis. The stimulation of O_2 consumption by artificial subarachnoid CSF (described in 4.4.4) mixtures containing platelets, but not those mixtures not containing platelets also corroborates this. As well as the observations mentioned above, staurosporine accelerated O_2 consumption at doses that inhibit the PKC isoform responsible for transient stimulation, mediated by α_1-adrenergic receptors specifically (1 nM). Protein kinase C is known to phosphorylate MLC_{20} at a separate site to MLCK[165]. This phosphorylation reduces the myosin ATPase activity two fold *in vitro*. The relief of this inhibitory effect by PKC inhibition may explain the acceleration in O_2 consumption. Acute activation of PKC results in raised intracellular calcium concentrations, as it results from α_1-adrenergic receptor agonism that leads to IP_3 production and opening of intracellular calcium stores (IP_3 gated calcium channels in the sarcoplasmic reticulum). There is some evidence to suggest that acute and sustained activation of protein kinase C, mediated by different PKC isoforms, are incompatible

events[52]. This concept was introduced in 4.1.1.3. This may explain the attenuation of CSF_S-induced stimulation of O_2 consumption by dobutamine and noradrenaline if the CSF induced tension is by way of the sustained, calcium-independent contraction. The activation of the calcium-independent (DAG dependent) pathway in vascular smooth muscle has been reported to be stimulated by products of blood clotting. Platelets release substances known as hydroxyeicosotetranoic acids (HETE) during the clotting process. One of these, 12-HETE, is produced from the subarachnoid clot 2-5 days after haemorrhage[201]. 12-HETE, in turn, leads to a slow accumulation of DAG, thought to be due to the inhibition of DAG kinase, the first enzyme in the catabolism of DAG, by 12-HETE. Significantly, this accumulation of DAG is over the same time course as the development of vasospasm in man (4-7 days)[294]. This increased concentration of DAG results in the sustained activation of a PKC isoenzyme thought to be PKCε. The data presented in this thesis seems to support the hypothesis of PKC induced tension with an inability to relax as the mechanism for subarachnoid haemorrhage induced cerebral vasospasm.

So, if this is the cause of the contraction, could it also be the source of the inhibition of phosphatase? Recently, an *in vivo* inhibitor of PP2A has been isolated and characterised[68]. This inhibitor peptide is phosphorylated and activated by PKC. This may well be the link between pathological contraction and the inability to relax. Alternatively, a separate molecule may cause the phosphatase inhibition and this should be the subject of continued research in the immediate future.

7.1.6 Agonist and inhibitor studies

The inhibitor and agonist studies presented in Chapter 4 (Table 4.2) tell us a great deal about the nature of the stimulation of O_2 consumption by CSF_S. There is a clear and significant level of protection afforded by pre-treatment with α_1- adrenergic receptor agonists. Some of the agonist and inhibitor data may be difficult to interpret because of the

stimulation of O_2 consumption of the inhibitor alone. Perhaps the most surprising result in this chapter is that of the ineffectiveness of endothelin inhibitors in reducing the activity of the CSF significantly. Endothelin was a prime candidate for the cause of delayed cerebral vasospasm, but the lack of protection afforded by the inhibitor and the fact that activity is maintained calls this into question.

The force measurement data allows us to compare our model to those data which already existed from previous authors[32]. A correlation is seen between O_2 consumption and force measurements with the oxygen consumption being much more sensitive in responding to CSF_S (Figure 4.7). There appears to be a threshold level of stimulation by a CSF_S sample of O_2 consumption, below which, tension is not generated. That both CSF_S and CSF_N elicit an acute contraction suggests the involvement of two processes: an acute activation of tension and a more sustained maintenance and slow increase in tension, or inhibition of relaxation, not seen with CSF_N. Again, these data are consistent with the proposal of a stimulation of contraction coupled with a pathological maintenance of tension.

The shift in the force-function relationship curve (Figure 4.6) also yields some important information. The shape of the CSF_S induced O_2 consumption/ force generation relationship is similar to the $[Ca^{2+}]$ induced relationship, although shifted to the right, indicating that contraction elicited by CSF_S requires greater ATP consumption (as assessed using oxygen consumption measurements) than tension elicited by calcium. There may be some loss of metabolic efficiency with the CSF_S stimulated tension case, but this right shift could equally suggest that there is an intermediate step between CSF_S stimulation and calcium activated tension generation. That is, the CSF_S may result in impaired calcium sensitivity or that a threshold calcium concentration may be necessary to activate contraction, such as activation of protein kinase C. Both of which would shift the curve to the right without changing the rate (Table 4.3). There is an increase in the concentration of the agonist before an increase in tension is seen with both cases.

7.1.7 Characterising the vasospastic molecule in CSF_S

What was elucidated regarding the structure of the vasospastic molecule(s) may prove useful in future studies. For instance, it was found to be a hydrophobic molecule, preferring the organic to the aqueous phase and perchloric acid extraction does not significantly decrease its activity, indicating that it is not a protein (Chapter 3). The molecule becomes more labile to light and freeze/ thaw cycles the more impurities are removed, which may indicate that it is stabilised by a protein or some such "binding molecule" *in vivo* and in its native solution. Possibly the most interesting observation with respect to the putative structure of the molecule is the dose dependent reduction in its activity when exposed to cholesterol esterase (Figure 4.8). This may mean that there is a planar, ring structure component attached, via an ester linkage, to a long, hydrophobic side group, which is essential for its activity.

7.2 Future research

In the immediate future, the development and refinement of the phosphatase assay will be pursued. It may be able to be developed into a rapid-throughput assay that could be made commercially available for diagnostic purposes and as a molecular-level model of vasospasm enabling development of intervention studies.

An obvious choice for the future of this research is to find the definitive cause of this pathology in terms of the physical and chemical characterisation of the causative molecule or molecules. PKC isoenzyme studies could be used to determine which isoenzymes are activated under certain conditions of stimulation. Moreover, the phosphorylation targets of these PKC isoenzymes and their control mechanisms need to be determined.

The changes in energy metabolism, may allow *in vivo* examination of vasospasm using ^{31}P magnetic resonance spectroscopy. This would be extremely useful in assessing the effectiveness of intervention therapy. Any changes in intracellular pH could be

assessed, as well as perhaps correlating severity of vasospasm with intracellular magnesium levels.

7.2.1 Clinical applications stemming from this research

The use of α_1-adrenergic receptor agonists or magnesium as therapies, based on the data presented in this thesis could also be a source of future clinical studies, as both these therapies have been applied to humans for many years. Development of new drugs may include specific MLCP activation substances, PKC isoenzyme specific inhibitors, 12-HETE antagonists or DAG kinase activators. All of these are, until the correct ætiology of vasospasm has been fully characterised and confirmed, speculations, but certainly provide fuel for the imagination of vascular smooth muscle and stroke researchers.

7.3 Conclusions

Several conclusions can be drawn from the work presented in this thesis. The main points that I feel are the most important in this thesis are:

- I have, from other researchers initial observations, developed and characterised a robust, sensitive and reproducible *in vitro* model of cerebral vasospasm after subarachnoid haemorrhage. This model can be used to investigate the ætiology of this pathology and compares very favourably to the *in vitro* and *in vivo* models currently available.

- Cerebrospinal fluid from patients with vasospasm stimulates O_2 consumption and tension generation in several vascular beds from different animals. The stimulation is not reversible by any known vasorelaxants except magnesium. The nature of this stimulation almost certainly contains an aspect of myosin light chain phosphatase inhibition.

- The inhibition of phosphatase activity is accompanied by a stimulation of contraction, which also occurs in response to CSF_N, where it may be overcome in the absence of

phosphatase inhibition. This stimulation of contraction may be due to a sustained activation of a particular PKC isoenzyme.

- The stimulation of O_2 consumption and tension is attenuated by α_1-adrenergic receptor agonists and magnesium and reversed by the acute application of magnesium followed by rinsing.

- The pathology of cerebral vasospasm is not a pathological constriction, but rather a pathological failure of the contracted tissue to relax in response to physiological signals.

8.Bibliography

1. Abedi, H. and I. Zachary (1998) Cytochalasin D stimulation of tyrosine phosphorylation and phosphotyrosine associated kinase activity in vascular smooth muscle cells. *Biochem. Biophys. Res. Commun.* **245:3.** 646-650

2. Adam, L. P., M. T. Franklin, G. J. Raff and D. R. Hathaway (1995) Activation of Mitogen Activated Protein Kinase in Porcine Carotid Arteries. *Circ. Res.* **76:2.** 183-90

3. Adam, L. P., J. R. Haeberle and D. R. Hathaway (1989) Phosphorylation of caldesmon in arterial smooth muscle. *J. Biol. Chem.* **264:13.** 7698-703

4. Adam, L. P., J. R. Haeberle and D. R. Hathaway (1995) Calponin is not phosphorylated during contractions of porcine carotid arteries. *Am. J. Physiol.* **268:Cell Physiol. 37.** C903-C909

5. Adam, L. P., L. Milio, B. Brengle and D. R. Hathaway (1990) Myosin light chain and caldesmon phosphorylation in arterial muscle stimulated with endothelin-1. *J. Mol. Cell. Cardiol.* **22:9.** 1017-23

6. Aksoy, M. O., R. A. Murphy and K. D. Kamm (1982) Role of calcium and myosin light chain phosphorylation in regulation of smooth muscle. *Am. J. Physiol.* **242:Cell Physiol. 11.** C109-C116

7. Alessi, D., L. K. MacDougall, M. M. Sola, M. Ikebe and P. Cohen (1992) The control of protein phosphatase-1 by targetting subunits. *Eur. J. Biochem.* **210:**1023-1035

8. Allen, G. S., H. S. Ahn, T. J. Preziosi and e. al (1983) Cerebral arterial spasm, a controlled trial of nimodipine in patients with subarachnoid haemorrhage. *N. Engl. J. Med.* **17:**619-624

9. Alvarez-Leefmans, F. Giraldez and S. M. Gamino (1986) Intracellular free magnesium in excitable cells: Its measurement and its biological significance. *Can. J. Physiol. Pharmacol.* **65:**915-925

10. Arnqvist, H. J. and L. Lundholm (1976) Influence of oxygen tension on the metabolism of vascular smooth muscle. *Atherosclerosis* **25:**245-253

11. Asano, T., K. Takakura, K. Sano, H. Kikuchi, H. Nagai, I. Saito, A. Tamura, C. Ochiai and T. Sasaki (1996) Effects of a hydroxyl radical scavenger on delayed ischaemic neurological deficits following aneurysmal subarachnoid hemorrhage: results of a multicenter, placebo controlled double blind trial. *J. Neurosurg.* **84:**792-803

12. Ataka, K., D. Chen, T. McCully, S. Levitsky and H. Feinberg (1993) Myocardial cytosolic calcium accumulation during ischaemia /reperfusion: The effects of aging and cardioplegia. *J. Mol. Cell. Cardiol.* **25:12.** 1387-1390

13. Atomi, Y., S. Yamada, R. Strohman and Y. Nonomura (1991) α- B crystallin in skeletal muscle: purification and localization. *J. Bioch. Tokyo.* **110:5.** 812-22

14. Auer, L. M. (1984) Acute operation and preventative nimodipine improve outcome in patients with ruptured cerebral aneurysms. *Neurosurgery.* **15:**57-66

15. Auer, L. M., L. Brandt, U. Ebeling, J. Gilsbach, U. Groeger, A. Harders, B. Ljunggren, F. Oppel, H. J. Reulen and H. Saevland (1986) Nimodipine and early aneurysm operation in good condition SAH patients. *Acta Neurochir. Wien.* **82:**7-13

16. Bakhramov, A., S. A. Hartley, K. J. Salter and R. Z. Kozlowski (1996) Contractile agonists preferentially activate Cl- over K+ currents in arterial myocytes. *BBRC* **227:**168-175

17. Barany, K. and M. Barany (1993) *FASEB J.* **7:**A1078

18. Barany, K., S. Csabina and M. Barany (1985) *Adv. Protein Phosphatases* **2:**37-58

19. Barany, K., R. F. Ledvora, V. Mougios and M. Barany (1985) Stretch induced myosin light chain phosphorylation and stretch-release induced tension development in arterial smooth muscle. *J. Biol. Chem.* **260:11.** 7126-7130

20. Barany, M. and K. Barany (1993) Calponin phosphorylation does not accompany contraction of various smooth muscles. *BBA* **1179:**229-233

21.

22. Barany, M., E. Polyak and K. Barany (1992) Protein phosphorylation during the contraction-relaxation-contraction cycle of arterial smooth muscle. *Arch. Biochem. Biophys.* **294:2.** 571-8

23. Barford, D. (1996) Molecular mechanisms of the protein serine/threonine phosphatases. *Trends in Bioch. Sci.* **21:11.** 407-412

24. Barron, J. T., S. J. Kopp, J. Tow and J. E. Parrillo (1994) Fatty acid, tricarboxylic acid cycle metabolites, and energy metabolism in vascular smooth muscle. *Am. J. Physiol.* **267:Heart Circ. Physiol.** H764-H769

25. Barron, J. T., S. J. Kopp, J. Tow and J. E. Parrillo (1996) Substrate dependent alteration in O2 consumption and energy metabolism in vascular smooth muscle. *Am. J. Physiol.* **270:Heart Circ. Physiol. 39.** H1869-H1877

26. Barron, J. T., S. J. Kopp, J. P. Tow and J. E. Parrilo (1991) Differential effects of fatty acids on glycolysis and glycogen metabolism in vascular smooth muscle. *Biochim. Biophys. Acta* **1093:**125-134

27. Battista, A. F., E. S. Flamm, M. Goldstein and L. S. Freedman (1976) Effect of dopamine-beta-hydroxylase inhibition on cerebral vasospasm in the cat. *J. Neurosurg.* **44:**168-172

28. Bitar, K. N., M. S. Kaminski, N. Hailat, K. B. Cease and J. R. Strahler (1991) Hsp27 is a mediator of sustained smooth muscle contraction in response to bombesin. *Biochem. Biophys. Res. Commun.* **181:3.** 1192-200

29. Boehm, E. A., J. F. Clark and G. K. Radda (1995) Metabolite utilization and compartmentation in porcine carotid artery: a study using beta guanidinopropionic acid. *Am. J. Physiol.* **268:Cell Physiol. 37.** C628-C635

30. Boker, D. K., L. Solymosi and H. Wassmann (1985) Immediate postangiographic intraarterial treatment of cerebral vasospasm after subarachnoid haemorrhage with nimodipine. Report on 3 cases. *Neurochirurgia* **28:1.** 118-120

31. Born, G. V. R. (1956) The relation between the tension and the high-energy phosphate content of smooth muscle. *J. Physiol.* **131:**704-711

32. Boullin, D. J. and J. Mohan (1977) Effects of (+) - and (-) - propanolol on the responses of the human isolated basilar artery to cerebrospinal fluid obtained from patients with subarachnoid haemorrhage and cerebral artery spasm. *Br. J. Clin. Pharmacol.* **4:**27-31

33. Boullin, D. J., J. Mohan and D. G. Grahame-Smith (1976) Evidence for the presence of a vasoactive substance (possibly involved in the aetiology of cerebral arterial spasm) in cerebrospinal fluid from patients with subarachnoid haemorrhage. *J. Neurol. Neurosurg. Psych.* **39:**756-766

34. Brandt, L., B. Ljunggren, H. Saveland, K.-E. Anderson and E. Vinge (1986) Cerebral vasospasm and calcium channel blockade. Nimodipine treatment in patients with aneurysmal subarachnoid haemorrhage. *Acta Pharmacol. Toxicol.* **58:2.** 151-155

35. Buckell, M. (1964) Demonstration of Substances Capable of Contracting Smooth Muscle in Haematoma Fluid from Certain Cases of Ruptured Cerebral Aneurysm. *J. Neurol. Neurosurg. Psych.* **27:**198-199

36. Burchfield, D. M. and J. A. Rall (1986) Temperature dependence of the crossbridge cycle during unloaded shortening and maximum isometric tetanus in frog skeletal muscle. *J. Muscle Res. Cell. Motil.* **7:4.** 320-326

37. Butler, T. M., M. J. Siegman and S. U. Mooers (1986) *Am. J. Physiol.* **267:Cell Physiol.** C1160-C1166

38. Butler, W. E., J. W. Peterson, N. T. Zervas and K. G. Morgan (1996) Intracellular calcium, myosin light chain phosphorylation and contractile force in experimental cerebral vasospasm. *Neurosurgery* **38:4.** 781-788

39. Carrier, O., R. K. Hester, H. A. Jurevics and T. E. Tenner (1976) Influence of magnesium on calcium and potassium related responses in vascular smooth muscle. *Blood Vessels* **13:**321-337

40. Chabrier, P. E., M. Auguet, P. Roubert, M. O. Lonchampt, V. Gillard, J. M. Guillon, S. Delaflotte and P. Braquet (1989) Vascular mechanism of action of endothelin 1: effect of calcium antagonists. *J. Cardiovasc. Pharmacol.* **13:5.** s32-5

41. Chace, K. V. and R. Odessey (1981) The utilization by rabbit aorta of carbohydrates, fatty acids, ketone bodies and amino acids as substrates for energy production. *Circ. Res.* **48:6.** 850-858

42. Clark, J. F. (1994) The Creatine Kinase System in Smooth Muscle. *Mol. Cell. Biochem.* 221-232

43. Clark, J. F. and P. F. Dillon (1995) Phosphocreatine and creatine kinase in energetic metabolism of the porcine carotid artery. *J. Vasc. Res.* **32.** 24-30

44. Coburn, R. F. and W. S. Fillers (1989) Oxidative metabolism contraction coupling in smooth muscle. *Muscle Energetics* 391-404

45. Cohen, P. (1985) The role of protein phosphorylation in the hormonal control of enzyme activity. *Eur. J. Biochem.* **151:**439-448

46. Cohen, P. (1989) The structure and regulation of protein phosphatases *Ann. Rev. Biochem.* **58:**453-508

47. Cohen, P., S. Klumpp and D. L. Schelling (1989) An improved procedure for identifying and quantitating protein phosphatases in mammalian tissues. *FEBS Lett.* **250:2.** 596-600

48. Colburn, J. C., C. H. Michnoff, L. C. Hsu, C. A. Slaughter, K. E. Kamm and J. T. Stull (1988) Sites phosphorylated in myosin light chain in contracting smooth muscle. *J. Biol. Chem.* **263:35.** 19166-19173

49. Cook, D. A. (1995) Mechanisms of cerebral vasospasm in subarachnoid haemorrhage. *Pharmac. Ther.* **66:**259-284

50. Cornwell, T. L., E. Arnold, N. J. Boerth and T. M. Lincoln (1994) *Am. J. Physiol.* **406:**C1405-1413

51. Cramer, H., W. Muller-Esterl and C. Schroeder (1998) Sub-type Specific Endothelin-A and Endothelin-B Receptor Desensitization Correlates With Differential Receptor Phosphorylation. *J. Cardiovasc. Pharm.* **31:1.** S203-6

52. Danthuluri, N. R. and N. C. Deth (1984) Phorbol ester induced contraction of arterial smooth muscle and inhibition of alpha adrenergic response. *Biochem. Biophys. Res. Commun.* **125:3.** 1103-1109

53.

54. Demolle, D., M. Lecomte and J. M. Boeynaems (1988) Pattern of protein phosphorylation in aortic endothelial cells. Modulation by adenine nucleotides and bradykinin. *J. Biol. Chem.* **263:34.** 18459-65

55.

56. Dillon, P. F., M. O. Aksoy, S. P. Driska and R. A. Murphy (1981) Myosin phosphorylation and the cross bridge cycle in arterial smooth muscle. *Science (Wash. D.C.)* **211:**495-497

57. Dillon, P. F. and R. A. Murphy (1982) Tonic force maintenance with reduced shortening velocity in arterial smooth muscle. *Am. J. Physiol.* **242:Cell Physiol. 11.** C102-C108

58. Dinischiotu, A., M. Beullens, W. Stalmans and M. Bollen (1997) Identification of sds22 as an inhibitory subunit of protein phosphatase-1 in rat liver nuclei. *FEBS Lett.* **402:**141-144

59. DiSalvo, J., D. Gifford and A. Kokkinakis (1985) *Adv. Enzyme Reg.* **23:**103-122

60. Driska, S. (1987) High myosin light chain phosphatase activity in arterial smooth muscle: can it explain the latch phenomenon? *Prog. Clin. Biol. Res.* **Regulation and contraction of smooth muscle:**387-398

61. Driska, S. P., M. O. Aksoy and R. A. Murphy (1981) Myosin light chain phosphorylation associated with contraction in arterial smooth muscle. *Am. J. Physiol.* **240:Cell Physiol. 9.** C222-C233

62. Duckles, S. P., R. D. Bevan and J. A. Bevan (1976) An in vitro study of prolonged vasospasm of rabbit cerebral artery. *Stroke* **7:2.** 174-8

63. Ekmehag, B. L. and P. Hellstrand (1989) Shortening velocity, myosin light chain phosphorylation and Ca2+ dependance of force during metabolic inhibition in smooth muscle of rat portal vein. *Acta Physiol. Scand.* **136:**367-376

64. Endo, M. (1977) Calcium release from the sarcoplasmic reticulum. *Physiol.Rev.* **57:1.** 71-108

65. Endo, S. and J. Suzuki (1977) Experimental cerebral vasospasm after subarachnoid hemorrhage: development and degree of vasospasm. *Stroke* **8:6.** 702-707

66.

67. Erdodi, F., A. Rokolya, M. Barany and K. Barany (1988) Phosphorylation of the 20,000-Da myosin light chain isoforms of arterial smooth muscle by myosin light chain kinase and protein kinase C. *J. Biochem. Biophys.* **306:2.** 583-591

68. Eto, M., T. Ohmori, M. Suziki, K. Furuya and F. Morita (1995) A novel protein phosphatase-1 inhibitory protein potentiated by protein kinase C. isolation from porcine aorta media and characterisation. *J. Biochem.* **118:**1104-1107

69. Fadel, M. M., P. L. Foley, N. F. Kassell and K. S. Lee (1995) Histidine attenuated cerebral vasospasm in a rabbit model of subarachnoid haemorrhage. *Surg. Neurol.* **43:**52-58

70. Filenko, A. M., V. M. Danilova and A. Sobieszek (1997) Smooth muscle myosin light chain kinase, supramolecular organisation, modulation of activity, and related conformational changes. *Biophys.J.* **73:**1593-1606

71. Fisher, C. M., J. P. Kistler and J. M. Davis (1980) Relation of cerebral vasospasm to subarachnoid haemorrhage visualized by computer tomographic scanning. *Neurosurgery* **6:1.** 1-9

72. Ford, G. D. and S. P. Driska (1986) Influence of altering cellular magnesium content on vascular smooth muscle contractility. *Am. J. Physiol.* **251:Cell Physiol 20.** C687-C695

73. Fujii, T., A. Oomatsuzawa, N. Kuzumaki and Y. Kondo (1994) Calcium-dependent regulation of smooth muscle calponin by S100 . *J. Biochem. (Tokyo)* **116:**121-127

74. Fujimura, M., T. Sugawara, H. Seki, T. Oku, K. Niimura, Y. Otawara and H. Higuchi (1996) Perivascular coating with fibrin glue of cerebral arteries in patients with aneurysmal subarachnoid haemorrhage: incidence of chronic hydrocephalus. *Tohoku J. Exp. Med.* **179:4.** 267-272

75. Fukunaga, K., T. Kobayashi, S. Tamura and E. Miyamoto (1993) Dephosphorylation of autophosphorylated Ca2+/ calmodulin-dependent protein kinase 2 by protein phosphatase 2C. *J. Biol. Chem.* **268:1.** 133-137

76. Gailly, P., M. C. Gong, A. V. Somlyo and A. P. Somlyo (1997) Possible Role of Atypical Protein Kinase C Activated by Arachidonic Acid in Ca 2+ Sensitization of Rabbit Smooth Muscle. *J. Physiol.* **500:1.** 95-109

77. Gailly, P., X. Wu, T. A. J. Haystead, A. P. Somlyo, P. T. W. Cohen, P. Cohen and A. V. Somlyo (1996) Regions of the 110-kDa regulatory subunit M110 required for regulation of myosin light chain phosphatase activity in smooth muscle. *Eur. J. Biochem.* **239:**326-332

78. Gilsbach, J. M., H. J. Reulen, B. Ljunggren, L. Brandt, H. v. Holst, M. Mokry, C. v. Essen and M. A. Conzen (1990) Early aneurysm and preventive therapy with intravenously administered Nimodipine. A multicentre, double-blind, dose-comparison study. *Neurosurgery* **26:**458-464

79. Gong, M. C., P. Cohen, T. Kitazawa, M. Ikebe, M. Masuo, A. P. Somlyo and A. V. Somlyo (1992) Myosin light chain phosphatase activities and the effects of phosphatase inhibitors in tonic and phasic smooth muscle. *J. Biol. Chem.* **267:21.** 14662-14668

80. Griendling, K. K., S. E. Rittenhouse, T. A. Brock, L. S. Ekstein, L. M. Gimbrone and R. W. Alexander (1986) Sustained diacylglycerol formation from inositol phospholipids in angiotensin II stimulated smooth muscle cells. *J. Biol. Chem.* **261:**5901-5906

81. Grotenhuis, J. A. and W. Bettag (1986) Prevention of symptomatic vasospasm after subarachnoid haemorrhage by constant venous infusion of Nimodipine. *Neurol. Res.* **8:**243-249

82. Grotenhuis, J. A., W. Bettag and B. J. Fiebach (1984) Intracarotid slow bolus injection of nimodipine during angiography for treatment of cerebral vasospasm after subarachnoid haemorrhage. *J. Neurosurg.* **61:**231-240

83. Gupta, R. K., J. L. Benovic and Z. B. Rose (1978) The determination of the free magnesium level in the human red blood cell by 31P NMR. *J. Biol. Chem.* **253:17.** 6172-6176

84. Gupta, R. K., P. Gupta, W. D. Yushok and Z. B. Rose (1983) On the Noninvasive Measurement of Intracellular Free Magnesium by 31P NMR Spectroscopy. *Physiological Chemistry and Physics and Medical NMR* **15:**265-281

85. Haeberle, J. R., J. W. Hott and D. R. Hathaway (1985) Regulation of isometric force and isotonic shortening velocity by phosphorylation of the 20,000 dalton myosin light chain of rat uterine smooth muscle. *Pfluger's Arch.* **403:**215-219

86. Hai, C.-M. and R. A. Murphy (1988) Cross bridge phosphorylation and regulation of latch state in smooth muscle. *Am. J. Physiol.* **254:Cell Physiol. 23.** C99-106

87. Haller, H. and J. I. Smallwood (1990) Protein kinase C translocation in intact vascular smooth muscle strips. *Biochem. J.* **270:**375-381

88. Halvorson, H. R., A. M. Q. Vande Linde, J. A. Helpern and K. M. A. Welch (1992) Assessment of magnesium concentrations by 31P NMR *in vivo. NMR in Biomedicine.* **5:**53-58

89. Handa, Y., M. Kaneko, T. Matuda, H. Kobayashi and T. Kubota (1997) In vivo proton magnetic resonance spectroscopy for metabolic changes in brain during chronic cerebral vasospasm in primates. *Neurosurgery* **40:4.** 773-781

90. Harada, T., M. Seto, Y. Sasaki, S. London, Z. Luo and M. Mayberg (1995) The time course of myosin light chain phosphorylation in blood induced vasospasm. *Neurosurgery* **36:**1178-1183

91. Harders, A. G. and J. M. Gilsbach (1987) Time course of blood velocity changes related to vasospasm in the circle of Willis measured by transcranial Doppler ultrsound. *J. Neurosurg.* **66:**718-728

92.

93. Hartshorne, D. J. and T. Kawamura (1992) Regulation of contraction-relaxation in smooth muscle. *News Physiol. Sci.* **7:**59-64

94. Hasegawa, Y., K. Tanahashi and F. Morita (1990) Regulatory mechanism by the phosphorylation of 20kDa light chain of porcine aorta smooth muscle myosin. *J. Biochem. (Tokyo)* **108:**909-913

95. Healy, M. D., J. A. Ward and P. Wang (1984) Inhibition of calcium by magnesium in the contraction of rat aortic smooth muscle. *Magnesium* **3:**63-72

96. Heath, D. L. and R. Vink (1997) Magnesium sulphate improves neurologic outcome following severe closed head injury in rats. *Neuroscience Lett.* **228:**175-178

97. Hellstrand, P. (1979) Mechanical and metabolic properties related to contraction in smooth muscle. *Acta Physiologica Scand.* **464:supplementum.** 1-54

98. Hellstrand, P. and A. Arner (1980) Contraction of the rat portal vein in hypertonic and isotonic medium: mechanical properties and effects of magnesium. *Acta Physiol. Scand.* **110:1.** 59-67

99. Hellstrand, P., C. Jorup and M.-L. Lydrup (1984) O2 consumption, aerobic glycolysis and tissue phosphagen content during activation of the Na+/K+ pump in rat portal vein. *Eur. J. Physiol.* **401:**119-124

100. Helpern, J. A., A. M. Q. Vande Linde, K. M. A. Welch, S. R. Levine, L. R. Schultz, R. J. Ordidge, H. R. Halvorson and J. W. Hugg (1993) Acute elevation and recovery of intracellular [Mg2+] following human focal cerebral ischaemia. *Neurology* **43:**1577-1581

101. Hemric, M. E. and J. M. Chalovich (1988) Effect of caldesmon on the ATPase activity and binding of smooth and skeletal myosin subfragments to actin. *J. Biol. Chem.* **263:4.** 1878-1885

102. Herlihy, J. T. and R. Murphy (1973) Length-tension relationship of smooth muscle of the hog carotid artery. *Circ. Res.* **33:**275-283

103. Hickey, E., S. E. Brandon, R. Potter, G. Stein and L. E. Weber (1986) Sequence and organization of genes encoding the human 27kDa heat shock protein. *Nucleic Acid Res.* **14:10.** 4127-4145

104. Hino, A., B. K. Weir, R. L. Macdonald, R. A. Thisted, C. J. Kim and L. M. Johns (1995) Prospective, randomized, double-blind trial of BQ-123 and Bosentan for prevention of vasospasm following subarachnoid hemorrhage in monkeys. *J. Neurosurg.* **83:3.** 503-509

105. Hirashima, Y., S. Endo, R. Kato and A. Takaku (1996) Prevention of cerebrovasospasm following subarachnoid hemorrhage in rabbits by the platelet activating factor antagonist, E5880. *J. Neurosurg.* **84:**826-830

106. Honda, M. and H. Terao (1997) Experimental vasospasm produced without blood cell components-- hypothesis for the development of cerebral vasospasm. *Neurol. Med. Chir.(Tokyo)* **37:5.** 373-378

107. Hongo, K. and S. Kobayashi (1993) Calcium antagonists for the treatment of vasospasm following subarachnoid haemorrhage. *Neurolog. Res.* **15:**218-224

108. Hopf, C. and W. Hoch (1998) Tyrosine Phosphorylation of the Muscle-Specific Kinase is Exclusively Induced by Acetylcholine Receptor-Aggregating Agrin Fragments. *Eur. J. Biochem.* **253:2.** 382-389

109. Horiuchi, K. Y., M. Samuel and S. Chacko (1991) The mechanism for the inhibition of acto-heavy meromyosin ATPase by the actin-calmodulin binding domain of caldesmon. *Biochemistry* **30:3.** 712- 717

110. Horn, E. (1906) To Tilfaelde af Eclampsia Gravidarum Behandlet med Suflas Magnesicus Ijiceret: Zygmanens Subarachnoidalium. *Medicinsk Rev.* **32:**264-272

111. Horowitz, A., C. B. Menice, R. Laporte and K. G. Morgan (1996) Mechanisms of smooth muscle contraction. *Physiological Reviews* **76:4.** 967-1003

112. Hug, H. and T. F. Sarre (1993) Protein kinase C isoenzymes: Divergence in signal transduction? *Biochem. J.* **291:**329-343

113. Hughes, J. T. and P. M. Schianchi (1978) Cerebral artery spasm. *J. Neurosurg.* **48:**515-525

114. Hunt, T. M., G. H. Du Boulay, W. P. Blaso, D. M. C. Forster and D. J. Boullin (1979) Relationship between presence of vasoconstrictor activity in cerebrospinal fluid and time after subarachnoid haemorrhage from rupture of cerebral arterial aneurysms. *J. Neurol. Neurosurg. Psych.* **42:**625-634

115. Ichikawa, K., M. Ito and D. J. Hartshorne (1996) Phosphorylation of the large subunit of myosin phosphatase and inhibition of phosphatase activity. *J. Biol. Chem.* **271:9.** 4733-4740

116. Ignarro, L. J., R. E. Byrns and K. S. Wood (1987) Endothelium dependent modulation of cGMP levels and intrinsic smooth muscle tone in isolated bovine intrapulmonary artery and vein. *Circ. Res.* **60:1.** 82-92

117. Iijima, K., L. Lin, A. Nasjletti and M. S. Goligorsky (1991) Intracellular ramification of endothelin signal. *Am. J. Physiol.* **260:Cell Physiol. 29.** C982-992

118. Ikebe, M., J. Barsotti, S. Hinkins and D. J. Hartshorne (1984) Effects of magnesium chloride on smooth muscle actomyosin adenosine 5' triphosphatase activity. *Biochemistry* **23:**5062-5068

119. Ikebe, M., D. J. Hartshorne and M. Elzinga (1986) Identification, phosphorylation, and dephosphorylation of a second site for myosin light chain kinase on the 20, 000 Dalton light chain of smooth muscle myosin. *J. Biol. Chem.* **261:1.** 36-39

120. Ingebritsen, T. S. and P. Cohen (1983) The protein phoshatases involved in cellular regulation: 1. Classification and substrate specificities. *Eur. J. Biochem.* **132:**255-261

121. Ishida, Y. and H. Honda (1992) Underlying mechanisms for hypoxia induced relaxation of the guinea pig isolated aorta. *Jpn. J. Pharmacol.* **58:suppl II.** 307p

122.

123. Ishida, Y. and R. J. Paul (1990) Effects of Hypoxia on High Energy Phosphagen Content, Energy Metabolism and Isometric Force in Guinea Pig Taenia Caeci. *J. Physiol.* **424:**41-56

124. Ishida, Y., I. Riesinger, T. Wallimann and R. J. Paul (1994) I-3 compartmentation of ATP synthesis and utilisation in smooth muscle: roles of aerobic glycolysis and creatine kinase. *Mol. Cell. Biochem.* **133/134:**39-50

125. Ishida, Y. and K. Takagi (1983) Spontaneous contractions and carbohydrate metabolism of the isolated guinea pig Taenia coli. *Jpn. J. Pharmacol.* **33:**171p

126. Ishida, Y. and K. Takagi-Ohta (1996) Lactate Production of Mammalian Intestinal and Vascular Smooth Muscles Under Aerobic and Hypoxic Conditions. *J. Smooth Muscle Research* **32:2.** 61-67

127. Ishihara, H., B. L. Martin, D. L. Brautigan, H. Karaki, H. Ozaki, Y. Kato, N. Fusetani, S. Watabe, K. Hashimoto, D. Uemara and D. J. Hartshorne (1989) *BBRC* **159:**871-877

128. Ishikawa, T., T. Chijiwa, M. Hagiwara, S. Mamiya, M. Saitoh and H. Hidaka (1988) ML-9 inhibits the vascular contraction via the inhibition of myosin light chain phosphorylation. *Mol. Pharmacol.* **33:6.** 598-603

129. Ito, M. and D. J. Hartshorne (1990) Phosphorylation of myosin as a regulatory mechanism in smooth muscle. *Front. Smooth Musc. Res.* **327:**57-72

130. Jaworowski, A. and A. Arner (1998) Temperature sensitivity of force and shortening velocity in maximally activated skinned smooth Muscle. *J. Muscle Res. Cell Motil.* **19:3.** 247-255

131. Johnson, R. C. and S. N. Shah (1979) Presence in human cerebrospinal fluid of cholesterol esterifying enzyme utilizing free fatty acids. *Brain Res.* **162:2.** 353-357

132. Kalsner, S. (1995) Coronary artery spasm. Multiple causes and multiple roles in heart disease. *Biochem. Pharmacol.* **49:7.** 859-71

133. Kamm, K. E. and J. T. Stull (1989) Second messenger effects on the myosin phosphorylation system in smooth muscle *Muscle Energetics* 265-278

134. Kaoutzanis, M., M. Yokota, R. Sibilia and J. W. Peterson (1993) Neurologic evaluation in a canine model of single and double subarachnoid hemorrhage. *J. Neurosci. Methods* **50:3.** 301-307

135. Karczewski, P., S. Bartel and E.-G. Krause (1993) Protein phosphorylation in the regulation of cardiac contractility and vascular smooth muscle tone. *Curr. Opin. in Nephrol. Hypertension* **2**:33-40

136. Kemp, B. E. and R. B. Pearson (1985) Spatial requirements for location of basic residues in peptide substrates for smooth muscle myosin light chain kinase. *J. Biol. Chem.* **260:6.** 3355-3359

137. Kenney, R. E., P. E. Hoar and G. L. Kerrick (1990) The relationship between ATPase activity, isometric force, and myosin light chain phosphorylation and thiophosphorylation in skinned smooth muscle fiber bundles from chicken gizzard. *J. Biol. Chem.* **265:15.** 8642-8649

138. Kim, P., J. D. Jones and T. M. J. Sundt (1992) High energy phosphate levels in cerebral artery during chronic vasospasm after subarachnoid haemorrhage. *J. Neurosurg.* **76:6.** 991-996

139. Kim, P., Y. Yoshimoto, M. Iino, S. Tomio, T. Kirino and Y. Nonomura (1996) Impaired calcium regulation of smooth muscle during chronic vasospasm following subarachnoid haemorrhage. *J. Cereb. Blood Flow Metab.* **16**:334-341

140. Kistler, J. P., R. M. Crowell, K. R. Davis, R. Heros, R. G. Ojemann, T. Zervas and C. M. Fisher (1983) The relation of cerebral vasospasm to the extent and location of subarachnoid blood visualized by computer tomographic scanning: A prospective study. *Neurology* **33:4.** 424-436

141. Kiyohara, Y., K. Ueda, Y. Hasuo, J. Wada, H. Kawano, I. Kato, A. Sinkawa, T. Ohmura, H. Iwamoto and T. Omae (1989) Incidence and prognosis of subarachnoid haemorrhage in a Japanese rural community. *Stroke* **20**:1150-1155

142. Klumpp, S., D. Selke and J. Hermesmeier (1998) Protein phosphatase type 2C active at physiological Mg2+: stimulation by unsaturated fatty acids. *FEBS Letters* **437:**229-232

143. Kokubu, K., E. Tani, M. Nakano, N. Minami and H. Shindo (1989) Effects of ML-9 on experimental delayed cerebral vasospasm. *J. Neurosurg.* **71:**

144. Kraus, G. E., R. D. Bocholz, K.-W. Yoon, M. M. Knuepfer and K. R. Smith (1991) Cerebrospinal fluid endothelin 1 and endothelin 3 levels in normal and neurosurgical patients : A clinical study and literature review. *Surg. Neurol.* **35:**20-29

145. Krebs, E. G. and J. A. Beavo (1979) Phosphorylation and dephosphorylation of Enzymes. *Annu. Rev. Biochem.* **48:**923-59

146. Krebs, H. A. and K. Henseleit (1932) Untersuchungen uber die harnstoffbildung im tierkorper. *Z. Physiol. Chem.* **210:**33-66

147. Kuffler, S. W. (1953) The two skeletal nerve-muscle systems in frog. *Pflugers Arch.* **220:**116-135

148. Kurihawa, H., M. Yoshizumi, T. Sugiyama, K. Yamaoki, R. Nagai, F. Takaku, H. Satoh, J. Inui, M. Yanagisawa, T. Masaki and Y. Yazaki (1989) The possible role of endothelin 1 in the pathogenesis of coronary vasospasm. *J. Cardiovasc. Pharmacol.* **13:5.** S132-7

149. Laher, I. and J. A. Bevan (1987) Protein kinase C activation selectively augments a stretch induced, calcium dependent tone in vascular smooth muscle. *J. Pharmacol. Exp. Ther.* **242:2.** 566-572

150. Lassegue, B. R., W. Alexander, M. Clark, M. Akers and K. K. Griendling (1993) Phosphatidyl choline is a major source of phosphatidic acid and diacyl glycerol in angiotensin II stimulated vascular smooth muscle cells. *Biochem. J.* **292:**509-517

151. Li, H.-C. (1981) Phosphoprotein phosphatases. *Curr. Topics in Cell. Reg.* **21:**129-174

152. Linder, M. (1983) Inhibition by dipyridamole of cerebral vasospasm induced in vitro by whole blood. *J. Neurosurg.* **58:3.** 352-355

153. Ljunggren, B. C., J. L. Brandt and H. G. Saveland (1986) Outcome in patients subjected to early aneurysm operation and intravenous nimodipine. *Minerva Med.* **77:**1087-1092

154. Lowe, P., A. Hoiseth and T. Nordhus (1978) Spasm of the superior mesenteric artery complicating methysergide maleate therapy. *Br. J. Radiol.* **612:**1014-1016

155. Lowry, O. H., N. J. Rosebrough, A. L. Farr and R. J. Randall (1951) Protein measurement with the Folin phenol reagent. *J. Biol. Chem.* **193:**265

156. Lynch, R. M. and R. J. Paul (1983) Compartmentation of glycolytic and glycogenolytic metabolism in vascular smooth muscle. *Science* **222:**1344-1346

157. Macdonald, R. L., M. Bassiouny, L. Johns, M. Sajdak, L. S. Marton, B. K. Weir, E. D. Hall and P. K. Andrus (1998) U74389G prevents vasospasm after subarachnoid hemorrhage in dogs. *Neurosurgery* **42:6.** 1339-1346

158. Macdonald, R. L., M. C. Wallace and T. J. Coyne (1994) The Effect of Surgery On the Severity of Vasospasm *Journal of Neurosurgery* **80:3.** 433-439

159. Macdonald, R. L. and B. K. Weir (1994) Cerebral vasospasm and free radicals. *Free Rad. Biol. Med.* **16:5.** 633-643

160. Macdonald, R. L., B. K. A. Weir, M. G. A. Grace, M. H. Chen, T. P. Martin and J. D. Young (1992) Mechanism of cerebral vasospasm following subarachnoid hemorrhage in monkeys *Can. J. Neurol. Sci.* **19:**419-427

161.

162. Matsui, T. and T. Asano (1994) Effects of new 21-aminosteroid tirilazad mesylate (U74006F) on chronic cerebral vasospasm in a "two-hemorrhage" model of beagle dogs. *Neurosurgery* **34:6.** 1035-1039

163. Matsui, T., H. Kaizu, S. Itoh and T. Asano (1994) The role of active smooth muscle contraction in the occurrence of chronic vasospasm in the canine two haemorrhage model. *J. Neurosurg.* **80:**276-282

164. Matsui, T., T. Nagafuji, K. Tsutsumi, H. Uchida, T. Miyauchi and T. Asano (1994) The effect of nicorandil on chronic cerebral vasospasm. *Acta Neurochir (Wien)* **126:**165-169

165. Matsui, T., Y. Takuwa, H. Joshita, K. Yamashita and T. Asano (1991) Possible role of protein kinase C-dependent smooth muscle contraction in the pathogenesis of chronic cerebral vasospasm. *J. Cereb. Blood Flow Met.* **11:**143-149

166. Mattsson, E., I. Jansen, L. Edvinsson and D. Bergqvist (1993) Endothelin does not contribute to the vasospasm after balloon angioplasty in vitro. *J. Surg. Res.* **55:3.** 298-303

167. Mayberg, M. R., H. H. Batjer, R. Dacey, M. Diringer, E. C. Haley, R. C. Heros, L. L. Sternau, J. Torner, H. P. J. Adams, W. Feinberg and W. Thies (1994) Guidlines for the management of aneurysmal subarachnoid hemorrhage; A statement for healthcare professionals from a special writing group of the stroke council, American Heart Association. *AHA Medical/ Scientific Statement* **1:1.** 2592-2605

168. Mayer-Jaekel, R. E. and B. A. Hemmings (1994) Protein phosphatase 2A- a "menage a trois". *T.I.C.B* **4:**287-291

169. McClean, R. M. (1994) Magnesium and its therapeutic uses: A review. *Am. J. Med.* **96:**63-76

170. McDonald, T. F., S. Pelzer, W. Trautwein and D. J. Pelzer (1994) Regulation and modulation of calcium channels in cardiac, skeletal and smooth muscle cells. *Physiol. Rev.* **74:2.** 365-507

171. Mellor, H. and P. J. Parker (1998) The extended protein kinase C superfamily. *Biochem. J.* **332:**281-292

172. Merlevede, W., G. Defreyn, J. Goris, L. R. Kalala and J. Roosemont (1976) Regulation of glycogen phosphorylase phosphatase activity by ATP-Mg2+ and cyclic AMP. *Arch. Int. Physiol. Biochim.* **84:2.** 359-378

173. Miki, M., M. P. Walsh and D. J. Hartshorne (1992) The mechanism of the inhibition of the actin-activated myosin MgATPase by calponin. *Biochem. Biophys. Res. Commun.* **187:2.** 867-871

174. Mitsui, T., M. Inagaki and M. Ikebe (1992) Purification and characterisation of smooth muscle myosin-associated phosphatase from chicken gizzards. *J. Biol. Chem.* **267:23.** 16727-16735

175. Mitsui, T., T. Kitazawa and M. Ikebe (1994) Correlation between high temperature dependence of smooth muscle myosin light chain phosphatase activity and muscle relaxation rate. *J. Biol. Chem.* **269:8.** 5842-5848

176. Moreland, R. S. and G. D. Ford (1981) The influence of magnesium on calcium-activated, vascular smooth muscle actomyosin ATPase activity. *Arch. Biochem. Biophys.* **208:2.** 325-333

177. Moreland, S. (1994) Endothelin receptor antagonists: A brief review. *Can. J. Physiol. Pharmacol.* **72:**1469-1471

178. Mrwa, U., M. Troschka, G. Gross and L. Katzinski (1980) Calcium sensitivity of pig carotid actomyosin ATPase in relation to phosphorylation of the regulatory light chain. *Eur. J. Biochem.* **103:**415-419

179. Muir, K. W. and K. R. Lees (1995) A Randomised, double blind, placebo controlled pilot trial of intravenous magnesium sulfate in acute stroke. *Stroke* **1995:26.** 1183-1188

180. Mukai, H. and Y. Ono (1994) *Biocem. Biophys. Res. Commun.* **199:**897-904

181. Mulvany, M. J. (1979) The undamped and damped series elastic components of a vascular smooth muscle. *Biophys. J.* **26:**401-414

182. Murphy, R. A. (1994) What is special about smooth muscle? The significance of covalent cross bridge regulation. *FASEB J.* **8:**311-318

183. Murphy, R. A., D. F. Bohr and D. L. Newman (1969) Arterial actomyosin: Mg, Ca, and ATP ion dependencies for ATPase activity. *Am. J. Physiol.* **217:3.** 666-673

184. Murphy, R. A., P. H. Ratz and C. M. Hai (1987) Determinants of the latch state in vascular smooth muscle. *Prog. Clin. Biol. Res.* **Regulation and contraction of smooth muscle:**411-413

185. Murphy, R. A., C. M. Rembold and C.-M. Hai (1990) Contraction in smooth muscle. What is latch? *Front. Smooth Musc. Res.* **327:**39-50

186. Naka, M., Y. Kureishi, Y. Muroga, K. Takahashi, M. Ito and T. Tanaka (1990) Modulation of smooth muscle calponin by protein kinase C and calmodulin. *Biochem. Biophys. Res. Commun.* **171:3.** 933-937

187. Nakashima, T., K. Takenaka, S. Fukazawa, T. Ando, N. Sakai, H. Yamada, Y. Banno and Y. Nozawa (1997) Purification of a factor from CSF in patient after SAH which

induces the cytosolic free calcium elevation in vascular smooth muscle cells. *Neurol. Res.* **19:**51-56

188. Nakayama, S. and H. Nomura (1995) Mechanisms of intracellular Mg2+ regulation affected by amiloride and ouabain in the guinea-pig taenia caeci. *J. Physiol.* **488:1.** 1-12

189. Nakayama, S., H. Nomura and T. Tomita (1994) Intracellular free magnesium in the smooth muscle of guinea pig taenia caeci: A concomitant analysis for magnesium and pH upon sodium removal. *J. Gen. Physiol.* **103:**833-851

190. Nakayama, S., Y. Seo, A. Takai, T. Tomita and H. Watari (1988) Phosphorus compounds studied by 31-P NMRS in the taenia of guinea pig caecum. *J. Physiol.* **402:**565-578

191. Nakayama, S. and T. Tomita (1990) Depletion of intracellular free magnesium in magnesium and calcium free solution in the taenia isolated from guinea pig caecum. *J. Physiol.* **421:**363-378

192. Nakayama, S. and T. Tomita (1991) Regulation of intracellular free magnesium concentration in the taenia of guinea pig caecum. *J. Physiol.* **435:**559-572

193. Neil-Dwyer, G., M. E., D. Dorrance and D. Lowe (1987) Early intervention with Nimodipine in subarachnoid haemorrhage. *Eur. Heart J.* **8:K.** 41-47

194. Ngai, P. K., C. A. Carruthers and M. P. Walsh (1984) Isolation of the native form of chicken gizzard myosin light-chain kinase. *Biochem. J.* **218:3.** 863-870

195. Ngai, P. K. and M. P. Walsh (1987) Purification of smooth muscle myosin free of calmodulin and myosin light chain kinase. *Biochem. J.* **246:**205-211

196. Nishida, W., M. Abe, K. Takahashi and K. Hiwada (1990) Do thin filaments of smooth muscle contain calponin? *FEBS Lett.* **268:**165-168

197. Nishikawa, M., P. de Lanerolle, T. M. Lincoln and R. S. Adelstein (1984) Phosphorylation of mammalian myosin light chain kinases by the catalytic subunit of cyclic AMP dependent protein kinase and by cyclic GMP dependent protein kinase. *J. Biol. Chem.* **259:13.** 8429-8436

198. Nishiye, E., A. V. Somlyo, K. Torok and A. P. Somlyo (1993) The effects of MgADP on cross bridge kinetics: a laser flash photolysis study of guinea pig smooth muscle. *J. Physiol.* **460:**247-271

199. Nowak, G., F. Rainer and A. Sobieszek (1993) Purification and characterisation of the myofibrillar form of myosin light-chain phosphatase from turkey gizzard smooth muscle. *Biochim. Biophys. Acta* **1203:**230-235

200. Ohman, J., A. Servo and O. Heiskanen (1991) Long term effects of Nimodipine on cerebral infarcts and outcome after aneurysmal subarachnoid haemorrhage and surgery. *J. Neurosurg.* **74:**8-13

201. Ohta, S., J. Nishihara, Y. Oka, H. Todo, Y. Kumon and S. Sakaki (1995) Possible mechanism to induce protein kinase C-dependent arterial smooth muscle contraction after subarachnoid haemorrhage. *Acta Neurochir. (Wien)* **137:**217-225

202. Ohya, Y. and N. Sperelakis (1989) ATO regulation of the slow calcium channels in vascular smooth muscle cells of guinea pig mesenteric artery. *Circ. Res.* **64:**145-154

203. Okashiro, T., H. Tokuno, T. Fukumitsu, H. Hyashi and T. Tomita (1992) Effects of intracellular ATP on calcium current in freshly dispersed single cells of guinea pig portal vein. *Exp. Physiol.* **77:**719-731

204. Olsson, H. and P. Belfrage (1987) The regulatory and basal phosphorylation sites of hormone-sensitive lipase are phosphorylated by protein phosphatase-1, 2A and 2C but not by protein phosphatase 2B. *Eur. J. Biochem.* **168:**399-405

205. Onishi, H., J. Umeda, H. Uchiwa and S. Watanabe (1982) Purification of Gizzard Myosin Light Chain Phoshatase, and Reversible Changes in the ATPase and Superprecipitaion Activities of Actomyosin in the Presence of Purified Preparation of Myosin Light Chain Phosphatase and Kinase. *J. Biochem. Tokyo.* **91:1.** 265-271

206. Ono, Y., T. Fujii, U. Kikkawa, K. Igarishi and Y. Nishizuka (1988) *J. Biol. Chem.* **263:**6927-6932

207. Ono, Y., T. Fujii, K. Ogita, U. Kikkawa, K. Igarishi and Y. Nishizuka (1989) *Proc. Natl. Acad. Sci. USA.* **86:**3099-3103

208. Oriowo, M. A. and R. R. Ruffolo (1992) Activation of a single alpha 1 adrenoreceptor subtype in rat aorta mobilizes intracellular and extracellular pools of calcium. *Pharmacology* **44:**139-149

209. Padron, R., N. Pante, H. Sosa and J. Kendrick-Jones (1991) X-ray diffraction study of the structural changes accompanying phosphorylation of tarantula muscle. *J. Muscle Res. Cell Motil.* **12:**235-241

210. Palaty, V. (1971) Distribution of magnesium in the arterial wall. *J. Physiol.* **218:**353-368

211. Palaty, V. (1974) Regulation of the cell magnesium in vascular smooth muscle. *J. Physiol.* **242:**555-569

212. Park, S. and H. Rasmussen (1986) Carbachol-induced protein phosphorylation changes in bovine tracheal smooth muscle. *J. Biol. Chem.* **261:33.** 15734-9

213.

214. Pato, M. D., R. S. Adelstein, D. Crouch, B. Safer, T. S. Ingebritsen and P. Cohen (1983) The protein phosphatases involved in cellular regulation: 4. Classification of two homologous myosin light chain phosphatases from smooth muscle as protein phosphatase-

2A1 and 2C, and a homologous protein phosphatase from reticulocytes active as protein synthesis initiation factor eIF-2 as protein phosphatase-2A2. *Eur J. Biochem.* **132:**283-287

215. Pato, M. D. and E. Kerc (1988) Purification of smooth muscle myosin phosphatase from turkey gizzard. *Methods in Enzymol.* **159:**446-453

216. Paul, R., J., C. Hardin, J. Campbell and L. Raeymaekers (1989) Compartmentation of metabolism and function in smooth muscle *Muscle Energetics* **315:**381-390

217. Paul, R., J., C. Hardin, J. Campbell and L. Raeymaekers (1989) Compartmentation of metabolism and function in smooth muscle. *Muscle Energetics* **315:**381-390

218. Paul, R. J. (1983) Coordination of metabolism and contractility in vascular smooth muscle. *Federation Proc.* **42:**62-66

219. Paul, R. J. (1983) Functional compartmentalization of oxidative and glycolytic metabolism in vascular smooth muscle. *Am. J. Physiol.* **244:Cell physiol 13.** C399-409

220. Paul, R. J., M. Bauer and W. Pease (1979) Vascular smooth muscle: aerobic glycolysis linked to sodium and potassium transport processes. *Science* **206:**1414-1416

221.

222. Paul, R. J. and C. J. Ruegg (1988) Role of magnesium in activation of smooth muscle. *Am. J. Physiol.* **255:Cell Physiol. 24.** C465-C472

223. Pearson, R. B., R. Jakes, J. Kendrick-Jones and B. E. Kemp (1984) *FEBS Lett.* **168:**108-112

224. Pickard, J. D., G. D. Murray, R. Illingworth, M. D. Shaw, G. M. Teasdale, P. M. Foy, P. R. Humphrey, D. A. Lang, R. Nelson, P. Richards, J. Sinar, S. Bailey and A. Skene (1989) Effect of oral Nimodipine on cerebral infarction and outcome after subarachnoid haemorrhage: british aneurysm Nimodipine trial. *British Med. J.* **298:6674.** 636-642

225. Pierre, L. N. and A. P. Davenport (1995) Autoradiographic study of endothelin receptors in human cerebral arteries. *J. Cardiovasc. Pharmacol.* **26:suppl. 3.** S326-S328

226. Poe, M. (1969) Kinetic studies of temperature changes and oxygen uptake in a differential calorimeter: energy balance during calcium accumulation by mitochondria *Arch. Bioch. Biophys.* **132:**377-387

227. Pyne, G. J., T. A. D. Cadoux-Hudson and J. F. Clark (1998) Force-Function Relations in Vascular Smooth Muscle During Cerebral Vasospasm. *Biophys. J.* **74:2(pt2).** A256

228. Pyne, G. J., T. A. D. Cadoux-Hudson, Z. Domingo, G. K. Radda and J. F. Clark (1997) Vascular Smooth Muscle Oxidative Metabolism During Vasospasm. *Biophys. J.* **72:2(pt2).** A59

229. Pyne, G. J., T. A. D. Cadoux-Hudson, Z. Domingo, G. K. Radda and J. F. Clark (1997) Vascular Smooth Muscle Oxidative Metabolism During Vasospasm. *FASEB J.* **11:3.** A59

230. Ranatunga, K. W. (1982) Temperature-dependence of shortening velocity and rate of isometric tension development in rat skeletal muscle. *J. Physiol (Lond)* **329:**465-483

231. Redman, C. e. a. and T. E. T. C. Group. (1995) Which Anti-Convulsant for Women With Eclampsia? Evidence from the Collaborative Eclampsia Trial. *Lancet* **345:**1455-1463

232. Romani, A., C. Marfella and A. Scarpa (1993) Cell magnesium transport and homeostasis: role of intracellular compartments. *Miner. Electrolyte Metab.* **19:4-5.** 282-9

233. Ruegg, J. C. (1971) Smooth muscle tone. *Physiol. Rev.* **51:1.** 201-248

234. Ruegg, J. C. and R. J. Paul (1982) Calmodulin and cyclic AMP-dependent protein kinase alter calcium sensitivity in porcine carotid skinned fibres. *Circ. Res.* **50:**394-399

235. Russell, W. E. (1973) Insolubilisation and activation of arterial actomyosin by bivalent cations. *Eur. J. Biochem.* **33:**459-466

236. Salter, K. J. and R. Z. Kozlowski (1998) Differential electrophysiological actions of Endothelin-1 on Cl- and K+ currents in myocytes isolated from aorta, basilar and pulmonary artery. *J. Pharmacol. Exp. Ther.* **284:3.** 1122-1131

237. Sarti, C., J. Tuomilehto, V. Salomaa, J. Sivenious, E. Kaarsalo, E. V. Narva, K. Salmi and J. Torppa (1991) Epidemiology of subarachnoid haemorrhage in Finland from 1983 to 1985. *Stroke* **22:**848-853

238. Sasajima, H., H. Shima, Y. Toyoda and I. Nishio (1995) Role of protein kinase C in the relationship between Ca++ and contractile elements in rat alpha toxin permeabilised Mesenteric artery. *Japan. Circul. J.* **59:**103-111

239. Scarpa, A. (1974) Indicators of Free Magnesium in Solution *Biochemistry* **13:14.** 2789-2794

240. Seifert, V., B.-M. Loffler, M. Zimmermann, S. Roux and D. Stolke (1995) Endothelin concentrations in patients with aneurysmal subarachnoid hemorrhage. *J. Neurosurg.* **82:**55-62

241. Seiler, R. W., P. Grolimund and H. R. Zurbruegg (1987) Evaluation of the calcium antagonist Nimodipine for the prevention of vasospasm after aneurysmal subarachnoid haemorrhage. *Acta Neurochir Wien* **85:**7-16

242. Seiler, R. W. and A. C. Nirkko (1990) Effect of Nimodipine on cerebrovascular response to CO2 in assymptomatic individuals and patients with subarachnoid haemorrhage. A transcranial Doppler ultrasound study. *Neurosurgery* **27:**247-251

243. Sherry, J. M., A. Gorecka, M. O. Askoy, R. Dabrowska and D. J. Hartshorne (1978) Roles of calcium and phosphorylation in the regulation of the activity of gizzard myosin. *Biochemistry* **17:21.** 4411-4419

244. Shibuya, M., Y. Suzuki, K. Sugita, I. Saito, T. Sasaki, K. Takakura, I. Nagata, H. Kikuchi, T. Takemae, H. Hidaka and M. Nakashima (1992) Effect of AT877 on cerebral vasospasm after aneurysmal subarachnoid haemorrhage. *J. Neurosurg.* **76:**571-577

245. Shigeno, T., M. Clozel, S. Sakai, A. Saito and K. Goto (1995) The effect of bosentan, a new potent endothelin receptor antagonist, on the pathogenesis of cerebral vasospasm. *Neurosurgery* **37:1.** 87-91

246. Shimamura, K., N. Kurozumi, K. Yamamoto and S. Sunano (1989) Electrical and mechanical properties of spontaneous contraction in hypertensive rat portal vein. *Pflugers Arch.* **414:1.** 37-43

247. Shimizu, H., M. Ito, M. Miyahara, K. Ichikawa, S. Okubo, T. Konishi, M. Naka, T. Tanaka, K. Hirano, D. J. Hartshorne and T. Nakano (1994) Characterisation of the myosin binding sub-unit of smooth muscle myosin phosphatase. *J. Biol. Chem.* **269:48.** 30407-30411

248. Shiota, T., D. H. Bernanke, A. D. Parent and K. Hasui (1996) Protein kinase C has two different major roles in lattice compaction enhanced by cerebrospinal fluid from patients with subarachnoid haemorrhage. *Stroke* **27:**1889-1895

249. Shirazi, A., K. Iizuka, P. Fadden, C. Mosse, A. P. Somlyo, A. V. Somlyo and T. A. J. Haystead (1994) Purification and characterisation of the mammalian myosin light chain phosphatase holoenzyme. *J. Biol. Chem.* **269:50.** 31598-31606

250. Siegman, M. J., T. M. Butler, S. U. Mooers and R. E. Davies (1980) Chemical energetics of force development, force maintenance and relaxation in mammalian smooth muscle. *J. Gen. Physiol.* **76:609-629.** 609-629

251. Siegman, M. J., D. Funabara, S. Kinoshita, S. Watabe, D. J. Hartshorne and T. M. Butler (1998) Phosphorylation of a twitchin-related protein controls catch and calcium sensitivity of force production in invertebrate smooth muscle. *Proc. Natl. Acad. Sci. USA* **95:9.** 5383-8

252.

253. Sjogren, A. and L. Edvinsson (1988) The influence of magnesium on the release of calcium from intracellular depots in vascular smooth muscle cells. *Pharmacol. Toxicol.* **62:**17-21

254. Skonieczna, M., J. Kruszewska, J. Nowak and W. Bicz (1986) Influence of increased environmental temperature on oxidation processes in rat liver mitochondria. *Acta Physiol. Pol.* **37:4-5.** 157-167

255. Skonieczna, M., A. Piech and W. Bicz (1986) Influence of repeated exposure to elevated environmental temperature on the activity of respiratory enzymes of rat liver mitochondria. *Medycyna Pracy* **37:4.** 227-235

256. Sloane, B. F., A. Scarpa and A. P. Somlyo (1978) Vascular smooth muscle mitochondria; magnesium content and transport. *Arch. Biochem. Biophys.* **189:2.** 409-416

257. Small, J. V., D. O. Furst and J. De Mey (1986) Localization of Filamin in Smooth Muscle *J. Cell. Biol.* **102:1.** 210-220

258. Sobieszek, A., J. Borkowski and V. S. Babiychuk (1997) Purification and characterisation of a smooth muscle myosin light-chain kinase-phosphatase complex. *J. Biol. Chem.* **272:11.** 7034-7041

259. Somlyo, A. P. and A. V. Somlyo (1994) Signal transduction and regulation in smooth muscle. *Nature (London)* **372:231-236.** 231-236

260. Somlyo, A. V. and A. P. Somlyo (1968) Electromechanical and pharmacomechanical coupling in vascular smooth muscle. *J. Pharmacol. Exper. Ther.* **159:1.** 129-145

261.

262. Stromer, M. H. and M. Bendayan (1990) Immunocytochemical identification of cytoskeletal linkages to smooth muscle cell nuclei and mitochondria. *Cell. Motil. Cytoskel.* **17:1.** 11-18

263.

264. Sumner, M. J., T. R. Cannon, J. W. Mundin, D. G. White and I. S. Watts (1992) Endothelin ETA and ETB receptors mediate vascular smooth muscle contraction. *Br. J. Pharmacol.* **107:**858-860

265. Suzuki, M., M. Nishina, M. Endo, K. Matsuhita, M. Tetsuka, K. Shima and S. Okuyama (1997) Decrease in cerebral free magnesium concentration following closed head injury and effects of VA-045 in rats. *Gen. Pharmacol.* **28:1.** 119-121

266. Tachibana, K., P. J. Scheuer, Y. Tsukitani, H. Kikuchi, D. Van Engen, J. Clardy, Y. Gopichand and F. J. Schmitz (1981) Okadaic acid, a cytotoxic polyether from two marine sponges of the genus *Halichondria. J. Am. Chem. Soc.* **103:**2469-2471

267. Taggart, M. J. and S. Wray (1998) Hypoxia and smooth muscle function: key regulatory events during metabolic stress. *J. Physiol.* **509:2.** 315-325

268. Takahashi, K., K. Hiwada and T. Kokobu (1986) Isolation and characterization of a 34,000 Dalton calmodulin and F-actin binding protein from chicken gizzard smooth muscle. *Biochem. Biophys. Res. Commun.* **141:1.** 20-26

269. Takahashi, K. and B. Nadal-Ginard (1991) Molecular cloning and sequence analysis of smooth muscle calponin. *J. Biol. Chem.* **266:20.** 13284-13288

270. Takahashi, T., Y. Kawahara, T. Taniguchi and M. Yokoyama (1998) Tyrosine phosphorylation and association of p130Cas and c-Crk II by ANG II in vascular smooth muscle cells. *Am. J. Physiol.* **274:Heart Circ. Physiol. 43.** H1059-65

271. Takai, Y., K. Kaibuchi, T. Matsubara and Y. Nishizuke (1981) Inhibitory action of guanosine 3'5' monophosphate on thrombin-induced phosphatidylinositol turnover and protein phosphorylation in human platelets. *Biochem. Biophys. Res. Commun.* **101:1.** 61-67

272. Takai, Y., A. Kishimoto, Y. Iwasa, Y. Kawahara, T. Mori and Y. Nishizuka (1979) *J. Biol. Chem.* **254:**3692-3695

273. Takayasu, M. and R. G. Dacey (1990) Effects of HA 1077, a novel calcium antagonistic spasmolytic agent on intracerebral arterioles of rats. *Acta Neurochir (Wien)* **103:**67-70

274. Takayasu, M., Y. Suzuki, M. Shibuya, T. Asano, M. Kanamori, T. Okada, N. Kageyama and H. Hidaki (1986) The effects of HA compound calcium antagonists on delayed cerebral vasospasm in dogs. *J. Neurosurg.* **65:**80-85

275. Takeishi, Y., G. Chu, D. M. Kirkpatrick, Z. Li, H. Wakasaki, E. G. Kranias, G. L. King and R. A. Walsh (1998) *In vivo* phosphorylation of cardiac troponin I by protein kinase C beta 2 decreases cardiomyocyte calcium responsiveness and contractility in transgenic mouse hearts. *J. Clin. Invest.* **102:1.** 72-78

276. Takuwa, Y., N. Takuwa and H. Rasmussen (1986) Carbachol induces a rapid and sustained hydrolysis of polyphosphoinositide in bovine tracheal smooth muscle measurements of the mass of polyphosphoinositides , 1, 2 diacylglycerol and phosphatidic acid. *J. Biol. Chem.* **261:31.** 14670-14675

277. Tamura, S., K. R. Lynch, J. Larner, J. Fox, A. Yasui, K. Kikuchi, Y. Suzuki and S. Tsuiki (1989) Molecular cloning of rat type 2C (1A) protein phosphatase mRNA. *Proc. Natl. Acad. Sci. USA.* **86:**1796-1800

278. Taylor, J. S., D. B. Vigneron, J. Murphy-Boesch, S. J. Nelson, H. B. Kessler, L. Coia, W. Curran and T. R. Brown (1991) Free magnesium levels in normal human brain and brain tumours: 31P chemical shift imaging measurements at 1.5T. *Proc. Natl. Acad. Sci. USA* **88:**6810-6814

279. Thompson, D. F., N. A. Letassy and G. D. Thompson (1988) Fibrin glue: A review of its preparation, efficacy, and adverse effects as a topical hemostat. *Drug Intell. Clin. Pharm.* **22:12.** 946-952

280. Touyz, R. M., P. Laurent and E. L. Schiffrin (1998) Effect of Magnesium on Calcium Responses to Vasopressin in Vascular Smooth Muscle Cells of Spontaneously Hypertensive Rats. *J. Pharm. Exp. Therap.* **284:**998-1005

281. Trinkle-Mulcahy, L., K. Ichikawa, D. J. Hartshorne, M. J. Siegman and T. M. Butler (1995) Thiophosphorylation of the 130kDa subunit Is associated with a decreased activity of myosin light chain phosphatase in alpha toxin- permeabilised smooth muscle . *J. Biol. Chem.* **270:31.** 18191-18194

282. Turlapaty, P. D. M. V. and B. M. Altura (1978) Extracellular magnesium ions control calcium exchange and content of vascular smooth muscle. *Eur. J. Biochem.* **52:**421-423

283. Varsos, V., T. M. Liszczak, D. Hee Lan, J. P. Kistler, J. Vielma, P. McL Black, R. C. Heros and N. T. Zervas (1983) Delayed cerebral vasospasm is not reversible by aminophylline, nifedipine or papaverine in a "two-hemorrhage" canine model. *J. Neurosurg.* **58:**11-17

284. Verheggen, R. and K. Schror (1993) Effect of naftidrofuryl on platelet-induced vasospasm in vitro. Role of antiserotonergic actions. *Arzeimittelforschung* **43:3.** 330-4

285. Vernon, W. B. (1988) The role of magnesium in nucleic acid and protein metabolism. *Magnesium* **7:**234-248

286. Vink, R., T. McIntosh, P. Demediuk, M. W. Weiner and A. I. Faden (1988) Decline in intracellular free magnesium is associated with irreversible tissue injury after brain trauma. *J. Biol. Chem.* **263:2.** 757-761

287. Walker, J. S., C. J. Wingard and R. A. Murphy (1994) Energetics of crossbridge phosphorylation and contraction in vascular smooth muscle. *Hypertension* **23:**1106-1112

288. Wallnofer, A., S. Weir, U. Ruegg and C. Cauvin (1989) The mechanism of action of endothelin 1 as compared with other agonists in vascular smooth muscle. *J. Cardiovasc. Pharmacol.* **13:5.** s23-31

289. Walsh, M. P., A. Horowitz, O. Clement-Chomienne, J. E. Andrea, B. G. Allen and K. G. Morgan (1996) Protein kinase C mediation of Ca2+-independent contractions of vascular smooth muscle. *Biochem. Cell. Biol.* **74:**485-502

290. Walsh, M. P., G. J. Kargacin, J. Kendrick Jones and T. M. Lincoln (1995) Intracellular Mechanisms Involved in the Regulation of Vascular Smooth Muscle Tone. *Can. J. Physiol. Pharmacol.* **73:**565-573

291. Watanabe, T., T. Asano, T. Shimizu, Y. Seyama and K. Takakura (1988) Participation of lipooxygenase products from arachidonic acid in the pathogenesis of cerebral vasospasm. *J. Neurochem.* **50:**1145-1150

292. Weber, A., R. Herz and I. Reiss (1969) The role of magnesium in the relaxation of myofibrils. *Biochemistry* **8:6.** 2266-2271

293. Weir, B. (1995) The pathophysiology of cerebral vasospasm. *Br. J. Neurosurg.* **9:**375-390

294. Weir, B., M. Grace, J. Hansen and C. Rothberg (1978) Time course of vasospasm in man. *J. Neurosurg.* **48:**173-178

295. Wellum, G. R., J. W. Peterson and N. T. Zervas (1985) The relevance of in vitro smooth muscle experiments to cerebral vasospasm. *Stroke* **16:4.** 573-581

296. Wera, S. and B. A. Hemmings (1995) Serine/ threonine protein phosphatases. *Biochem. J.* **311:**17-29

297. Werth, D. K., J. R. Haeberle and D. R. Hathaway (1982) Purification of a myosin phosphatase from bovine aortic smooth muscle. *J. Biol. Chem.* **257:13.** 7306-9

298. Wetsel, W. C., W. A. Khan, I. Merchenthaler, H. Rivera, A. E. Halpern, H. M. Phung, A. Negro- Vilar and Y. A. Hannun (1992) Tissue and cellular distribution of the extended family of protein kinase C isoenzymes. *J. Cell Biol.* **117:1.** 121-133

299. White, D. G., T. R. Cannon, H. Garratt, J. W. Mundin, M. J. Sumner and I. S. Watts (1993) Endothelin ETA and ETB receptors mediate vascular smooth muscle contraction. *J. Cardiovasc. Pharm.* **22:8.** S144-S148

300. White, R. E. and H. C. Hartzell (1989) Magnesium ions in cardiac function. regulator of ion channels and second messengers. *Biochem. Pharmacol.* **38:6.** 859-867

301. Whitfield, P. C. and J. D. Pickard (1994) Nimodipine. *Br. J. Hosp. Med.* **52:10.** 539-540

302. Wills, F. L., W. D. McCubin and C. M. Kay (1994) Smooth muscle calponin-caltropin interaction: effect on biological activity and stability of caloponin. *Biochemistry* **33:**5562-5569

303. Winder, S. J., M. D. Pato and M. P. Walsh (1992) Purification and characterization of calponin phosphatase from smooth muscle. *Biochem. J.* **286:**197-203

304. Winder, S. J. and M. P. Walsh (1990) Smooth muscle calponin. Inhibition of actomyosin MgATPase and regulation by phosphorylation. *J. Biol. Chem.* **265:**10148-10155

305. Winder, S. J. and M. P. Walsh (1993) Calponin, thin filament-linked regulation of smooth muscle contraction. *Cell. Signalling* **5:**677-686

306. Wingard, C. J., A. K. Browne and R. A. Murphy (1995) Dependence of force on length at constant cross-bridge phosphorylation in the swine carotid media. *J. Physiol.* **488:3.** 729-739

307. Wingard, C. J., R. J. Paul and D. A. Murphy (1997) Energetic cost of activation processes during contraction of swine arterial smooth muscle. *J. Physiol.* **501:1.** 213-223

308. Wingard, C. J., R. J. Paul and R. A. Murphy (1994) Dependence of ATP consumption on cross bridge phosphorylation in swine carotid smooth muscle. *J. Physiol.* **481:1.** 111-117

309. Wronski, J., R. Abraszko, W. Berny and J. Mierzwa (1990) Clinical experiences with Nimodipine treatment in patients after SAH and aneurysm surgery. *Zentralbl. Neurochir.* **51:**21-23

310. Yakubu, M. A. and C. W. Leffler (1996) Role of endothelin-1 in cerebral hematoma-induced modification of cerebral vascular reactivity in piglets. *Brain Res.* **734:**149-156

311. Yanisagawa, M., H. Kurihawa, S. Kimura, Y. Tomobe, M. Kobayashi, Y. Mitsui, Y. Yazaki, K. Goto and T. Masaki (1988) A novel, potent vasoconstrictor peptide produced by vascular endothelial cells. *Nature* **332:**411-415

312. Yokota, M., J. W. Peterson, M. C. Kaoutzanis, K. Yamakawa, R. Sibilia and N. T. Zervas (1995) Protein kinase C and diacyl glycerol content in basilar arteries during experimental cerebral vasospasm in the dog. *J. Neurosurg.* **82:**834-840

313. Yoshimoto, Y., P. Kim, T. Sasaki and K. Takakura (1993) Temporal profile and significance of metabolic failure and trophic changes in the canine cerebral arteries during chronic vasospasm after subarachnoid hemorrhage. *J. Neurosurg.* **78:**807-812

314. Yu, H.-Y., J. A. Hypolite, A. J. Wein and R. M. Levin (1995) Effect of magnesium ions on rabbit detrusor contractility and intracellular free calcium. *Pharmacology* **51:**186-194

315. Zhang, A., T. P. O. Cheng and B. M. Altura (1992) Magnesium regulates intracellular free ionized calcium concentration and cell geometry in vascular smooth muscle cells. *Biochim. Biophys. Acta* **1134:**25-29

316. Zhang, H. and D. Cook (1994) Cerebral vascular smooth muscle potassium channels and their possible role in the management of vasospasm. *Pharmacol. Toxicol.* **75:**327-336

317. Zhang, Y., S. Moreland and R. S. Moreland (1993) Regulation of vascular smooth muscle contraction; myosin light chain phosphaorylation dependent and independent pathways. *Can. J. Physiol. Pharmacol.* **72:**1386-1391

318. Zimmermann, M. (1997) Endothelin in cerebral vasospasm. clinical and experimental results. *J. Neurosurg. Sci.* **41:2.** 139-151

319. Zuccarello, M., A. Romano, M. Passalacqua and R. M. Rapoport (1995) Endothelin 1 induced endothelin 1 release causes cerebral vasospasm *in vivo*. *J. Pharm. Pharmacol.* **47:**702

320. Zuccarello, M., G. B. Soattin, A. I. Lewis, V. Breu, H. Hallak and R. M. Rapoport (1996) Prevention of subarachnoid haemorrhage induced vasospasm by oral administration of endothelin receptor antagonists. *J. Neurosurg.* **84:**503-507